The Geochemistry of Rare Earth Element-Bearing Minerals and their Relationship to Copper Sulphide Mineralisation at the Carrapateena Deposit, South Australia

Thesis submitted in accordance with the requirements of the University of Adelaide for an Honours Degree in Geology

Brooke North

November 2020

THE GEOCHEMISTRY OF RARE EARTH ELEMENT-BEARING MINERALS AND THEIR RELATIONSHIP TO COPPER SULPHIDE MINERALISATION AT THE CARRAPATEENA DEPOSIT, SOUTH AUSTRALIA.

REE MINERALS AT CARRAPATEENA

ABSTRACT

Carrapateena is an Iron Oxide Copper-Gold (IOCG) deposit which is located on the eastern margin of the Gawler Craton, within the Olympic Copper-Gold Province. In addition to Cu and Au, Carrapateena contains elevated concentrations of REE. Three mineralogical zones are distinguished in the deposit largely based on Cu abundance: the barren zone, chalcopyrite zone and bornite zone, where the latter is the highest-grade Cu ore zone. Each zone exhibits distinct whole-rock REE profiles, warranting an investigation into the relationship between REE and Cu mineralisation. However, limited research has been completed in this space, and on Carrapateena in general. This project aims to investigate the textural relationships between Cu- and REE-bearing minerals, perform U-Pb geochronology on the REE-bearing minerals, and characterise their geochemistry in each zone of the deposit. This will ultimately improve understanding of the temporal development of Carrapateena.

Monazite, xenotime and apatite are the most abundant REE-bearing minerals in studied samples. Textural relationships show that while monazite was part of the main Cu-mineralising stage in the formation of Carrapateena, apatite and xenotime were part of a paragenetically earlier mineral assemblage. The geochronology of all three minerals record multiple remobilisation events, almost all of which post-date the published deposit age of ca. 1590 Ma. Based on textural relationships, the dates produced from monazite may be a more appropriate estimate of the introduction of Cu into the Carrapateena mineral system at ca. 1450 Ma. Apatite displays three distinct chondrite-normalised REE fractionation trends corresponding to the bornite, chalcopyrite and barren zones of Carrapateena. For the first time, these trends have been compared to those from other IOCG deposits in the Olympic-Cu-Au Province, and offer insight into evolving fluid physiochemistry during IOCG deposit formation. These findings are encouraging for the future applicability of apatite geochemistry to mineral exploration.

KEYWORDS

Carrapateena, IOCG, Rare Earth Elements, Copper, Monazite, Xenotime, Apatite, Chalcopyrite, Bornite, Geochemistry, Olympic Copper-Gold Province, REE.

TABLE OF CONTENTS

LIST OF FIGURES

LIST OF TABLES

1 INTRODUCTION

The Carrapateena IOCG deposit is located on the eastern margin of the Gawler Craton, 160 km north of Port Augusta in South Australia, within the Olympic Copper-Gold Province (Hayward & Skirrow, 2010; Skirrow et al., 2007). Discovered in 2005, Carrapateena has a current mineral resource of 970 Mt at 0.5% Cu and 0.2 g/t Au with an estimated mine life of 20 years (OZ Minerals, 2019). It belongs to the hematite breccia-hosted endmember of the Iron Oxide Copper-Gold (IOCG) group of deposits (Barton, 2014; Corriveau & Potter, 2019; Daly, Heithersay & McGeough 2007; Dmitrijeva et al., 2019; Williams et al., 2005).

The primary Cu-bearing sulphides at Carrapateena are bornite and chalcopyrite (with minor chalcocite), which formed by replacement of early pyrite or as open space infill (Porter, 2010; Sawyer et al., 2017). Economic mineralisation is hosted within the Carrapateena Breccia Complex (CBC), which comprises Mesoproterozoic polymictic hematite-granite breccia and is enclosed by Donington Suite granite (ca. 1850 Ma) (Mortimer et al., 1988). Sulphide minerals are zoned both vertically and laterally within the deposit, leading to the broad characterisation of the CBC into bornite, chalcopyrite and barren zones of interest to this study. The age of the initial phase of sulphide mineralisation is reported as 1598 ± 6 Ma as determined by Re-Os isotopic analysis of pyrite from hematite breccias (Sawyer et al., 2017). As such, Carrapateena is proposed to have formed during the major tectonothermal event associated with the Hiltaba magmatic event, the same proposed origin as the world-class Olympic Dam IOCG deposit, located 100 km north-west of Carrapateena (Ehrig et al., 2012; Oreskes & Einaudi 1990; Verdugo et al., 2019).

In addition to copper and gold, the Carrapateena deposit is enriched in rare earth elements (REE), particularly the light REE (LREE) cerium and lanthanum, relative to heavy REE (HREE), which is typical of IOCG deposits (Hitzman et al., 1992; Sawyer et al., 2014; Williams, 2012). Beyond some initial petrology and textural interpretations by Taylor (2014) and Williams (2012), very limited research has been completed on which REE-bearing mineral phases are present at Carrapateena, and their relationship with Cu-sulphides. The importance of understanding REE mineralogy is exemplified by the unique geochemical signatures exhibited by each of the three zones of the deposit, which potentially offers insight into the geological evolution of Carrapateena and IOCG deposits in general.

To begin to explore the relationship between Cu and REE, this study aims to investigate the paragenetic evolution of Cu- and REE-bearing minerals, perform U-Pb geochronology on the REE-bearing minerals and characterise their geochemistry in each of the three mains zones of the deposit.

2 BACKGROUND GEOLOGY

2.1 Regional Geology

The Carrapateena deposit is located on the eastern margin of the Gawler Craton within the Olympic Cu-Au Province, which also hosts the Olympic Dam, Prominent Hill, Moonta and Hillside deposits and several other mineralised prospects (Figure 1) (Dmitrijeva et al., 2019).

The tectonic evolution of the region is complex, involving multiple orogenic events, extensional basin development and volcanic activity. Beginning at approximately 1850 Ma, Meso-to-Neoarchean to early Paleoproterozoic igneous and metamorphic rocks comprising the core of the Gawler Craton were overlain by dominantly clastic rocks of the Dark Peake Group (Hand et al., 2007; Reid & Hand, 2012; Spunzar et al., 2011;).

During the Cornian Orogeny 1850 Ma, which involved crustal thickening followed by crustal extension associated with mafic magmatism (Reid & Hand., 2008), metaluminous granodiorites of the Donington Suite intruded the eastern margin of the craton. Hayward & Skirrow (2010) suggested that Donington Suite magmatism was related to subduction under the eastern margin of the Olympic Domain (Betts and Giles, 2006; Ferris et al., 2002).

In the Olympic Cu-Au Province, a series of extensional basins formed between 1790 and 1740 Ma that accommodated deposition of the Wallaroo Group, which includes intrusive and extrusive felsic and mafic igneous rocks with carbonates and clastic sediments (Cowley et al., 2003; Reid, 2019). The Gawler Craton was then affected by the Kimban Orogeny at ca. 1735 – 1690 Ma (Hand et al., 2007; Reid & Hand, 2012).

The effects of the Kimban Orogeny within the Olympic Cu-Au Province are still poorly understood, and its affects appear to be absent in the southern Olympic Cu-Au Province. Between 1630 to 1615 Ma, magmatism was focused in the southwest of the craton (including the St Peter Suite and Nuyts Volcanics) and is interpreted to define a late Palaeoproterozoic magmatic arc (Swain et al., 2008). Immediately following this, magmatism migrated to the east and then evolved to encompass much of the southern Gawler Craton to form a felsic igneous province covering over 25,000 km^2 (Hand et al., 2007). This was associated between 1595 – 1575 Ma with the formation of the Hiltaba Suite and the 1592 – 1589 Ma bimodal Gawler Range Volcanics (GRV) and is interpreted to be contemporaneous with the breakup of the supercontinent Columbia (Allen et al., 2008; Budd, 2006; Creaser and White, 1991; Flint et al., 1993).

Hand et al. (2008) proposed that GRV volcanism took place in an orogenic foreland setting, and there is extensive evidence for high-grade metamorphism and deformation associated with the Hiltaba Suite (Cutts et al., 2011; Forbes et al., 2012; Morrissey et al., 2013; Reid & Hand, 2012). The granitoids of the Hiltaba Suite are variably enriched in uranium, fluorine and other high field strength elements (Budd, 2006; Fraser & Nuemann, 2010), however, their role in IOCG mineralisation is not well constrained.

Tectonic and hydrothermal events affecting the eastern Gawler Craton subsequent to GRV volcanism are poorly constrained until the intrusion of the NW-trending Gairdner Dyke Swarm at 825 Ma. This dyke swarm marked the start of a long history of rifting that eventually lead to fragmentation of Australia and Laurentia (Powell, 1998; Preiss, 2000) and accumulation of the Adelaide Rift Complex, which comprise a sequence of Neoproterozoic to Cambro-Ordovician sediments including the Tapley Hill Formation (643 ± 2.4 Ma) (Kendall at al., 2006; Preiss, 1987; Reid, 2019). It was also during the Neoproterozoic to the Lower Palaeozoic that the unconformable sedimentary cover sequence of Carrapateena and other deposits on the Stuart Shelf, comprising marine mudstones, sandstones and lake sediments, was deposited (Murphy et al., 2012; Preiss & Forbes, 1981).

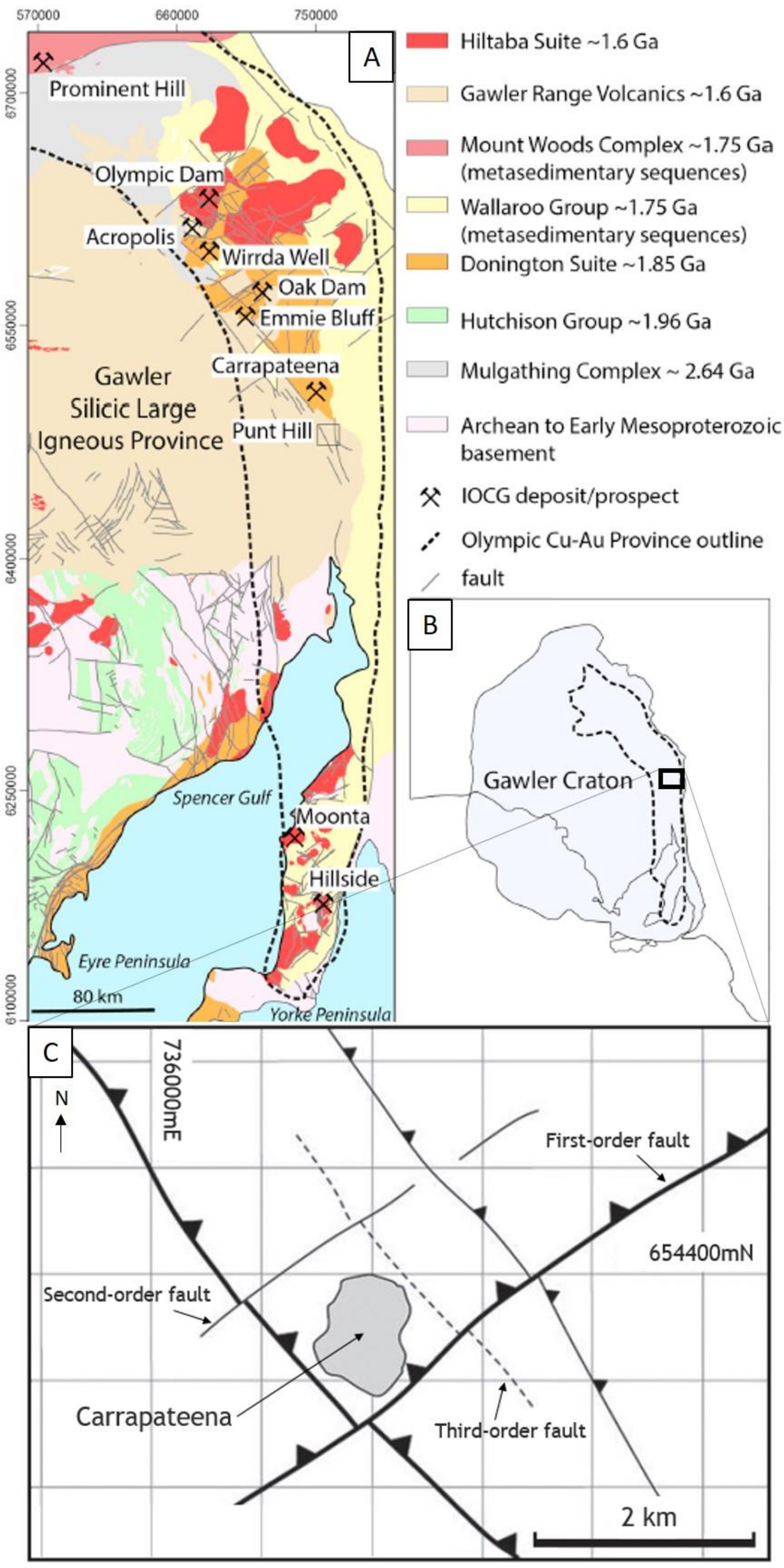

Figure 1: a) Geological map of the eastern Gawler Craton and b) Regional-scale location of Carrapateena (after Dmitrijeva et al., 2019). c) Deposit-scale basement structural geology interpretations for Carrapateena based on aeromagnetic and gravity imagery (adapted from Hayward & Skirrow, 2010).

2.2 Deposit Geology

Carrapateena is situated beneath ~480 m of Neoproterozoic Stuart Shelf sedimentary units of the Umberatana and Wilpena groups (Vella & Emerson, 2009). The Wilpena Group (ca. 640–540 Ma) includes quartzite, sandstone and shale which overlie the Whyalla sandstone (640–635 Ma) and Nucaleena Formation (~635 Ma) (Lloyd et al., 2020). A thin horizon of basal conglomerate separates the unmineralised cover sequence from the Carrapateena Breccia Complex (CBC), which is a steeply plunging pipe-like body of hematite-sericite-chlorite-carbonate (HSCC) altered polymictic hematite-granite breccia that hosts all economic mineralisation. The diameter of the CBC is approximately 500 m, with mineralisation extending to at least 1900 m below the unconformity (Sawyer et al., 2017). A small gossan has been recognised at the paleo-unconformity, with associated supergene Cu minerals including chalcocite, digenite and covellite (Sawyer et al., 2014).

The geology of the deposit is a combination of mineralised hematite-altered breccias, barren hematite breccias, granite breccias, chlorite-altered granite breccias, dykes and rare rocks with a proposed sedimentary origin (Sawyer et al., 2014). Breccia clasts are predominantly derived from the Donington Suite that encloses the CBC, but vary in composition from medium grained gneissic diorite to hematite-dominated clasts of earlier breccia phases within a hematite and sericite altered matrix. The gneissic quartz-granite and quartz diorite of the Donington Suite that encloses the CBC have been foliated and/or sheared to varying degrees, most probably during the 1730 – 1700 Ma Kimban Orogeny (Reid et al., 2008).

Carrapateena is proposed to have formed at approximately 1595 – 1575 Ma during the major tectonothermal event that resulted in the intrusion of the Hiltaba Suite and Gawler Range Volcanics (GRV) (e.g. Payne et al., 2017; Sawyer et al., 2017). This is the same time period proposed for the formation of the super-giant Olympic Dam deposit (e.g. Johnson and Cross, 1995; Ciobanu et al., 2013). The structural trap for mineral precipitation is speculated to have formed as a result of NNW – SSE extension coinciding with the GRV eruption and subsequent NW – SE to NNW – SSE contraction (Hand et al., 2007). Specifically, the deposit is located near the intersection of a NE-trending extensional fault with a NW-trending fault (Figure 1c) in the hanging wall of the crustal scale Elizabeth Creek Fault.

Hematite is present in two main forms at Carrapateena: earthy hematite and grey crystalline hematite. Earthy hematite is more dominant in the shallower levels of the deposit. Grey hematite becomes more prevalent in the mid-to-deep levels while magnetite is the dominant Fe-oxide at the deepest levels (Figure 2). This distribution is used to infer ‘oxidised’ and ‘reduced’ areas of the deposit, given that hematite has a higher oxidation state than magnetite (Otake et al., 2007).

2.3 Cu Zonation at Carrapateena

Copper sulphide minerals are present as disseminated grains that typically range in size from 0.1 – 4 mm (Sawyer et al., 2017). Cu sulphides are commonly hosted in the comminuted granite host rock fragments and in the matrix, both of which are overprinted by earthy or grey hematite (Sawyer et al., 2014). Textural relationships illustrate that the precipitation of chalcopyrite predominantly resulted from the replacement of an earlier pyrite stage, which formed as open space infillings and was the necessary source of reduced sulphur in the system (Sawyer et al., 2014). Bornite partially replaces (rims) both pyrite and chalcopyrite and is suspected to have completely replaced existing sulphides where bornite grains are found alone. Native gold and electrum are hosted within sulphides including pyrite and bornite (Sawyer et al., 2017). It is important to note that the ore genesis of South Australian IOCG systems, including Carrapateena and Olympic Dam, involves a multistage paragenesis including repetitive brecciation (e.g. Apukhtina et al., 2017; Ismail et al., 2014; Krneta et al., 2017a).

Sulphide minerals (bornite, chalcopyrite and pyrite) are zoned in abundance both vertically and laterally at Carrapateena. Trending from the reduced, deep zone of the deposit to the oxidised, upper barren zone, sulphide mineralisation zones from pyrite-chalcopyrite to chalcopyrite-bornite to bornite only (Sawyer et al., 2014). Three domains have been distinguished to reflect this zonation, which includes a main bornite zone, a chalcopyrite zone and a barren zone (Figure 2). The bornite zone is differentiated by a Cu/S ratio that indicates that bornite is the dominant Cu sulphide and at the core/hand specimen scale where bornite is visible. The chalcopyrite zone still contains some bornite, but chalcopyrite is the dominant Cu sulphide. The barren zone is located in the central-north of the CBC and only contains trace amounts of Cu (<100 ppm). It is visually distinctive at the core scale, with abundant earthy hematite alteration, a lack of Cu sulphides and typically contains barite and anhydrite. No siderite, magnetite or pyrite are present in the barren zone (M Neumann, personal communication, August 31, 2020).

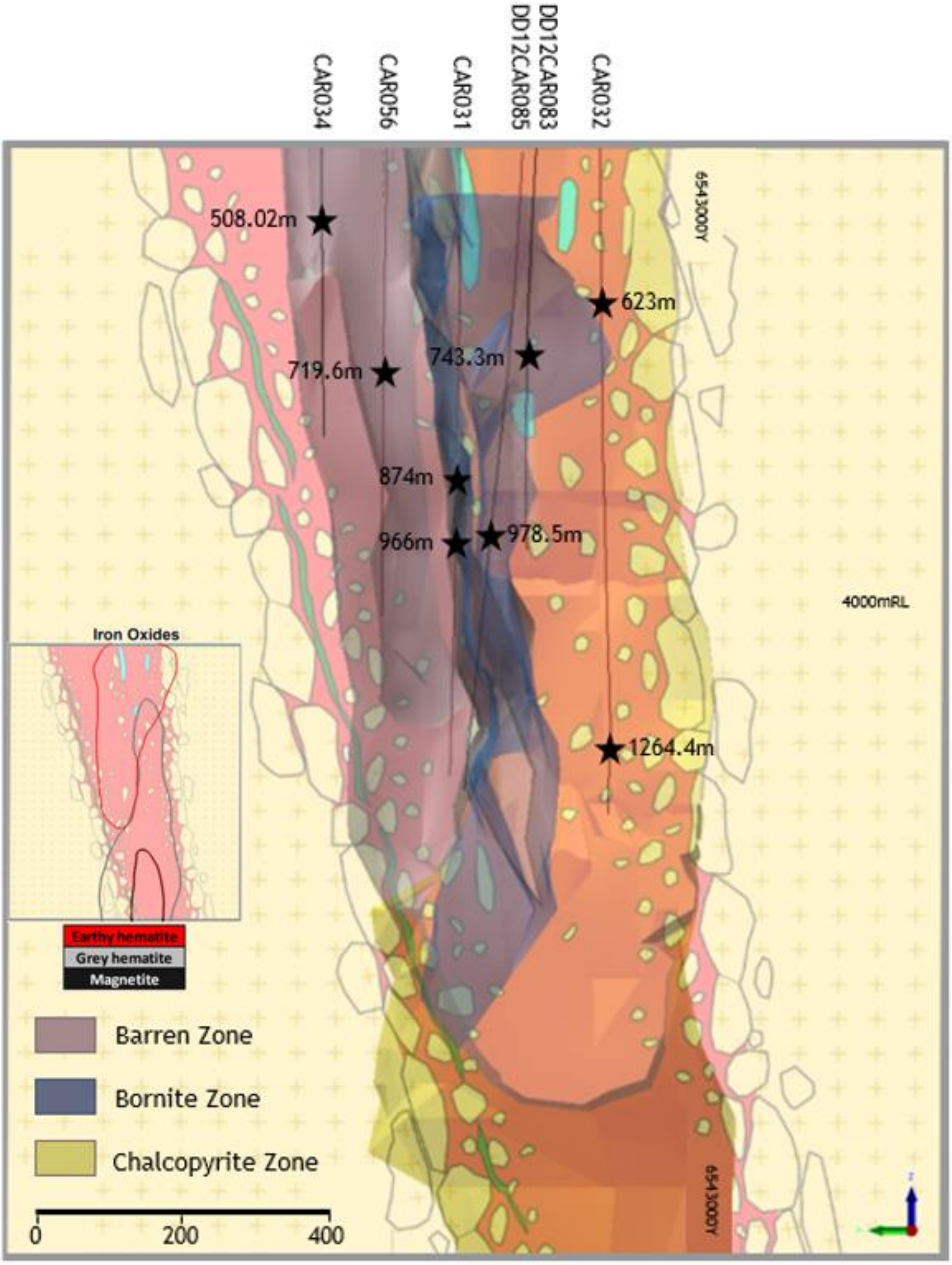

Figure 2: Section view of Carrapateena looking east showing the locations of studied samples (stars) in the delineated barren, chalcopyrite and bornite zones. Cartoon geology represents the volcanogenic conglomerate unit (light blue 'pods') and variably brecciated Donington granite enclosing the CBC. The cover sequence has been removed from this section. Inset image illustrates the zonation of iron oxides in the CBC, with the approximate same field of view. After Neumann (2019).

The bornite, chalcopyrite and barren zones can also be distinguished geochemically (Figure 3). Using the existing OZ Minerals whole-rock geochemical database, it is evident that the three zones exhibit different REE signatures in addition to Cu/S ratios (Figure 3, top and middle). The chondrite-normalised data from the bornite zone is most enriched in all REE, followed closely by the barren zone. There is a negative Y anomaly in the barren zone data only and this group also exhibits the highest concentrations of P (Figure 3, bottom). Note there does not appear to be a correlation between Cu sulphides and total REE concentration. However, there may be a range of different elemental distinctions between the three zones, which will be expanded in the Results and Discussion sections of this thesis.

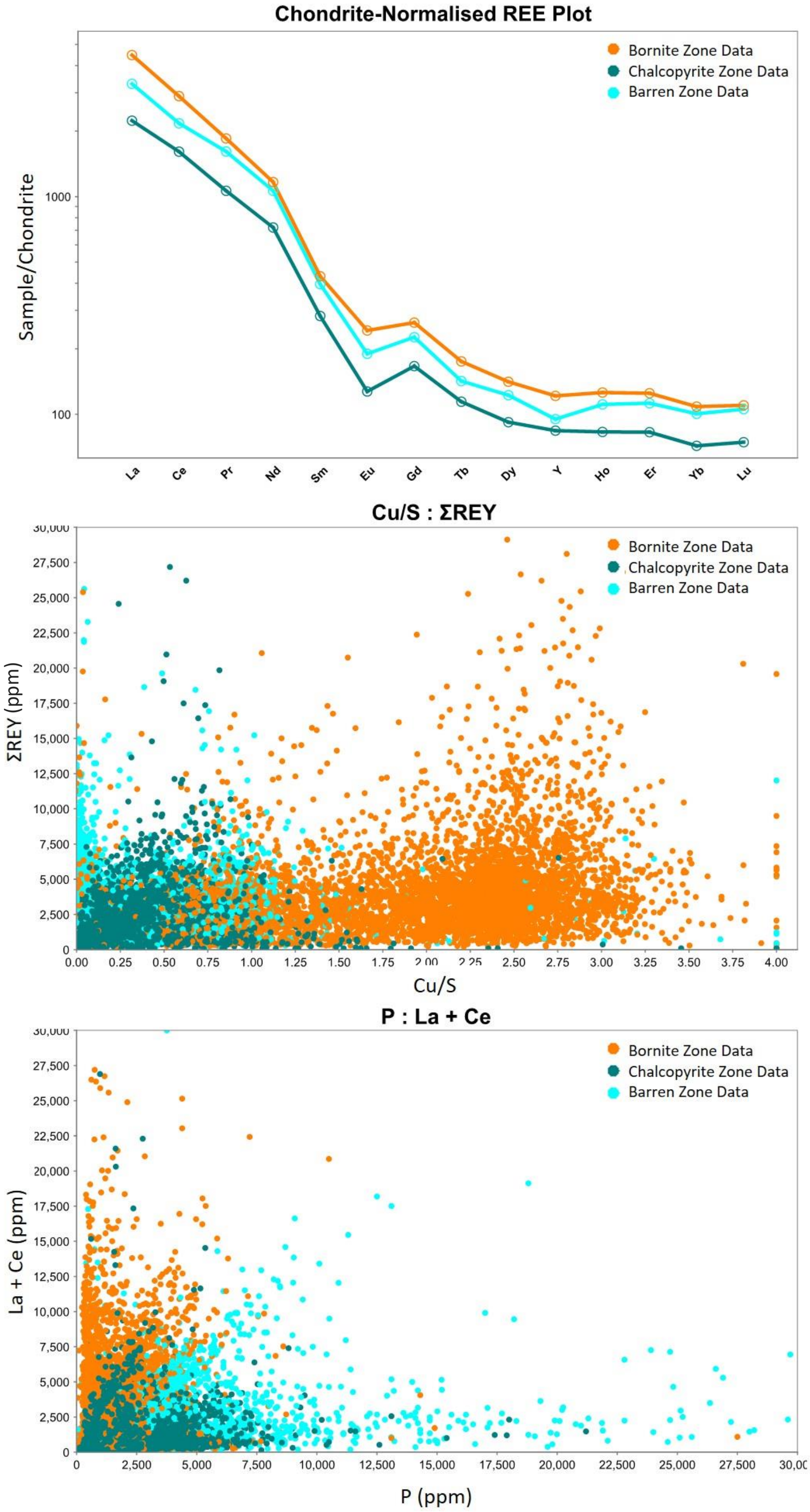

Figure 3: Trace element plots of whole-rock geochemical data from OZ Minerals database from the three different zones (Bornite, Chalcopyrite and Barren) within the Carrapateena deposit. Top: Averaged chondrite-normalized REE signatures of all data. n= 18154. Middle: Cu/S vs ΣREY (REY = REE + Y) plot demonstrating poor correlation between ΣREE and Cu sulphides. n= 18154. The y scale excludes 17/5811 bornite zone data points. Bottom: P vs La + Ce showing enrichment of P in the barren zone and absolute concentrations of La and Ce. The x and y scales exclude 3/4586 barren zone, 9/9304 bornite zone and 1/4264 chalcopyrite zone data points. n= 18345. All plots generated in ioGAS.

2.4 Rare Earth Elements at Carrapateena

REE mineralogy at Carrapateena is not extensively documented, however, florencite, monazite, parasite and an unidentified LREE phase that lacks Ca or P have been observed in previous petrology and SEM analyses (e.g. Williams, 2012). Monazite has been observed as discrete grains or very fine-grained aggregates, while florencite forms veinlets or partly aggregated grains associated with hematite and is hosted in chlorite and sericite (Williams, 2012). Florencite has been observed in the matrix of a chloritized granite crackle breccia (Sawyer et al., 2014) and monazite as discrete grains or very fine-grained aggregates, interpreted to be contemporaneous with Cu sulphide mineralisation (Taylor, 2014). Specifically, monazite has been recorded to have close spatial and temporal associations with bornite (Sawyer et al., 2017). The highest concentrations of REE are present in the bornite zone and barren zone and the more granite-rich domains of the deposit contain lower concentrations of REE, with the exception of chloritised granites (Sawyer et al., 2014).

3 METHODS

3.1 Sample Collection and Preparation

Field work was planned to be completed at Carrapateena during March 2020. However, travel restrictions enforced due to the global COVID-19 pandemic postponed all field work and collection of additional samples. Instead, 14 previously sampled slabs from two diamond drill holes in the bornite zone (DD12CAR083 and DD12CAR085) (Table 1) were selected. Five of these samples were sent to CSIRO and scanned using the Maia Mapper (Ryan et al., 2018) in addition to being made into thirteen 40 µm polished thin sections at Adelaide Petrographics. Additional thin sections were made available by OZ Minerals after the completion of Maia Mapping. Analysis of the OZ Minerals database in Micromine (3D) allowed for the selection of samples based on elevated lanthanum values and their location within the deposit. Two thin sections were chosen from each major zone: the bornite zone, the chalcopyrite zone and the barren zone, to provide a broad representation of the orebody.

3.2 Maia Mapper

The five samples of half core were polished to 600 grit and sent to CSIRO in Perth for scanning. The Maia Mapper is a micro XRF scanner for elemental imaging of unprepared cut drill core and polished rock (CSIRO, 2019; Ryan et al., 2018). The system combines a MetalJet D2 liquid metal micro-focused x-ray source from Excillium, custom detector arrays and a polycapillary lens with data capture hardware and spectral analysis algorithms to produce high-definition, quantitative element images in real-time. The element images are up to 80 M pixels with a spatial resolution of ~32 µm (Ryan et al., 2018). For these samples, the Maia Mapper collected an entire X-ray spectrum from ~2.2 keV to ~70 keV and ran at 3 ms per pixel. Data processing was completed using ImageJ and GeoPIXE to investigate the distribution of REE and Cu and their textural relationship to iron-oxides and brecciation events.

3.3 Petrology

Petrographic analyses were conducted using an Olympus BX51 System Microscope with a DP21 digital camera attached. A petrography report was completed for a total of 11 thin sections (Appendix A). Petrology was used to identify areas of interest for further examination using the Scanning Electron Microscope and Mineral Liberation Analyser (SEM-MLA) (discussed below).

3.4 Scanning Electron Microscope and Mineral Liberation Analyser

The FEI Quanta 600 SEM and MLA were used on 11 samples at Adelaide Microscopy, University of Adelaide. High resolution Electron Backscatter (EBS) images of individual mineral grains were taken on both the Quanta 600 and Quanta 450 SEM. These images were used for targeting monazite, xenotime and apatite crystals for the Laser Ablation Inductively Coupled Plasma Mass Spectrometry (LA-ICP-MS) (discussed below) and also aided analysis of textural relationships between minerals of interest and their hosts to establish paragenetic timing. The X-ray energy dispersive detector (EDS) was used to ensure the correct identification of minerals through acquisition of qualitative elemental compositions. The MLA was then used to produce modal mineralogy maps of the samples. The SEM parameters are presented in Table 1.

Table 1: SEM and MLA parameters for analysis of all thin sections.

Method	SEM 600 and MLA	SEM 450
Samples	11	5
Spot size	7.0	5.0
Beam Energy (Kv)	25.00	20.00
Working Distance (WD) (mm)	10	10

3.5 Laser Ablation Inductively Coupled Plasma Mass Spectrometry

LA-ICP-MS was conducted to obtain quantitative trace element data using the Agilent 7900x in conjunction with the RESOlution LR 193nm Excimer laser system at Adelaide Microscopy, University of Adelaide. In situ laser ablation for a total of nine samples was completed for monazite U-Pb (three samples), xenotime U-Pb (three samples) and apatite U-Pb (six samples). Simultaneous acquisition of isotopes (e.g. ^{202}Hg, ^{204}Pb, ^{206}Pb, ^{207}Pb, ^{208}Pb, ^{232}Th and ^{238}U) allowed for dating of the REE-bearing minerals (U-Pb geochronology) following the methods of Payne et al., 2008; Fletcher et al., 2004; Thomson et al., 2012 for monazite, xenotime and apatite, respectively. The LA-ICP-MS parameters are presented in Table 2.

Table 2: Summary methods table for LA-ICP-MS analysis of monazite, xenotime and apatite. Standards in blue were used for trace element analysis.

ICP-MS			
	Monazite	**Xenotime**	**Apatite**
Brand and model	Agilent 7900x ICP-MS	Agilent 7900x ICP-MS	Agilent 7900x ICP-MS
Forward power (W)	1350 W	1350 W	1350 W
Carrier (He)	0.35 L/min	0.35 L/min	0.35 L/min
Sample (Ar)	0.98 L/min	0.98 L/min	0.98 L/min
Laser			
Type of laser	ArF Excimer	ArF Excimer	ArF Excimer
Brand and model	RESOlution LR (Resonetics)	RESOlution LR (Resonetics)	Resolution LR (Resonetics)

		ICP-MS	
	Monazite	**Xenotime**	**Apatite**
Laser wavelength	193 nm	193 nm	193 nm
Pulse duration	20 ns	20 ns	20 ns
Spot size	13 µm	13 µm	30 µm
Repetition rate	5 Hz	5 Hz	5 Hz
Laser fluence	2.0 J/cm^{-2}	2.0 J/cm^{-2}	3.5 J/cm^{-2}
		Data Acquisition Parameters	
Data acquisition protocol	Time-resolved analysis	Time-resolved analysis	Time-resolved analysis
Scanned masses with dwell times (ms)	^{29}Si (5), ^{31}P (5), ^{43}Ca (5), ^{57}Fe (5), ^{65}Cu (5), ^{89}Y (5), ^{90}Zr (10), ^{139}La (5), ^{140}Ce (5), ^{141}Pr (5), ^{146}Nd (5), ^{147}Sm (5), ^{153}Eu (10), ^{157}Gd (5), ^{159}Tb (10), ^{163}Dy (10), ^{165}Ho (10), ^{166}Er (10), ^{169}Tm (10), ^{172}Yb (10), ^{175}Lu (10), ^{201}Hg (20), ^{204}Pb (20), ^{206}P (30), ^{207}Pb (60), ^{208}Pb (10), ^{232}Th (5), ^{238}U (10).	^{29}Si (5), ^{31}P (5), ^{43}Ca (5), ^{57}Fe (5), ^{65}Cu (5), ^{89}Y (5), ^{90}Zr (10), ^{139}La (5), ^{140}Ce (5), ^{141}Pr (5), ^{146}Nd (5), ^{147}Sm (5), ^{153}Eu (10), ^{157}Gd (5), ^{159}Tb (10), ^{163}Dy (10), ^{165}Ho (10), ^{166}Er (10), ^{169}Tm (10), ^{172}Yb (10), ^{175}Lu (10), ^{201}Hg (20), ^{204}Pb (20), ^{206}P (30), ^{207}Pb (60), ^{208}Pb (10), ^{232}Th (5), ^{238}U (10).	^{29}Si (5), ^{31}P (5), ^{35}Cl (5), ^{43}Ca (5), ^{51}V (10), ^{55}Mn (10), ^{57}Fe (5), ^{65}Cu (5), ^{88}Sr (10), ^{89}Y (10), ^{90}Zr (10), ^{139}La (10), ^{140}Ce (10), ^{141}Pr (10), ^{146}Nd (10), ^{147}Sm (10), ^{153}Eu (10), ^{157}Gd (10), ^{159}Tb (10), ^{163}Dy (10), ^{165}Ho (10), ^{166}Er (10), ^{169}Tm (10), ^{172}Yb (10), ^{175}Lu (10), ^{178}Hf (10), ^{201}Hg (5), ^{204}Pb (10), ^{206}P (100), ^{207}Pb (100), ^{208}Pb (10), ^{232}Th (20), ^{238}U (20).
Detection mode	Pulse counting	Pulse counting	Pulse counting
Background collection (s)	30 s	30 s	30 s
Ablation time (s)	30 s	30 s	30 s
Washout (s)	20 s	20 s	20 s
		Standardisation and Data Reduction	
Primary standards	MAdel, NIST610	MG-1, NIST610	MAD, NIST610
Secondary standards	222, Ambat	BS-1, NIST610_13 µm	401, OD306
Data reduction software	LADR, Excel	LADR, Excel	LADR, Excel

3.6 Data Reduction

Geochronology

LA-ICP-MS data was processed using LADR software (Norris Scientific) (Norris and Danyushevsky, 2018). IsoplotR (Vermeesch, 2018) was used to construct Tera-Wasserburg and Wetherill concordia plots for monazite, apatite and xenotime, and to produce $^{207}Pb/^{206}Pb$ weighted mean age plots for concordant data.

For U-Pb dating using LA-ICP-MS, U-Pb downhole fractionation and instrument drift need to be corrected for, as well as common Pb for apatite. The procedures that were followed for this are summarised in Payne et al. (2008) for monazite, Fletcher et al. (2004) for xenotime and Chew et al., (2014) for apatite. For all mineral analyses in this study, several known standards were distributed at periodic intervals between unknown data to correct for both down-hole elemental fractionation and instrument drift. U-Pb geochronology data for all standards are presented in Appendix B and C. The signals for individual analyses were bracketed during LADR processing due to fine-grained hematite inclusions and/or intergrowths with monazite, xenotime and apatite as evidenced by anomalous Fe concentrations. All minerals commonly had peaks of iron but where these interferences could not be isolated through bracketing, they were further filtered in Excel. Iron contamination was unavoidable even after high resolution imaging and target selection for individual grains. Other analyses with uncharacteristically high silica and low phosphorus concentrations were removed as they were contaminated by the surrounding matrix minerals.

4 OBSERVATIONS AND RESULTS

Petrographic analysis was conducted on a suite of 11 thin sections using optical microscopy and SEM-MLA imaging. Presented here are the key minerals and their textures present in studied samples, with full petrographic descriptions for each sample available in Appendix A. A summary table of the samples analysed is presented in Table 3.

Table 3: Summary table of samples analysed in this study.

Drill hole ID	Sample Depth	Lithology Description	Deposit Zone	Number of Thin Sections
DD12CAR083	743.3-743.4 m	Hematite ore breccia dominated by grey hematite and granite rock fragments, both of which have been overprinted by fine-grained red hematite.	Bornite Zone	3
DD12CAR085	978.5-978.6 m	Complex polymict hematite ore breccia containing abundant rock fragments, colloform hematite and grey hematite.	Bornite Zone	2
CAR031	874 m	Complex granite breccia significantly altered by chlorite with carbonate veining.	Bornite Zone	1
	966 m	Granite Breccia variably altered to chlorite and sericite.	Bornite Zone	1
CAR032	623 m	Hematised siltstone interbedded with sandstone.	Chalcopyrite Zone	1
	1264.4 m	Dolomite with cross cutting bladed hematite veins intergrown with anhydrite.	Chalcopyrite Zone	1
CAR034	508.02 m	Hematite breccia dominantly composed of grey hematite in various habits and polycrystalline quartz.	Barren Zone	1
CAR056	719.6 m	Colloform hematite clast cut by a smaller domain of a fine-grained, massive sericite matrix.	Barren Zone	1

4.1 General Petrographic Observations

The rocks of the Carrapateena deposit have been subjected to a multi-stage history of hydrothermal alteration and brecciation. The majority of the samples investigated in this study consist of complex breccias composed of fragments of Donington granite, grey-hematite (as blade-like crystals and after alteration of magnetite) and earthy hematite as well as a range of gangue minerals including sericite and anhydrite.

A prograde paragenetic sequence is well established for sulphide minerals present in studied thin sections; pyrite is replaced by chalcopyrite and chalcopyrite is replaced by bornite. Bornite is often observed as discrete grains and in veins, in addition to partially replacing (rimming) chalcopyrite and less commonly, pyrite. Chalcocite and covellite are retrograde alteration products of bornite and are focused along micro-fractures and at bornite grain boundaries (Figure 4a, b).

Earthy hematite is present as a cryptocrystalline breccia matrix component and as alteration of remnant clasts. Earthy hematite is most abundant in thin sections from the bornite zone. Grey hematite exhibits a range of textures but is commonly present as either coarse, crystalline clasts or as fine-grained blades infilling between clasts (Figure 4b). Colloform hematite (after magnetite) clasts are present in samples from the bornite and barren zones. This hematite forms feather-textured ‘branches’ that are sometimes intergrown with pyrite and chalcopyrite (Figure 4c). The petrology of REE bearing minerals is described in section 4.3.

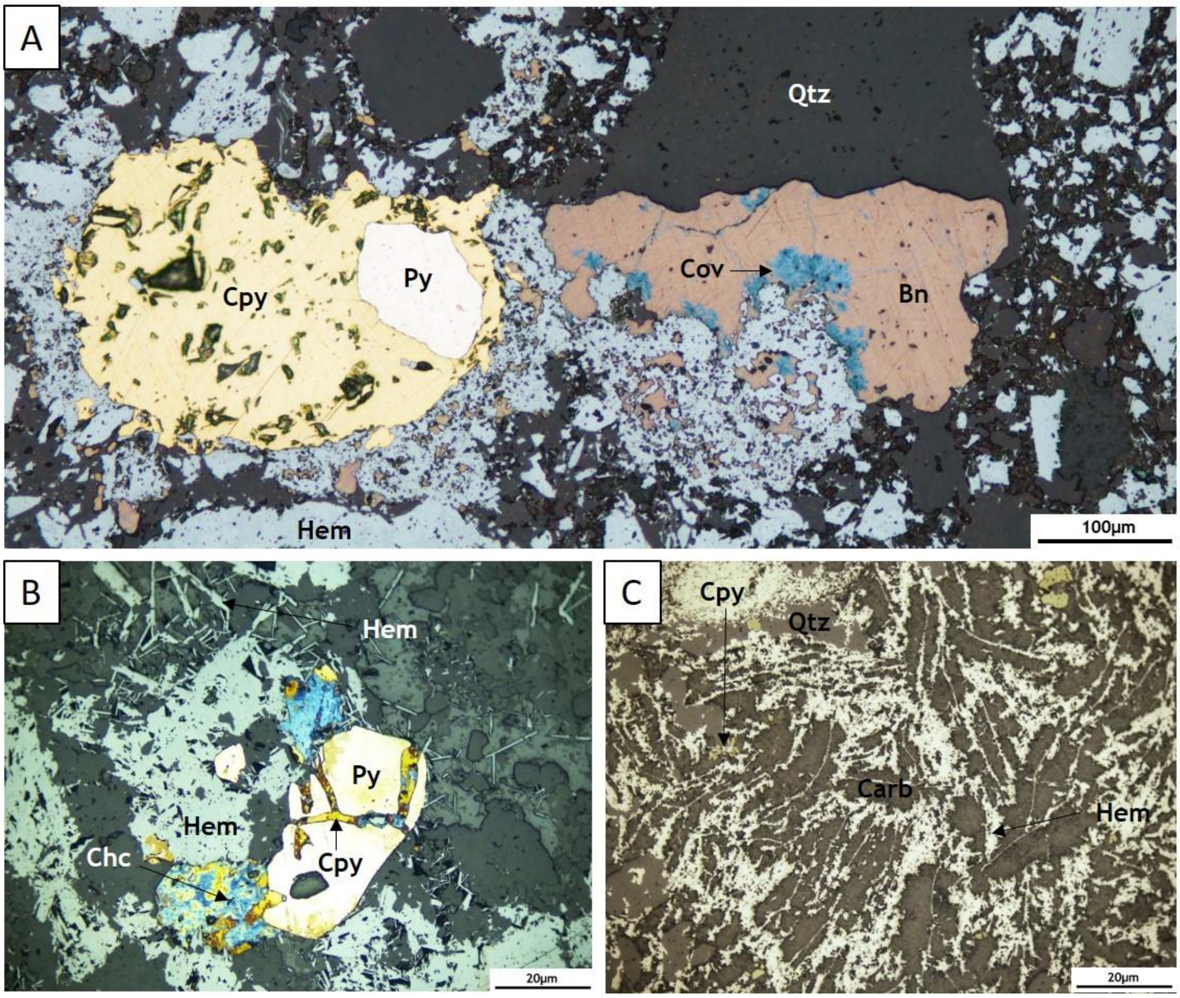

Figure 4: A) Photomicrograph of sulphide minerals showing pyrite being replaced by chalcopyrite and covellite (deep blue) replacing bornite along microfractures and bornite grain boundaries. Grey hematite pre-dates sulphide mineral infill. Image of sample DD12CAR083-743 m. B) Photomicrograph of two typical textures of hematite: clasts and blades. Note chalcopyrite veins being partially replaced by bornite (brown), which has subsequently been altered to chalcocite (pale blue). From sample DD12CAR083-743 m. C) Photomicrograph of a colloform hematite clast in which hematite forms feathered branches with chalcopyrite in a matrix of quartz and carbonate. From sample CAR032-1264.4 m.

Abbreviations: Cpy: chalcopyrite, Py: pyrite, Bn: bornite, Cov: covellite, Qtz: quartz, Hem: hematite, Chc: chalcocite, Carb: carbonate.

4.2 Maia Mapping – REE and Cu Relationship

MAIA mapping of samples DD12CAR083 – 743 m and DD12CAR085 – 978 m show that cerium (Ce) and yttrium (Y) are concentrated in rock fragments that are dominantly composed of quartz and overprinted by earthy hematite. Due to the textural complexity of the breccia, it is difficult to identify REE hosts in sample DD12CAR085 – 978 m. Y is noticeably less abundant than Ce in both samples (Figure 5 and Figure 6). Ce is present in lower concentrations throughout the matrix in sample DD12CAR083 – 743 m similarly to Cu. Additionally, Cu forms veins that cross-cut rock fragments, indicating that Cu mineralisation may be multi-generational, with at least one generation being paragenetically later than REE mineralisation. No spatial relationship between Cu and Ce and/or Y is observed.

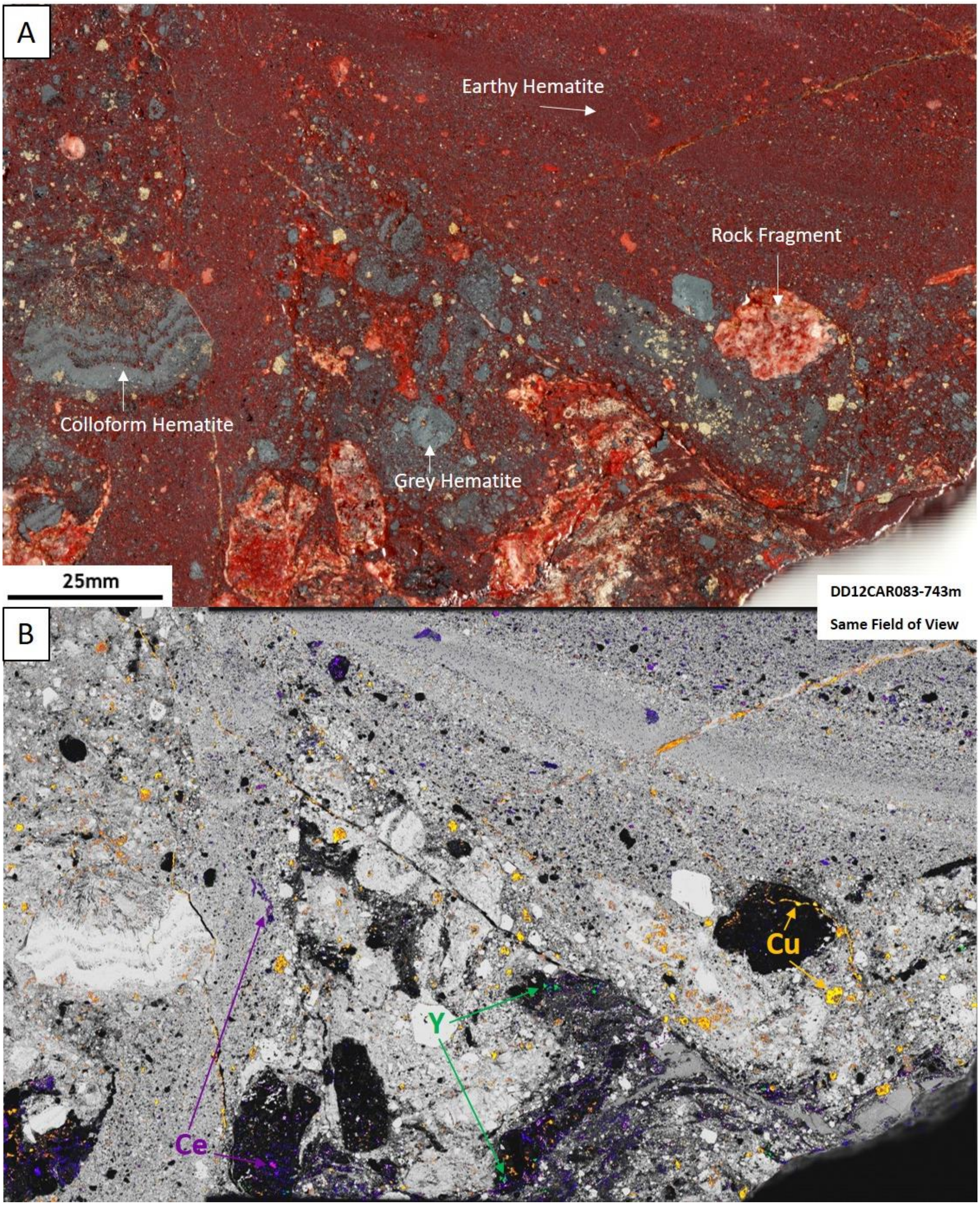

Figure 5: A) Reference core sample image that was scanned using the Maia Mapper. B) Maia map showing element hotspots overlaid on a grey-scale Fe map. Only Cu (yellow) and the two available REE: Ce (LREE proxy) (purple) and Y (HREE proxy) (green) are shown.

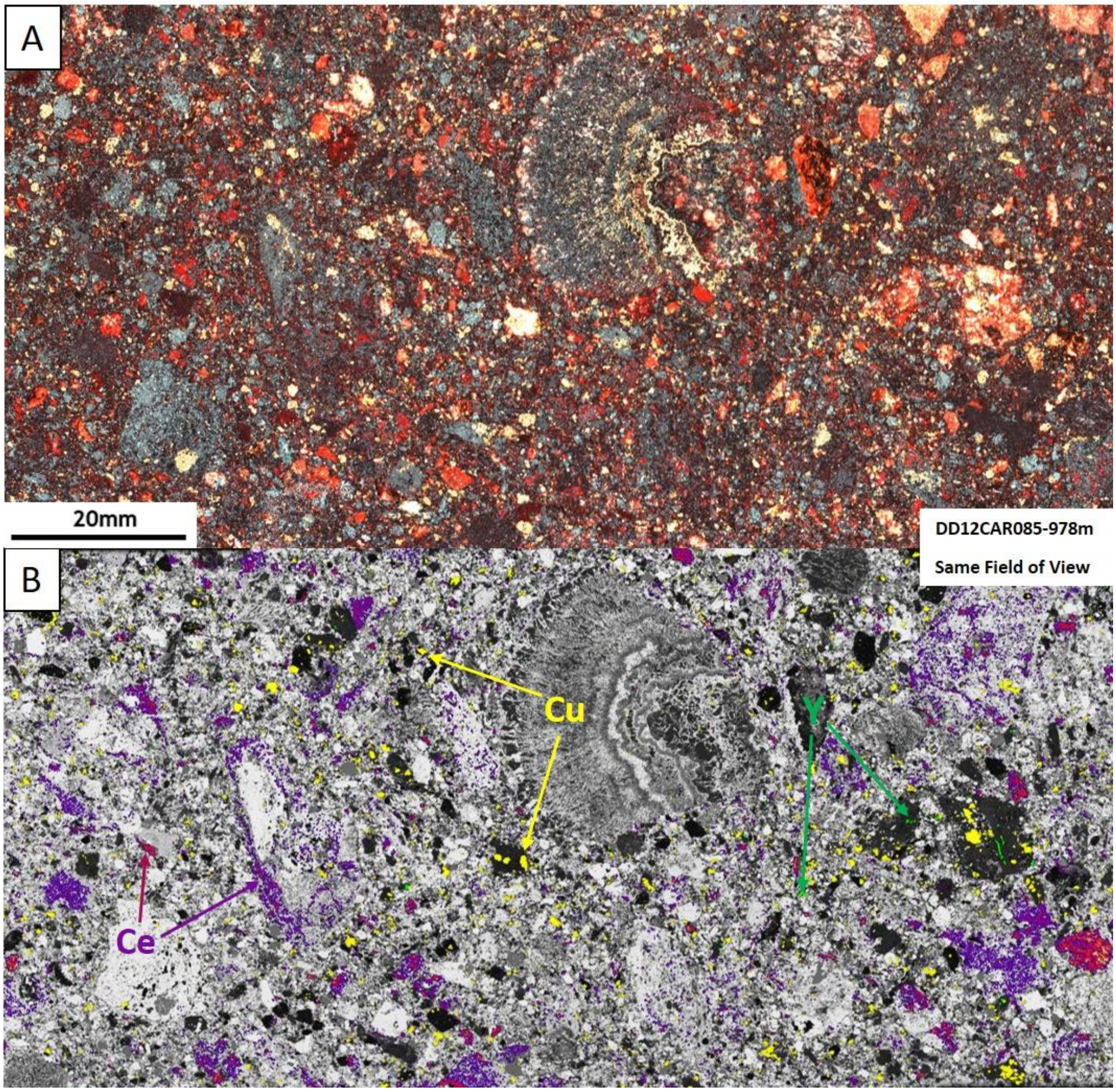

Figure 6: A) Reference core sample image that was scanned using the Maia Mapper. B) Maia map showing element hotspots overlaid on a grey-scale Fe map. Only Cu (yellow) and the two available REE: Ce (LREE proxy) (purple) and Y (HREE proxy) (green) are shown.

4.3 Monazite Petrology and Mineral Liberation Analysis

Monazite in samples from the bornite zone range in size from ~10–15 μm, and are present as scattered anhedral crystals with irregular morphology predominantly infilling around bladed grey hematite crystals (Figure 7a). In sample CAR031-874 m, monazite is unusually abundant and forms continuous clusters/micro-veins (Figure 7b). There are several subhedral apatite crystals in sample DD12CAR085-978 m from the bornite zone with reaction rims of monazite (Figure 7c), indicating that, in the limited number of samples analysed, monazite may be forming from the breakdown of apatite and therefore is paragenetically later than the apatite (see section 4.8). In the chalcopyrite zone, monazite occurs as coarser individual anhedral crystals up to 100 μm in diameter and was most commonly observed in carbonate and lesser so in quartz. Monazites in the barren zone form aggregates of variable size (up to 250 μm) hosted in grey hematite and quartz.

Additionally, florencite (another LREE-phosphate mineral) is intergrown with monazite in sample CAR056-719.6m from the barren zone only. The habit and texture of florencite is identical to monazite. However, due to its extremely low abundance, the mineral was not investigated further.

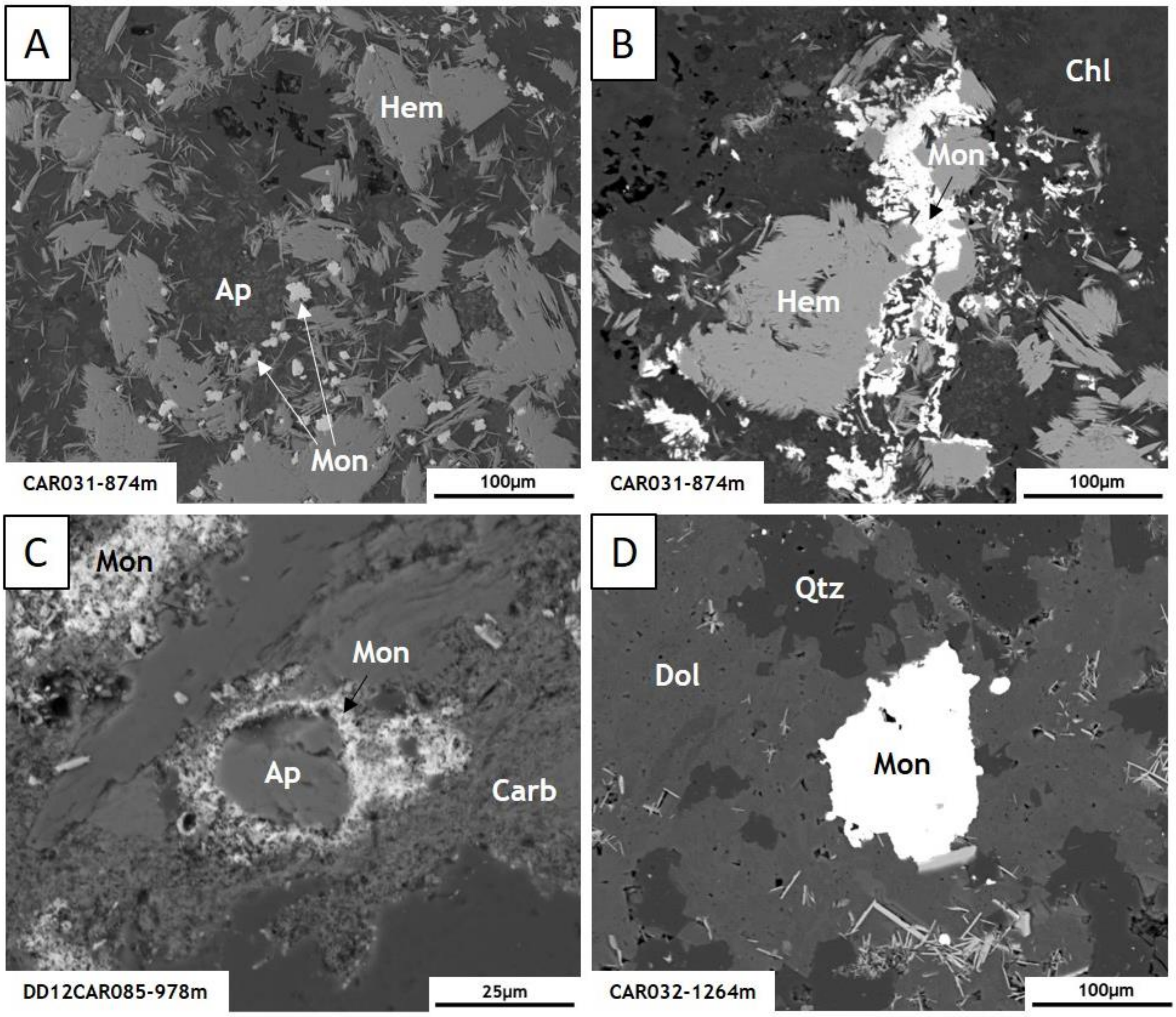

Figure 7: EBS images showing representative textures of monazite. A) Scattered anhedral monazite infilling around bladed grey hematite from the bornite zone. B) Micro-vein of monazite in grain contact with grey hematite in chlorite altered matrix from the bornite zone. C) Reaction rim of monazite around an apatite crystal from the bornite zone. D) Typical anhedral monazite crystal in samples from the chalcopyrite zone.

Abbreviations: Ap: apatite, Hem: hematite, Mon: monazite, Dol: dolomite, Chl: chlorite, Carb: carbonate, Qtz: quartz.

4.4 Xenotime Petrology and Mineral Liberation Analysis

Xenotime is less abundant than monazite in samples from all three zones and is often finer grained than monazite. In the bornite zone, xenotime is present as isolated grains with subhedral-euhedral (often prismatic) morphology (Figure 8a), and commonly occurs in carbonate fragments. The crystal habit of xenotime from the chalcopyrite zone is the same as described for xenotime from the bornite zone, and the main host minerals are polycrystalline quartz and dolomite (Figure 8b). In samples from the barren zone, rare clusters of xenotime up to 100 μm in length occur in addition to small isolated grains. Xenotime occurs in polycrystalline quartz and is commonly in contact with grey hematite in barren zone samples.

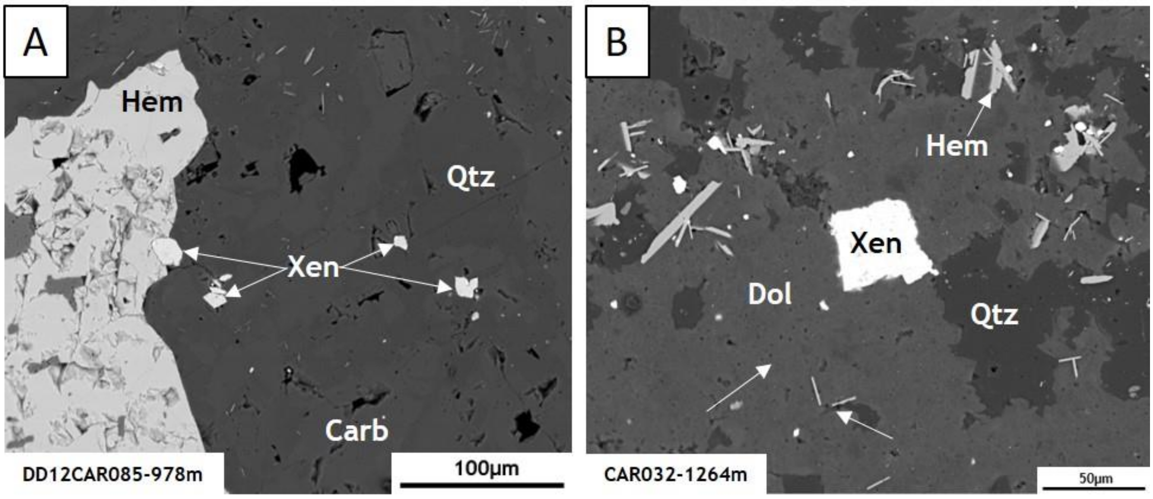

Figure 8: EBS images showing representative textures of xenotime. A) Four euhedral to subhedral crystals of xenotime in a sample from the bornite zone. B) Typical subhedral xenotime crystal present in all zones of the deposit. In this sample from the chalcopyrite zone, xenotime is hosted in dolomite and quartz.

Abbreviations: Xen: xenotime, Mon: monazite, Dol: dolomite, Hem: hematite, Qtz: quartz, Carb: carbonate.

4.5 Apatite Petrology and Mineral Liberation Analysis

In the bornite zone, apatite occurs as both individual subhedral crystals (up to ~125 μm) (Figure 9a and b), and as fine-grained crystals forming veins (Figure 9c and d). Bornite zone subhedral apatite is hosted in hematite, carbonate, sericite and quartz and in some instances has been partially replaced by monazite (Figure 7c above). In contrast, the apatite veins are commonly associated with sericite and are intergrown with monazite (Figure 7a, and Figure 8d). In the chalcopyrite zone, apatite is less abundant and ranges in size and shape from 15–25 μm anhedral grains to 50 μm subhedral crystals. Apatite in this zone is most commonly hosted in polycrystalline quartz and scapolite. Apatite in the barren zone is observed as 25–50 µm, euhedral (hexagonal), prismatic crystals and only occurs in veins of sericitic alteration, which also contain minor disseminated (secondary) covellite (Figure 9a).

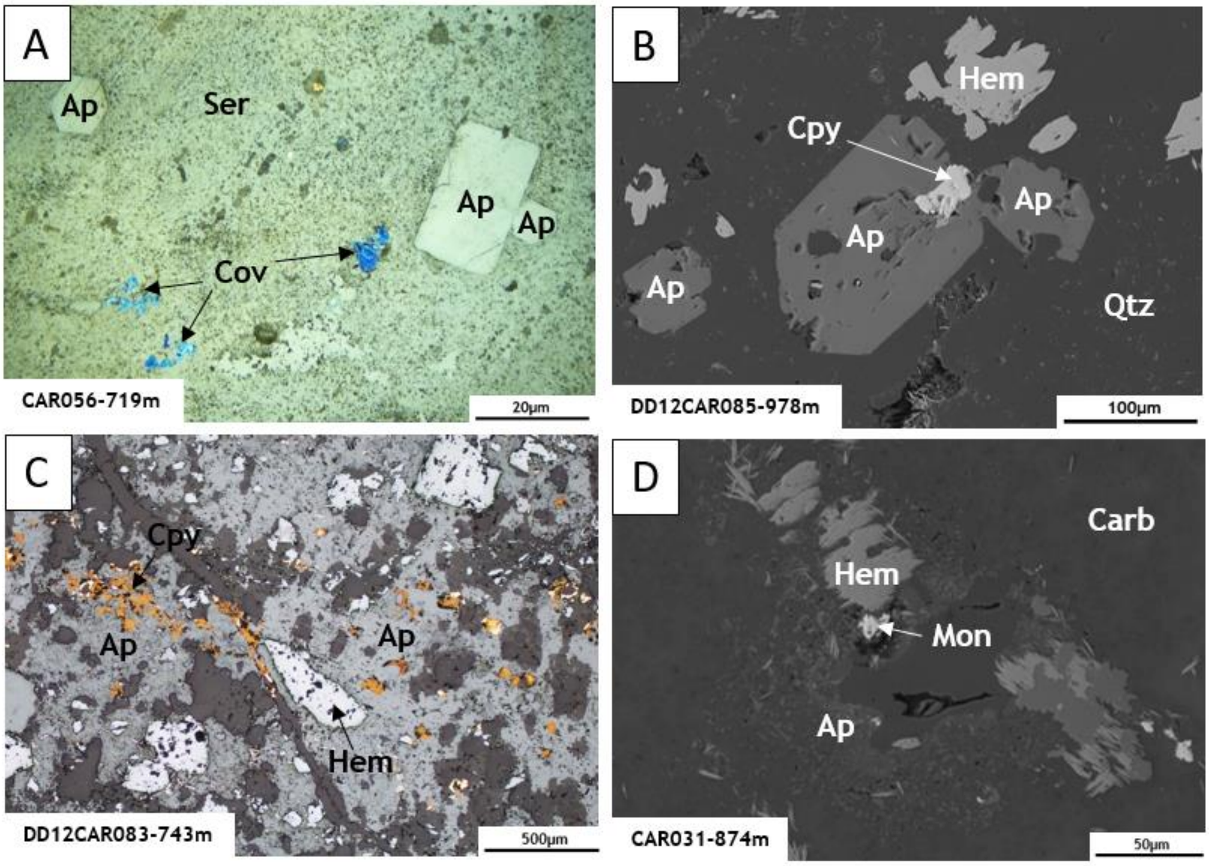

Figure 9: A) Photomicrograph of euhedral apatite crystals in sericite from the barren zone. B) EBS image of subhedral apatite crystals from the bornite zone with infill of chalcopyrite. C) Photomicrograph of veined fine-grained apatite from the bornite zone. Note overprint by chalcopyrite. D) EBS image showing very fine-grained apatite which are intergrown with monazite from the bornite zone.

Abbreviations: Ap: apatite, Cpy: chalcopyrite, Hem: hematite, Cov: covellite, Ser: sericite, Mon: monazite, Carb: carbonate, Qtz: quartz.

4.6 Relationship between Cu-Sulphides and REE-Bearing Minerals

Monazite occurs as inclusions within chalcopyrite and inclusions of chalcopyrite occur in monazite (Figure 10a and b). Bornite and monazite have not been seen together in the limited number of samples used in this study. However, bornite and monazite display similar textural overgrowth relationships with matrix minerals including grey hematite (Figure 10b and f). Xenotime is included in pyrite and chalcopyrite in addition to a subhedral crystal of apatite (Figure 10c and d). Similarly, there are abundant inclusions of subhedral apatite within pyrite and chalcopyrite (Figure 10e). However, fine-grained apatite also occurs as inclusions within bornite (Figure 10f), and is intergrown with monazite micro-veins (Figure 7a), which provides textural evidence for at least two generations of apatite.

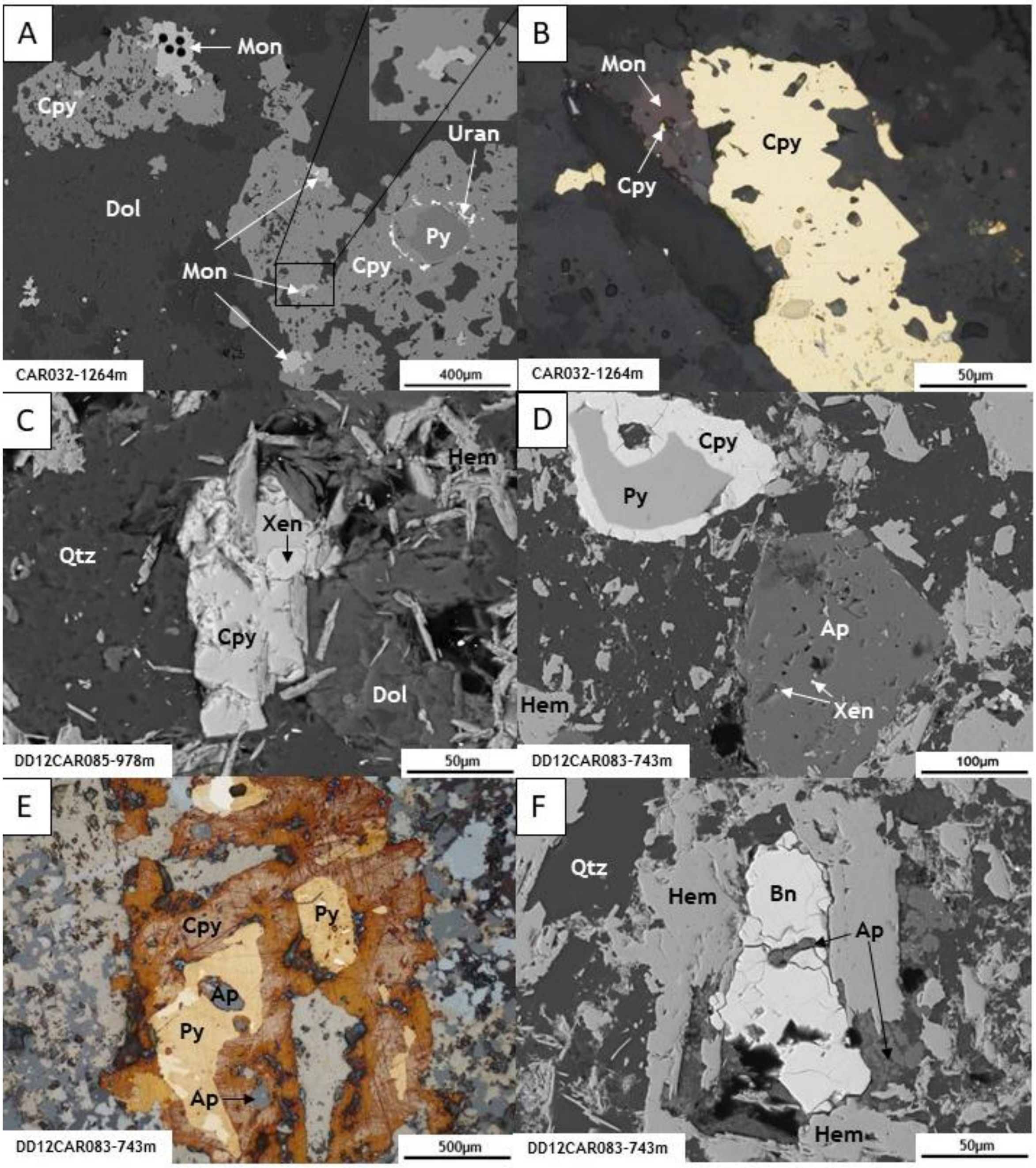

Figure 10: Images displaying textural relationships between REE-minerals and Cu-sulphides. A) BSE image of multiple inclusions of monazite in chalcopyrite in a matrix of dolomite. Circular features in the upper monazite are laser ablation spots. B) Photomicrograph showing an inclusion of chalcopyrite in monazite that is in grain contact with chalcopyrite. C) EBS image of an inclusion of xenotime in chalcopyrite. D) EBS image of xenotime inclusions in apatite. E) Photomicrograph of inclusions of apatite within pyrite and chalcopyrite. Note pyrite being replaced by chalcopyrite. Orange colour of chalcopyrite is from oxidation of thin section. F) Inclusion of fine-grained, anhedral apatite in bornite.

Abbreviations: Ap: apatite, Mon: monazite, Xen: xenotime, Cpy: chalcopyrite, Bn: bornite, Py: pyrite, Hem: hematite, Qtz: quartz, Dol: dolomite, Uran: uraninite.

4.7 Paragenesis

Petrographic observations regarding the paragenetic timing between ore and gangue minerals are consistent with those described by previous workers (Sawyer, 2014; Taylor, 2014; Williams, 2012), and a modified paragenetic evolution is presented in Figure 11 based on samples included in this study.

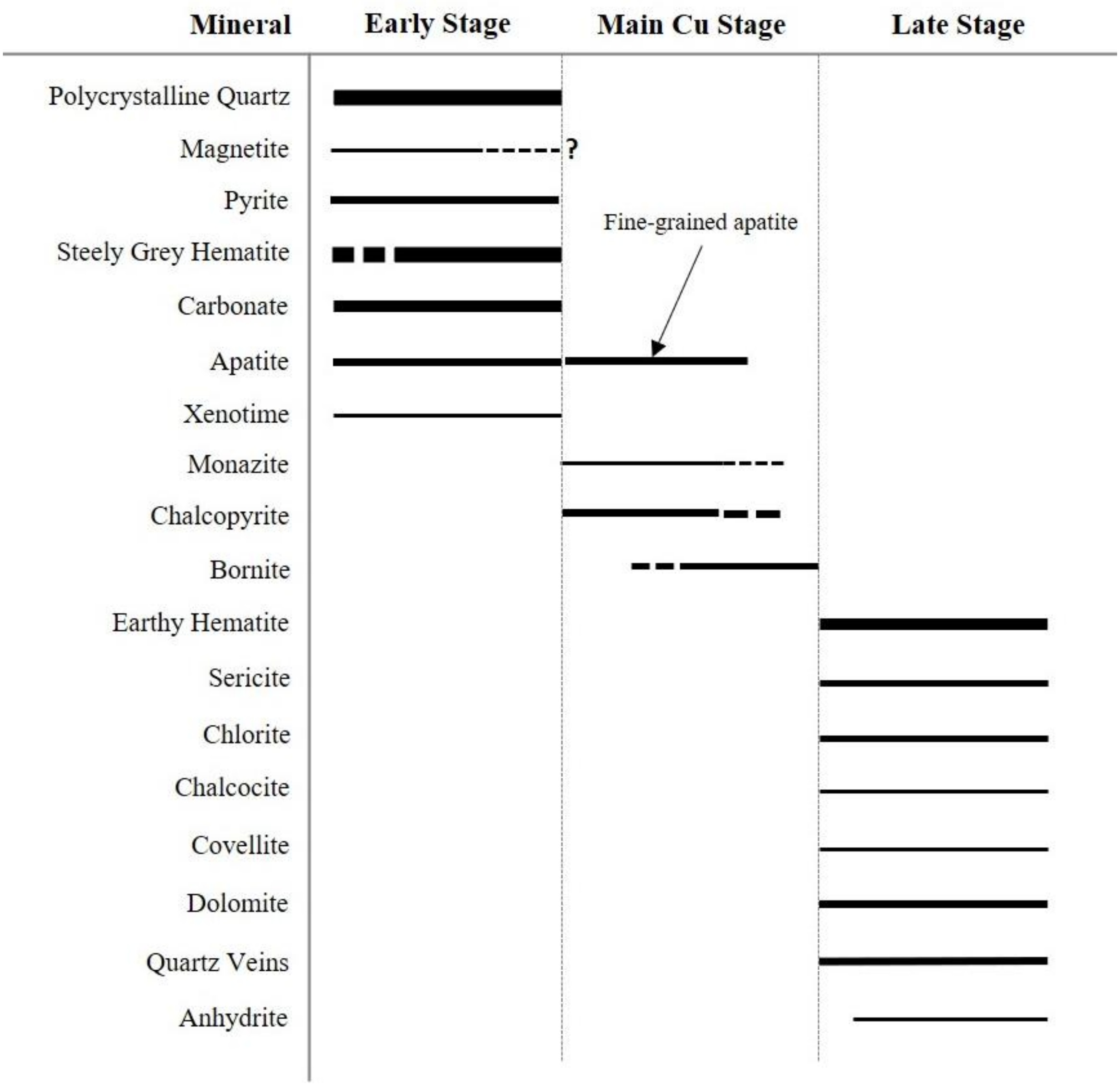

Figure 11: Summary paragenesis of minerals present in studied samples. Note the co-genetic relationship between monazite, fine-grained apatite and Cu-sulphides. Coarser-grained apatite and all xenotime are interpreted to pre-date Cu-sulphide mineralisation. Minor minerals are not included.

4.8 Monazite Geochronology

A total of 225 analyses were acquired in-situ from six different samples for monazite U-Pb geochronology. Monazite is rare in the analysed samples, with grains commonly 10 – 15 μm in diameter. Because of significant contamination, reflected by anomalous Fe and Si and/or common Pb, 132 analyses were removed from age determination considerations. Furthermore, for monazite analyses from the barren zone, only analyses with 30% or less error were used to constrain some level of precision for the common Pb composition. This excluded a further 28 analyses from age calculations. Concordia diagrams produced from the culled dataset for each of the three zones are presented in Figure 12. U-Pb geochronology data for individual analyses are presented in Appendix D.

For samples from the bornite zone (n=38), monazite grains show evidence of having experienced both common Pb loss and modern lead loss (which tracks parallel to the X axis in Tera Wasserburg space) (Figure 12a). The intercept of the line between common Pb and radiogenic Pb (red dashed line in Figure 12a) with the concordia yields an approximate age of ca. 1400 Ma.

Monazites in sample CAR032-1264.4 m from the chalcopyrite zone produced a ^{207}Pb corrected ^{206}Pb/^{238}U weighted mean age of 1427.09 ± 8.48 Ma (MSWD = 4.26) (Figure 12b). There is a single concordant analysis at ca. 1750 Ma.

For monazite analyses from sample CAR034-508.02 from the barren zone, no meaningful age could be produced due to variable modern Pb loss, high concentrations of common Pb and low concentrations of U. As such, an age of ~1400 Ma was approximated from the intercept of the line between common Pb and radiogenic Pb (red dashed line in Figure 12c) with the concordia.

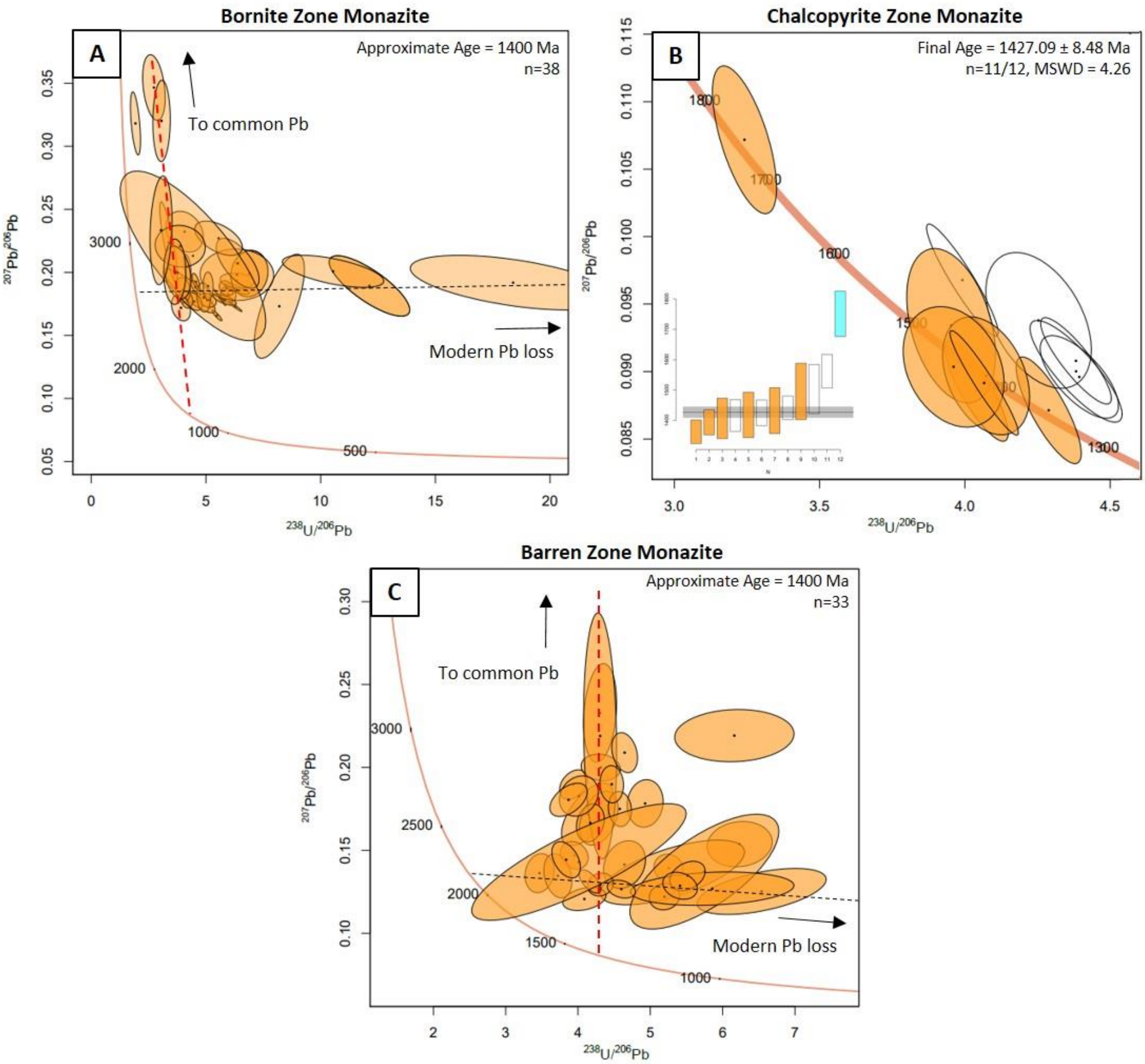

Figure 12: Annotated Tera Wasserburg concordia diagrams of in situ monazite U-Pb analyses. Uncoloured ellipses were not used to calculate weighted mean or intercept ages. n= sample population. All ellipses are presented with 2σ errors on both axes.

4.9 Xenotime Geochronology

A total of 111 individual analyses were acquired in situ from six different samples for xenotime U-Pb geochronology. Xenotime is rare in the analysed samples, with grains dominantly 10 – 15 µm in diameter. Because of significant contamination of analyses reflected by anomalous Fe and Si, 56 were removed. As a result, only 12 individual xenotime grains were present in samples from the bornite zone, and after compositional filtering, three remained. Therefore, no meaningful age could be acquired. For xenotime analyses from the barren zone, a 30% error threshold was applied to the U-Pb data to constrain some level of precision for the common Pb composition. This excluded a further three analyses from age calculations. Concordia diagrams produced from the processed dataset for the chalcopyrite and barren zones are presented in Figure 13. U-Pb geochronology data for individual analyses are presented in Appendix E.

Xenotime in sample CAR032-1264.4 m from the chalcopyrite zone produced a $^{207}Pb/^{206}Pb$ weighted mean age of 1489.99 ± 9.26 Ma (MSWD = 30.4) (Figure 13a). This age has extremely low precision due to the small sample population (n=7) after removing 28 analyses that failed compositional criteria. There is Pb loss at ca. 1100 Ma and a single concordant analysis at ca. 1590 Ma. The very high MSWD indicates there is substantial scatter in the data, and the estimate of ca. 1490 Ma should not be regarded as a definite age.

For xenotime in samples from the barren zone, a Wetherill concordia plot was produced with a fixed lower intercept to 0 Ma since they appeared to have undergone substantial modern Pb loss (Figure 13b). The xenotime analyses form a discordant linear array that intercepts the concordia at 1469.93 ± 7.8 Ma (MSWD = 2.5). This age has relatively high precision due to a large sample population (n= 45). There is a single concordant analysis at 1590 Ma not included in regression.

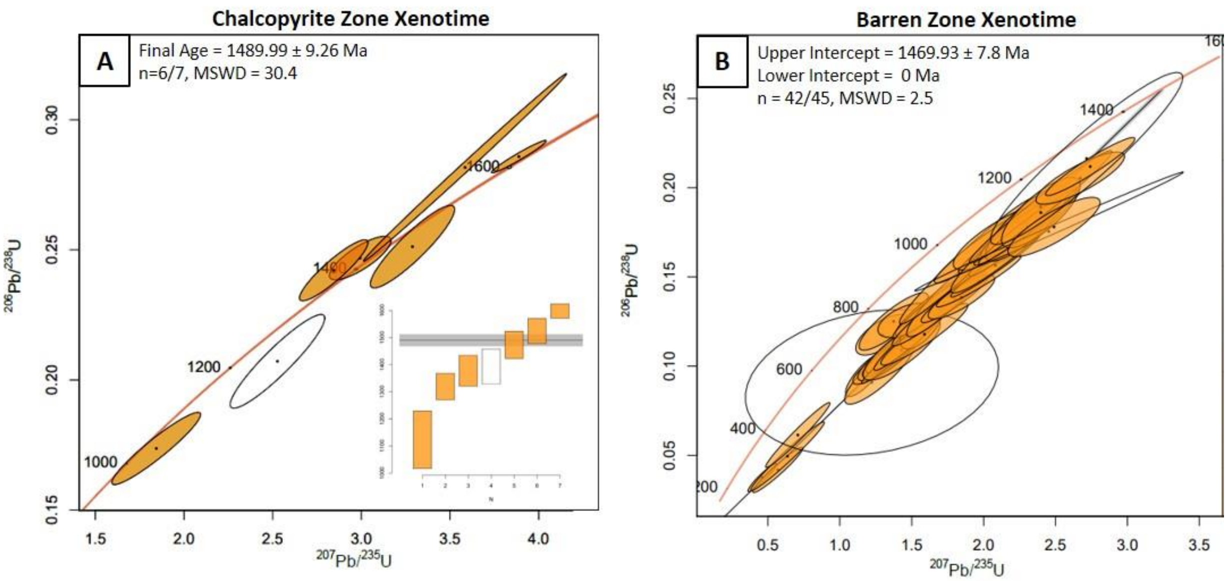

Figure 13: Annotated Wetherill concordia diagrams of in situ xenotime U-Pb analyses. Uncoloured ellipses were not used to calculate weighted mean or intercept ages. n= sample population. All ellipses are presented with 2σ errors on both axes.

4.10 Apatite Geochronology

A total of 560 individual analyses were acquired in situ from six different samples for apatite U-Pb geochronology. Apatite is the most abundant of the REE-bearing minerals across all samples, with grains ranging from 15 – 125 μm in diameter. Due to failing compositional criteria for apatite (including anomalous Fe concentrations), 128 analyses were removed. For apatite analyses from the chalcopyrite and barren zones, a 30% error threshold was applied to the U-Pb data to constrain some level of precision for the common Pb composition. This excluded a further 84 analyses from age calculations. Concordia diagrams produced from the reduced dataset are presented in Figure 14. U-Pb geochronology data for individual analyses are presented in Appendix F.

For samples from the bornite zone, apatite analyses form a discord that yields an approximate age of 1331.5 ± 8.84 Ma (MSWD=19, $^{207}Pb/^{206}Pb_o$ = 0.7788 ± 0.0160). The data appear to have undergone Pb loss that tracks in the direction of the dashed black arrows on Figure 14a. Of all plots produced, this has the largest sample population (n=205).

Apatite in samples from the chalcopyrite zone produce a discord which intercepts the concordia at approximately 1651.8 ± 53.3 Ma ($^{207}Pb/^{206}Pb_o$ = 0.676 ± 0.086) (Figure 14b). Fifty-nine of the 81 analyses were used to calculate this age since they had less than 30% error on U/Pb ratios, however, this threshold is still high, reducing the precision of the obtained age.

For samples from the barren zone, regardless of the applied 30% error threshold, the 79 analyses (out of 140) formed an imprecise discord age of approximately 587.2 ± 28.1 Ma (MSWD = 2.4). The data suggests that apatite may have experienced either growth or loss of Pb during the Neoproterozoic. The solid black line in Figure 14c highlights the deviation from the expected common Pb trend that tracks from 4.5 Ga to 1.6 Ga.

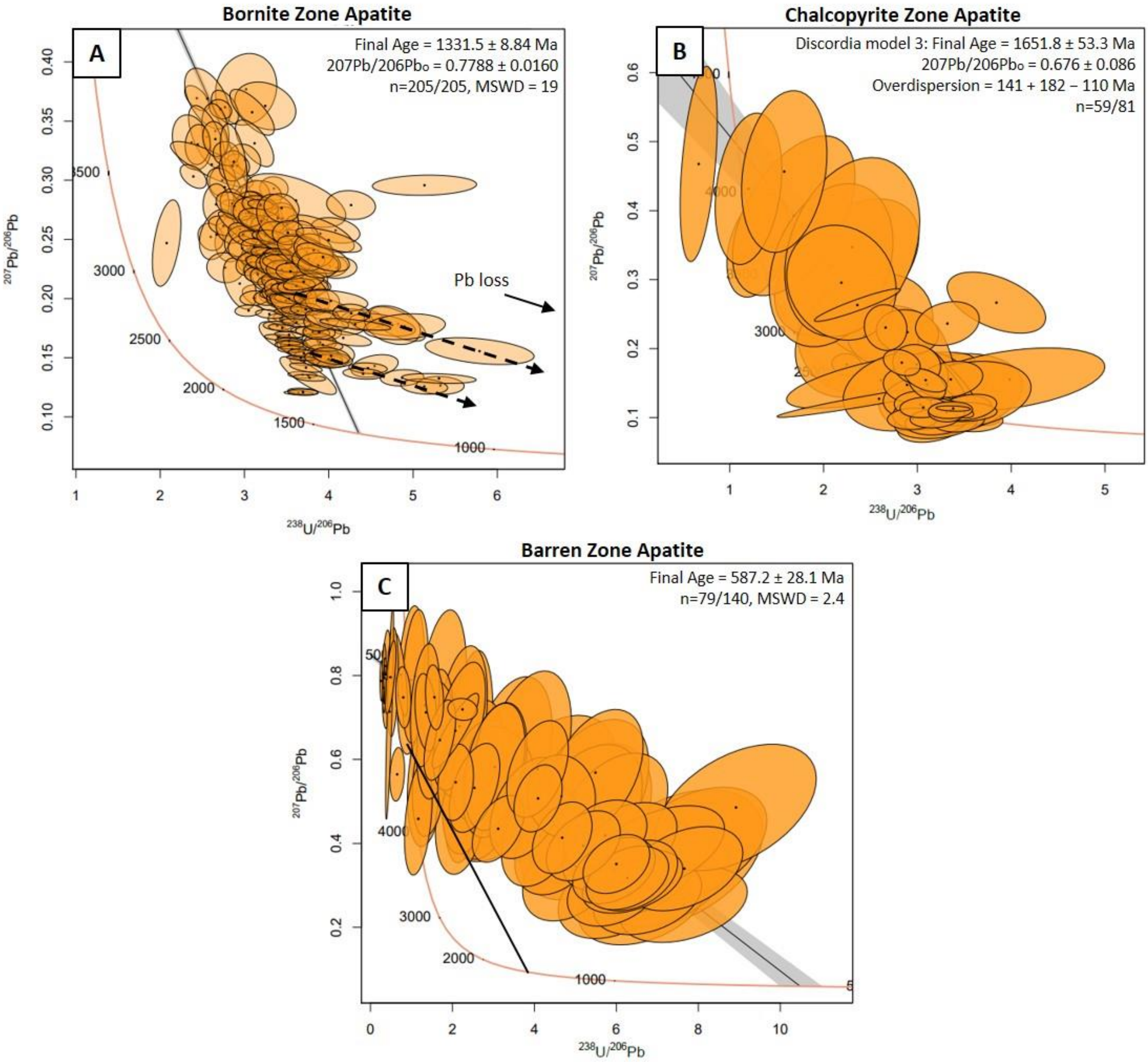

Figure 14: Annotated Tera Wasserburg concordia diagrams of in situ apatite U-Pb analyses. Uncoloured ellipses were not used to calculate weighted mean or intercept ages. n= sample population. All ellipses are presented with 2σ errors on both axes. The black solid line in (C) highlights the deviation from the expected common Pb trend that tracks from 4.5 Ga to 1.6 Ga.

4.11 LA-ICP-MS Monazite Trace Element Chemistry

For the investigation of REE compositional variation between minerals and samples, Y has been positioned between Dy and Ho on chondrite-normalised fractionation trends as in other studies (e.g. Bau, 1996). The chondrite normalised values are sourced from Sun and McDonough (1989). In this study, LREE refers to the elements La, Ce, Pr and Nd, MREE refers to Sm, Eu, Gd, and HREE refers to Tb, Dy, Y, Ho, Er, Yb and Lu. The La/Nd ratio represents the slope of the line between the LREE. For monazite, a major sink for LREE, variations in this ratio reflect either difference in fluid composition from which the monazite grew or the presence of a competing mineral phase for the LREE (Ferrero et al., 2019). The Gd/Y ratio represents the slope of the line between the MREE and HREE, quantifying the degree of HREE partitioning into each mineral. A negative Eu anomaly (i.e. an Eu deficiency) is conceivably inherited from the host rock and implies coeval crystallisation with feldspars (Holder et al., 2020; Schaltegger et al., 1999; Weill & Drake., 1973).

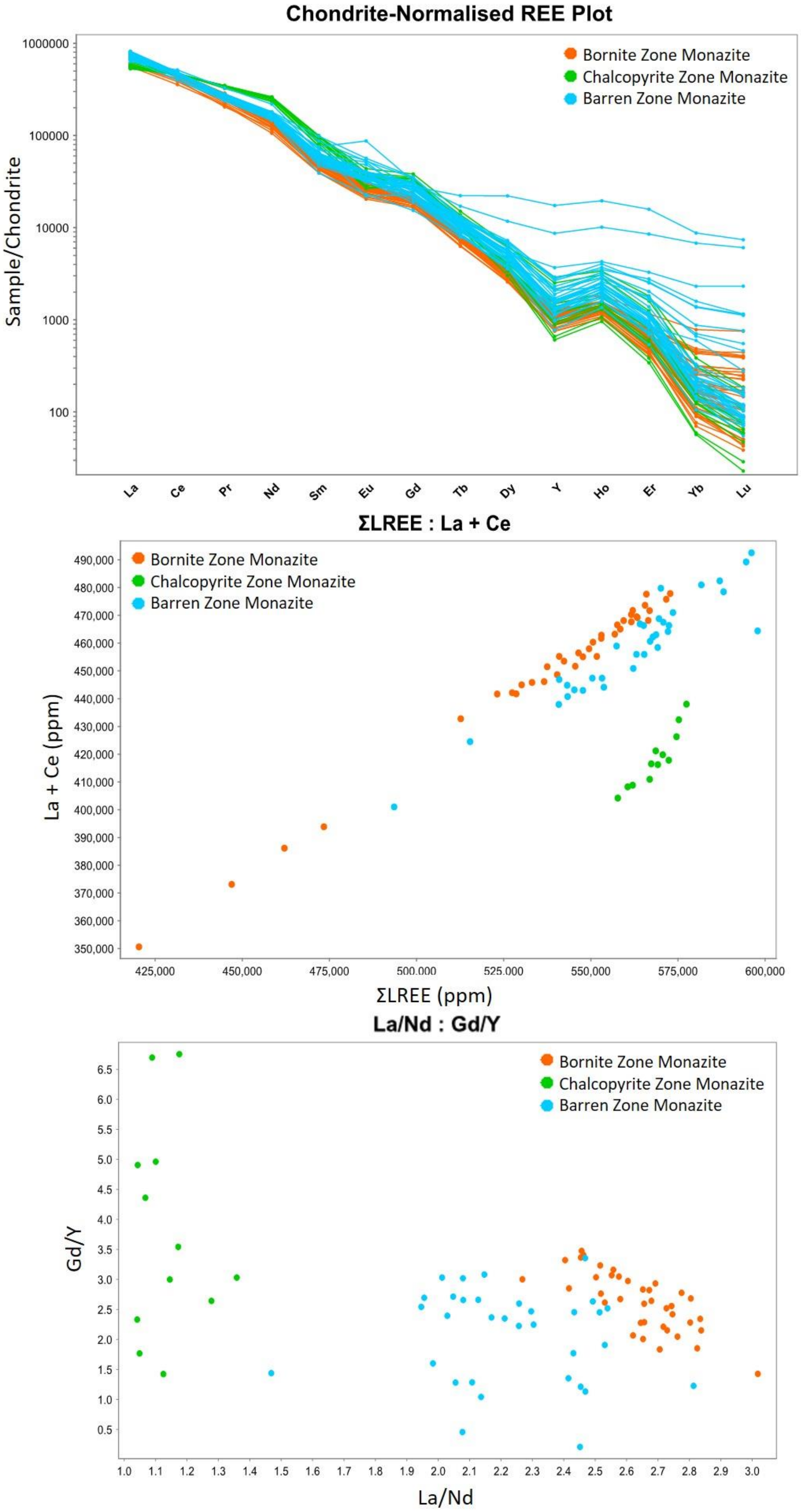

Figure 15: Trace element plots for monazite from three different zones within the Carrapateena deposit. Top: Chondrite-normalized REE signatures of monazite. Middle: Sum of LREE against La + Ca (all units in ppm), which discriminates three populations of monazite and highlights LREE enrichment in monazite from the barren zone. Bottom: La/Nd vs Gd/Y plot showing the relative degree of LREE, MREE and HREE partitioning into monazite.

The chondrite-normalised rare earth element fractionation patterns of monazite from all zones display a strong relative enrichment in LREE with a negative slope towards the HREE (Figure 15, top). A negative Y anomaly exists for monazite in all zones, however, a small negative Eu anomaly is only seen in monazite from the chalcopyrite zone. Monazite from the bornite zone contains slightly lower concentrations of all REE, with chalcopyrite zone monazite having the highest concentrations of Pr – Tb. There is a large spread of Yb and Lu concentrations in monazite from all zones, particularly from the barren and bornite zones.

The LREE trends are seen more clearly Figure 15 (middle) where monazite from the barren zone contains the highest concentrations of La + Ce and ΣLREE. Monazite from the chalcopyrite zone, although containing similar ΣLREE concentrations, contains lower La + Ce.

Monazite from all zones of the deposit are easily distinguished based on La/Nd and Gd/Y ratios (Figure 15, bottom). The La/Nd ratio is highest in monazite from the bornite zone, followed by monazite from the barren zone. Monazite from the chalcopyrite zone exhibits the highest Gd/Y values (>6.5), while monazite from the bornite and barren zones has a maximum Gd/Y value of ~3.5. The trace element concentrations for individual monazite analyses can be found in Appendix G.

4.12 LA-ICP-MS Xenotime Trace Element Chemistry

Chondrite-normalised fractionation trends for xenotime in all zones of the deposit show a smooth increase across the LREE-MREE with a high, plateaued HREE segment (Tb-Lu). Xenotime analyses from the barren zone display positive excursions from the LREE trend and contain the highest concentrations of HREE (Figure 16, top).

Xenotime from the chalcopyrite zone is more enriched in the LREE and MREE than xenotime from the bornite and barren zones. Xenotime from the barren zone displays a negative linear trend between Eu and HREE+Y/MREE (Figure 16, middle). Xenotime from the chalcopyrite zone generally contains higher concentrations of Eu and exhibits the highest Gd/Y ratio (~0.112) and generally the smallest La/Nd ratios along with bornite zone xenotime (Figure 16, bottom). However, the lack of analyses from the ore zones makes it difficult to definitively delineate differences. The trace element concentrations for individual xenotime analyses can be found in Appendix H.

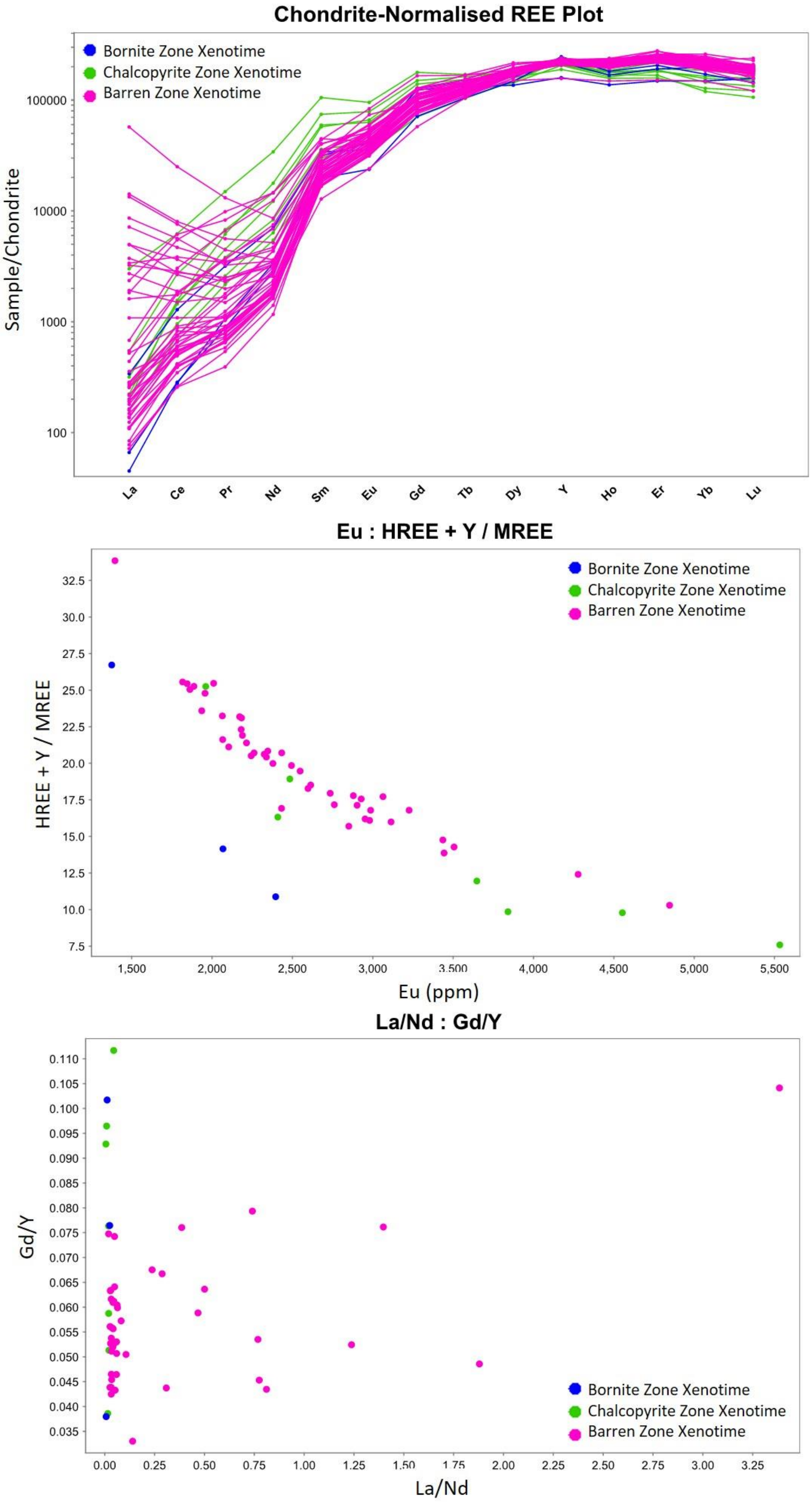

Figure 16: Trace element plots for xenotime from the three different zones within the Carrapateena deposit. Top: Chondrite-normalized REE signatures of xenotime. Middle: Eu vs HREE+Y/MREE plot discriminating three populations of xenotime. Bottom: La/Nd vs Gd/Y plot showing the relative degree of LREE, MREE and HREE partitioning into xenotime.

4.13 LA-ICP-MS Apatite Trace Element Chemistry

The chondrite-normalised REE fractionation trends for apatite differ for each zone of the deposit. Apatite from the barren zone displays a MREE-enriched and LREE- and HREE-depleted pattern, with a significant negative Y anomaly. Apatite from the bornite and chalcopyrite zones exhibits a relatively flat trend across all REE, and apatite from the chalcopyrite zone is the most enriched in LREE with La being enriched 10 times chondrite (Figure 17, top). This relative enrichment is highlighted in Figure 17 (middle), which gives absolute concentrations of La in ppm.

Barren zone apatite displays some positive excursions in LREE and no Eu anomaly is observed. Apatite from the chalcopyrite zone has a pronounced negative Eu anomaly, whereas only some analyses from the bornite zone display this pattern. The three populations of apatite are clearly defined in Figure 17 (bottom) with the high Gd/Lu ratios for apatite from the barren zone reflecting enrichment in MREE. The trace element concentrations for individual apatite analyses can be found in Appendix I.

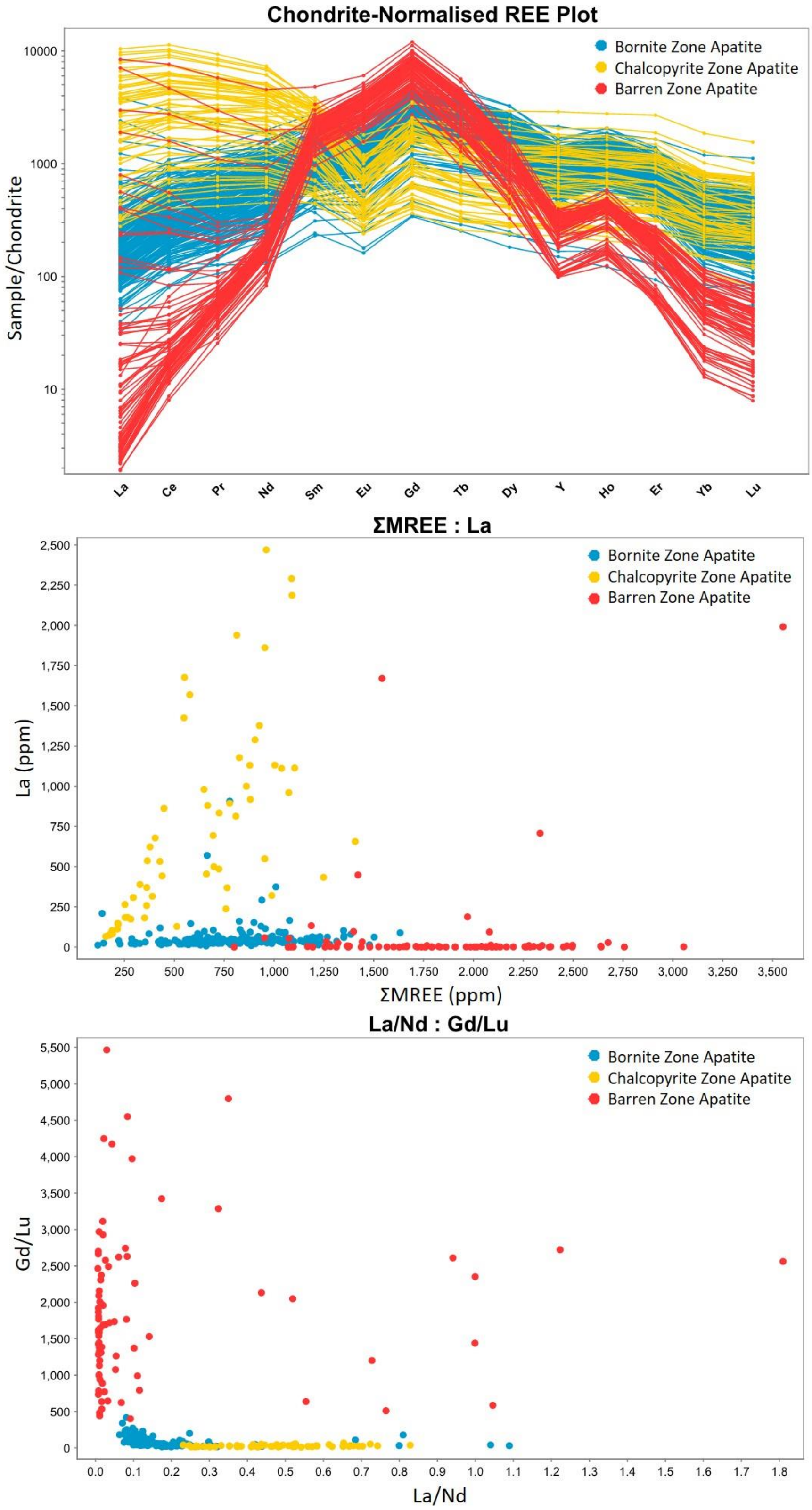

Figure 17: Trace element plots for apatite from the three different zones within the Carrapateena deposit. Top: Chondrite-normalized REE signatures of apatite. Middle: Sum of MREE against La (all units in ppm), which discriminates three populations of apatite and highlights La enrichment in apatite from the chalcopyrite zone. Bottom: La/Nd vs Gd/Y plot showing the relative degree of LREE, MREE and HREE partitioning into apatite.

5 DISCUSSION

To begin to explore the relationship between Cu and REE, the primary aims of this study are to investigate the textural relationships between Cu-sulphides and REE-bearing minerals, perform U-Pb geochronology of the REE-bearing minerals and characterise their geochemistry in each zone of the deposit.

5.1 Textural Relationships and Relative Timing of REE Minerals and Cu Sulphides

From petrographic observations, monazite occurs as inclusions in chalcopyrite, and chalcopyrite inclusions occur in monazite, suggesting co-crystallisation. Monazite and bornite were never observed together in the limited number of studied samples however, both minerals exhibit similar textural overgrowth relationships with matrix minerals. Previous studies identified monazite in grain contact with bornite and chalcopyrite (Williams, 2012), so it is likely that some monazite may have also co-crystallised with bornite. Xenotime is found as inclusions in pyrite and chalcopyrite suggesting that xenotime precipitated prior to sulphide mineralisation and is thus part of an early mineral assemblage.

Based on petrographic observations it is probable that at least two generations of apatite are present in the mineral system. Fine-grained apatite, which is only present in samples from the bornite zone, was not suitable for LA-ICP-MS analysis. Subhedral apatite crystals are present in all samples and are included in pyrite and chalcopyrite, indicating a pre-pyrite and Cu-sulphide timing. Additionally, some subhedral apatite crystals have reaction rims of monazite, which provides further evidence for apatite forming at an early stage in the deposit formation history. Conversely, the fine-grained apatite is intergrown with monazite and bornite and is therefore interpreted to be a paragenetically later phase than the subhedral apatite, and part of the main Cu mineralising stage. A summary of the paragenetic relationships observed in this study is presented in Figure 11.

At the Olympic Dam deposit, the major REE minerals are florencite and bastnasite, with minor synchysite, zircon, monazite, xenotime, and crandallite. These minerals are disseminated in both sulphide and gangue minerals (Ehrig et al., 2012). At least two generations of apatite are identified; early, magmatic apatite and a later, hydrothermal apatite (Krneta et al., 2017b). Hydrothermal apatite is associated with Cu sulphides and hematite at Olympic Dam, which, along with xenotime, is interpreted to have formed after REE-fluorocarbonates (eg. bastnasite and synchysite) (Schmandt et al., 2019). Monazite is extremely rare in studied samples from Olympic Dam but is noted to be found together with florencite replacing magmatic apatite (Krneta et al., 2017b). Observations from the present study concur with the mineralogical relationships at Olympic Dam.

The interpreted timing of key minerals at Carrapateena in this study is also consistent with those at the Oak Dam East prospect where apatite is part of the early magnetite mineral assemblage while monazite is part of the paragenetically later mineral assemblage associated with chalcopyrite. Xenotime is only known to be intergrown with uraninite which is also part of the latter assemblage. Interestingly, some monazite is documented to replace florencite in the Cu-rich zone (Davidson et al., 2007). Similarly, at the Hillside deposit, apatite occurs as inclusions in pyrite and is part of the early magnetite assemblage (Ismail et al., 2014). At Hillside, monazite is observed to rim apatite, as in this study, which is attributed to represent the transition from magmatic (apatite core) to hydrothermal (monazite rim) processes. More broadly, subsolidus growth of monazite and xenotime at the expense of apatite is well documented and is commonly related to post-magmatic fluid-influx at varying scales (e.g. Engi, 2017).

5.2 Geochronology Interpretation

The common Pb mixing trends of monazite from the bornite and barren zones at Carrapateena approaches the concordia at ca. 1400 Ma, although these data are not considered as reliable due to substantial dispersion, largely owing to Pb loss. Monazite from the chalcopyrite zone produced a similar age of 1427 ± 8 Ma.

Xenotime from the chalcopyrite and barren zones yielded ages of 1490 ± 9 Ma and 1470 ± 8 Ma, respectively. However, the MSWD is exceptionally high for the chalcopyrite zone age and as such, it should not be regarded as a robust age. Concordant analyses at around 1450 Ma suggest there may have been a xenotime growth event at that time. There is also a single concordant xenotime analysis at 1590 Ma in both the chalcopyrite and barren zones.

The greatest range of ages is recorded by apatite, with analyses from the bornite zone giving an age of 1332 ± 9 Ma compared to 587 ± 28 Ma from the barren zone and 1652 ± 53 Ma from the chalcopyrite zone. The latter is the only age in this study within overlap of the published deposit age near 1590 Ma (eg. Johnson & Cross, 1995; Sawyer at al. 2017). Additionally, it’s evident that the U-Pb data produced by apatite sampled from the bornite zone doesn’t define a cohesive age population and appears to have undergone both variable common Pb- and modern Pb-loss , as noted by other studies of U-Pb isotopic systems on the Stuart Shelf (eg. Apukhtina et al., 2017; Cherry et al., 2018; Davidson et al., 2007). The array of data has a comparatively well-defined lower value of $^{238}U/^{206}Pb$ and a more variable upper value of $^{238}U/^{206}Pb$ for a given interval of $^{207}Pb/^{206}Pb$. A visually fitted discordia is shown in Figure 18 that bisects the centres of the analyses that define the lowest $^{238}U/^{206}Pb$ values for the dataset which intersects the concordia at ~ 1450 Ma.

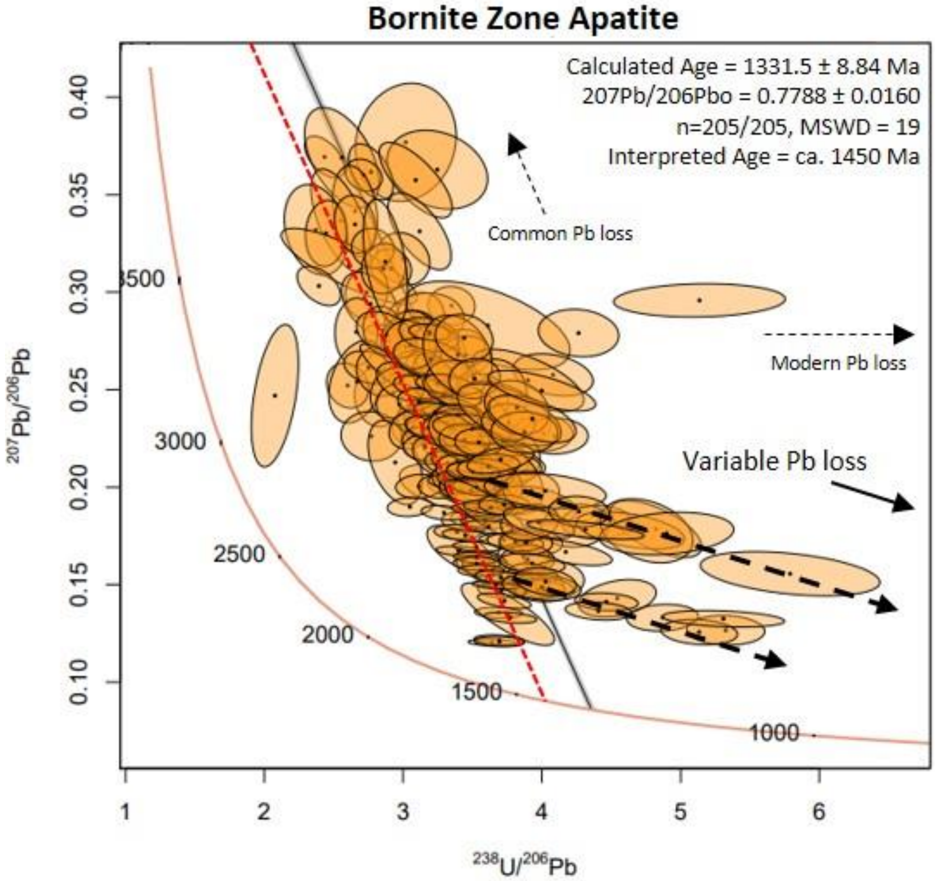

Figure 18: Annotated Tera Wasserburg concordia diagram of in situ apatite U-Pb analyses from bornite zone samples. A visually fitted discordia (dashed red line) bisects the centre of analyses that define the lowest $^{238}U/^{206}Pb$ values for the dataset. The lower intercept of this discordia on the concordia gives an age of ca. 1450 Ma. n= sample population. All ellipses are presented with 2σ errors on both axes.

A summary of regional crustal events and the geochronological data obtained from Carrapateena and other IOCG deposits on the Stuart Shelf is presented in Figure 19. Between ca. 1400 – 1500 Ma, magmatism, rift basin development, shear zone reactivation and isotope resetting are recognised in both the northern Gawler Craton and Laurentia which are suggested to have been connected during the Mesoproterozoic (Anderson & Bender, 1989; Bickford et al., 2015; Schmidt, 2014; Zhao et al., 2002). Additionally, the terrane-scale shear zone system in the Gawler Craton is proposed to have been reactivated during the Coorabie orogeny between ca. 1470 and 1450 Ma (Hand et al., 2007). Following this, a recent study by Morrissey et al. (2019) presented evidence for the existence of a magmatic and metamorphic event at ca. 1450 Ma in an interpreted extensional setting in the northern Gawler Craton. Ground water circulation is also linked to Pb loss from 1400 Ma at Olympic Dam (Reeve et al., 1990). REE-bearing minerals at Carrapateena may have been affected by fluids associated with these crustal-scale events potentially using associated extensional faulting as fluid pathways.

Apatite analysed from the barren zone yielded a significantly younger age of 587.2 ± 28.1 Ma which falls within a period of rifting, erosion and Adelaidean sedimentation (Preiss & Forbes, 1981). Regional-scale Rb-Sr dating of shales and basalts in the Adelaidean sequence produced an age of 586 ± 30 Ma which is interpreted by Foden et al. (2001) to represent the timing of intra-basinal fluid convection resulting from a new phase of extension.

There are two individual xenotime analyses, one from the chalcopyrite zone and one from the barren zone, which are concordant at 1590 Ma. Sawyer et al. (2017) report the age of the initial phase of sulphide mineralisation at Carrapateena as 1598 ± 6 Ma as determined by Re-Os isotopic analysis of pyrite. It is well documented that pyrite pre-dates the deposition of Cu sulphide mineralisation not only at Carrapateena, but at other Olympic Province IOCG deposits such as Olympic Dam. Therefore, it is quite possible this age does not represent the timing of all Cu mineralisation. Considering the evidence for the co-crystallisation of monazite and Cu sulphides (Figure 10), the dates produced from monazite in this study may be interpreted to be a more appropriate estimate of the introduction of Cu into the Carrapateena mineral system at ca. 1450 Ma.

The general paradigm is that IOCG deposits on the Stuart Shelf formed in a single magmatic-hydrothermal event near 1590 Ma (eg. Kirchenbaur et al., 2016). Thus implying that the bornite, chalcopyrite and barren zones at Carrapateena are just different domains of the same-aged ore system in which some components have undergone variable amounts of isotopic resetting. An alternative interpretation is that IOCG mineralisation and alteration developed episodically with individual phases related to discrete tectonic and hydrothermal events which span the evolution of the Gawler Craton and represent over ~1000 Ma of crustal evolution (e.g. Cherry et al., 2017; Macmillan et al., 2016; McPhie et al., 2011). Therefore, the barren, bornite and chalcopyrite zones at Carrapateena may represent discrete domains which have formed at different times in the evolution of the deposit. Given that there is evidence for apatite growth at ca. 1600 Ma, and that apatite has a closure temperature of 450 – 550°C (Dodson, 1973), it can be inferred that the younger ages obtained in this study are not a result of thermal resetting and therefore, are likely a result of post-formational hydrothermal and tectonic reworking events.

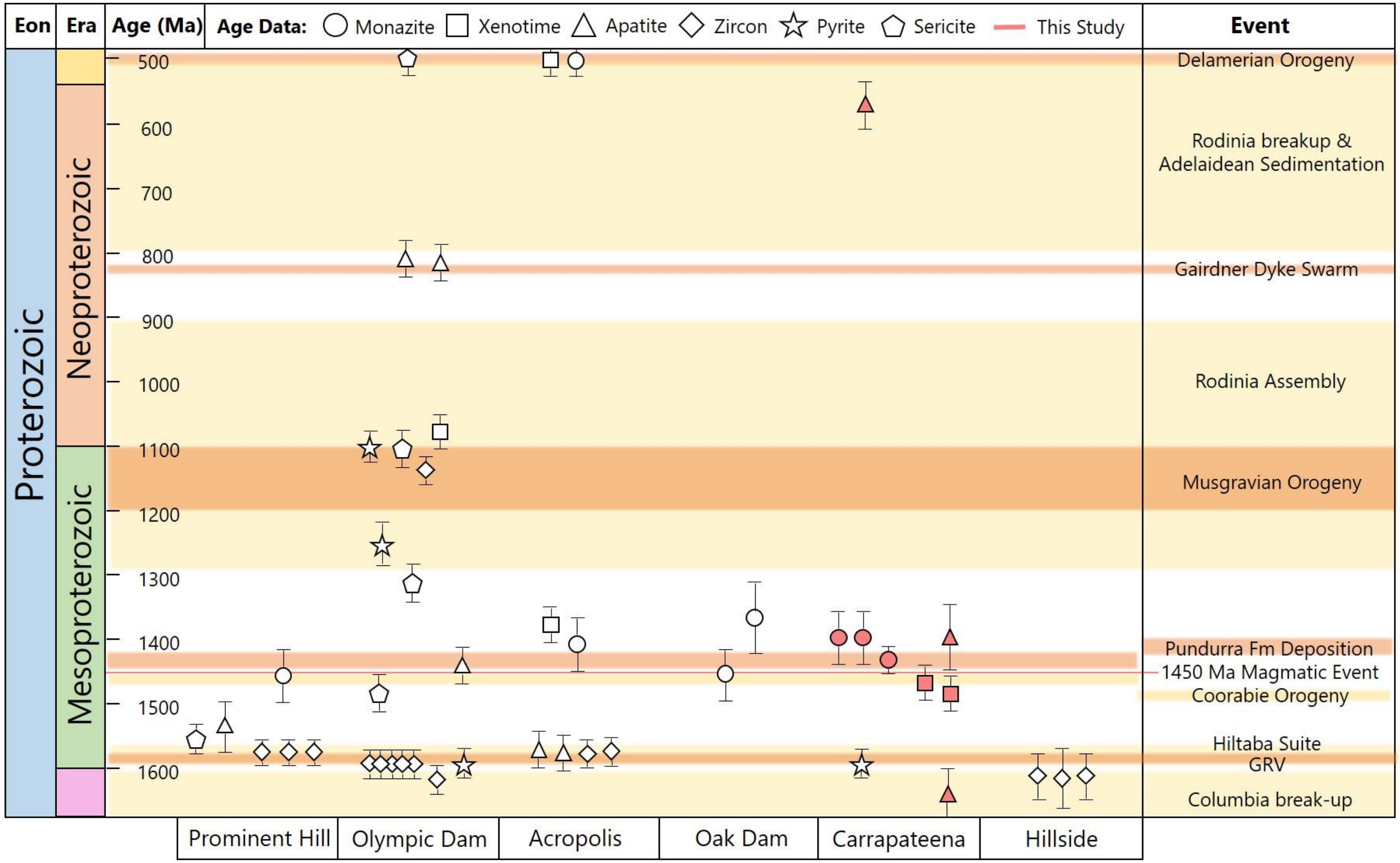

Figure 19: Temporal record of IOCG deposits on the Stuart Shelf, ordered from North (Prominent Hill) to South (Hillside), including geochronological data obtained from this study (pink shapes). Regional events that may be linked to various mineralisation ages are shown for reference. Approximate error bars are shown for each age. Age data for Prominent Hill sourced from Bowden et al. (2016) and Belperio et al. (2007). Age data for Olympic Dam is sourced from Gustafson and Compston (1979), Maas et al. (2011), McInnes et al. (2008), Cherry et al. (2017), Cherry et al. (2018), Jagodzinski (2014), Apukhtina et al. (2017), Huang et al. (2015) and Mcphie et al. (2020). Age data for Oak Dam (Oak Dam East) sourced from Davidson et al. (2007). Age data for Carrapateena sourced from Sawyer et al. (2017) and this study. Age data for Acropolis sourced from Cherry et al. (2018) and Mcphie et al. (2020). Age data for Hillside sourced from Gregory et al. (2011).

5.3 Trace Element Chemistry of Apatite

This project is a reconnaissance study with limited data (collected at the mineral-grain scale), and therefore, the chemistry of the individual minerals analysed cannot be directly related to bulk geochemical data shown in Figure 3. However, it is evident that the bornite, chalcopyrite and barren zones display overall bulk compositional differences in addition to Cu abundance as reflected by their respective REE signatures (Figure 3). This highlights the importance of understanding REE mineralogy in order to understand the processes by which these zones formed and how they led to differences in Cu endowment. Since monazite and xenotime are comparatively less abundant than apatite, and no definitive trends were differentiated according to their zonal location, their chemistry will not be discussed. However, the REE concentrations of monazite and xenotime analyses can be found in Appendix G and H.

Chondrite-normalised REE fractionation patterns of apatite have been used in numerous studies of IOCG deposits to determine the evolution of hydrothermal fluids during deposit formation (e.g.Ismail et al., 2014; Kontonikas-Charos et al., 2014; Krneta et al., 2017a; Krneta et al., 2017b). In these studies, LREE- enriched patterns with negative Eu anomalies are characteristic of early and reduced assemblages (early hydrothermal apatite) while MREE-enriched patterns, positive Eu anomalies and negative Y anomalies are characteristic of later and oxidised assemblages. More specifically, preferential depletion in the LREE and HREE in apatite is suggested to correspond to a shift in hydrothermal fluid conditions characteristic of the hematite-sericite overprinting assemblage, associated with a decrease in temperature, pH and salinity, accompanied by an increase in fO_2 (Krneta et al., 2017a; Ismail et al., 2014). These findings are comparable to the transition seen in this study, with apatite from the chalcopyrite zone displaying the early and reduced assemblage trend, apatite from the barren zone displaying the late and oxidised assemblage trend, and the bornite zone apatite displaying a combination of both trends with a relatively flat pattern. These signatures are also seen globally within magmatic-hydrothermal mineralisation (eg. Harlov et al., 2002a). The presence of monazite and xenotime inclusions in apatite has been noted extensively (eg. Harlov et al., 2002a; Harlov and Forster, 2004) which may be another contributing factor to the HREE- and LREE-depleted fractionation pattern seen in apatite from the barren zone.

There are striking similarities between the REE profiles of apatite from Carrapateena, Olympic Dam, Wirrda Well and Acropolis (Figure 20), although the absence of geochronological data from these studies makes it difficult to ensure accurate comparison between the same generations of apatite. Nonetheless, apatite data sampled from where bornite is the dominant sulphide at the Wirrda Well prospect closely follows the pattern of bornite zone apatite at Carrapateena (Kerneta et al., 2017a). Additionally, the REE signatures of samples with chalcopyrite mineralisation at Olympic Dam and Acropolis are similar to those from Carrapateena’s chalcopyrite zone (Figure 20). These sample sets contain the highest concentrations of LREE, with La being enriched 10 times chondrite, indicating that there were unfavourable physiochemical conditions for the formation of monazite or another LREE-bearing phase and/or a lack of available phosphate (Schmandt et al., 2019). Notably, the strongest MREE enrichment in apatite from Olympic Dam is observed in samples from bornite-bearing ore rocks (Schmandt et al., 2019) (Figure 20), rather than from the barren zone as seen at Carrapateena.

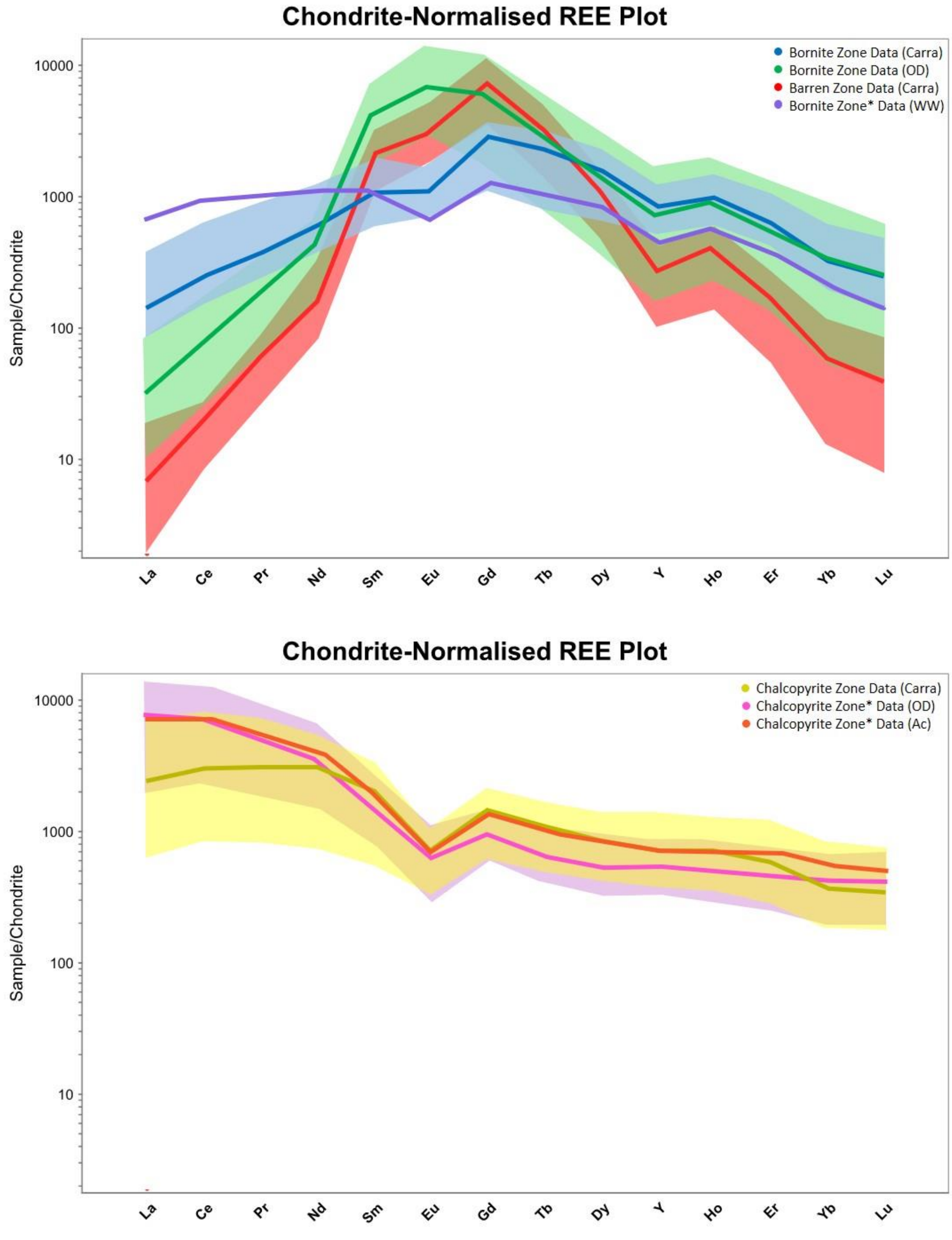

Figure 20: Chondrite-normalized REE signatures of apatite from Carrapateena, Olympic Dam, Acropolis and Wirrda Well. The shaded areas encompass the bulk spread of apatite analyses and the solid lines are the median REE signatures. Olympic Dam data sourced from Krneta et al. (2017b). Acropolis and Wirrda Well data sourced from Krneta et al. (2017a). The concentrations of REE for individual apatite analyses sampled from Carrapateena are provided in Appendix I.

5.4 Geochemistry of the Barren Zone

From analysis of whole-rock geochemical data, the barren zone contains lower concentrations of U and Cu but similar concentrations of Th to the bornite and chalcopyrite zones (Figure 21). Additionally, the chondrite-normalised REE fractionation pattern of apatite from the barren zone at Carrapateena looks remarkably similar to the pattern displayed by apatite from the bornite zone at Olympic Dam (Figure 20). Given the low solubility and thus immobility of Th in fluids (Hazen et al., 2009), these observations indicate that the barren zone may have been endowed with ore grade Cu at one stage but was subsequently leached. Perhaps this leaching event occurred during the late Neoproterozoic as evidenced by the geochronology of apatite analyses from the barren zone.

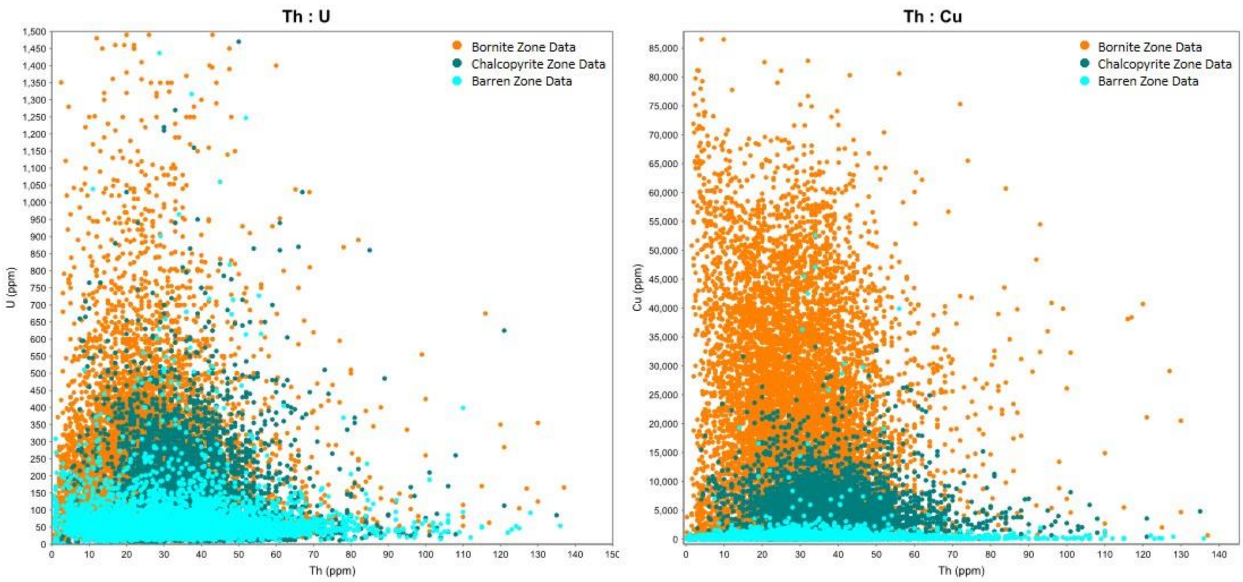

Figure 21: Whole-rock geochemical data from OZ Minerals. Left: Th vs U plot. n =18154. Right: Th vs Cu plot. n=18154.

5.5 Chemistry of IOCG Fluids in the Stuart Shelf Deposits

The ore genesis of IOCG deposits in general is controversial but the current hypothesis for the Olympic Cu-Au Province deposits is the mixing of two fluids, one of which is magmatic or a deeply circulated meteoric fluid while the other is a cooler, more oxidised meteoric fluid (Haynes et al. 1995; Oreskes & Einaudi, 1992; Verdugo et al., 2019). Hand et al. (2007) proposed that ore precipitation results from the oxidation of iron and the reduction of sulphate during mixing in a high-level sub-volcanic setting or more specifically, in a distal continental retro-arc foreland environment. The ore genesis model for Carrapateena is consistent with the fluid mixing model proposed for Olympic Dam, with the zonation of iron-oxides and sulphide species reflecting the potential involvement of an oxidising meteoric fluid. Williams (2012) proposed that Carrapateena evolved in two main stages whereby the system began with a reduced magnetite, carbonate and chlorite rich section at depth which was later overprinted by hematite, sericite, fluorite, barite and sulphides. Several studies have also inferred that REE-minerals co-precipitated with Cu, Au, Fe and U from a mutual hydrothermal fluid (e.g. Belperio et al., 2007; Davidson et al., 2007). Both interpretations are consistent with the findings of this study.

6 CONCLUSIONS

The paragenetic relationships observed, as well as the geochronology and trace element data obtained in this study provides evidence for a complex and prolonged evolution of the Carrapateena deposit. Textural relationships show that while monazite was part of the main Cu-mineralising stage in the formation of Carrapateena, apatite and xenotime were part of a paragenetically earlier mineral assemblage. Multiple stages of remobilisation are recorded by the geochronology of REE-bearing minerals at Carrapateena and other deposits on the Stuart Shelf. These stages post-date the published deposit age of ca. 1590 Ma and are related to regional tectonic events in the Gawler Craton. Based on textural relationships, the dates produced from monazite in this study may be a more appropriate estimate of the introduction of Cu into the Carrapateena mineral system at ca. 1450 Ma.

Apatite displays three distinct chondrite-normalised REE fractionation trends corresponding to the bornite, chalcopyrite and barren zones of Carrapateena. For the first time, these trends have been compared to those from Olympic Dam, Acropolis and Wirrda Well and offer insight into evolving fluid physiochemistry during IOCG deposit formation. These findings are encouraging for the future applicability of apatite geochemistry to mineral exploration.

7 RECOMMENDATIONS FOR FURTHER STUDY

Based on the data presented in this study and the textural relationships observed, the story of Cu endowment at Carrapateena requires further investigation. In the rare instances where chalcopyrite and bornite are intergrown, it is uncertain whether the bornite reflects dissolution and reprecipitation of existing Cu under a new set of physiochemical conditions or if it reflects a completely new Cu event. This question can be addressed with a focused study on the trace element chemistry of texturally intergrown chalcopyrite and bornite with the potential for the development of a new exploration model for the Gawler Craton.

The use of apatite geochemistry would likely have the greatest utility in exploration when drilling in rocks with no Cu mineralisation. As such, succeeding research could involve acquiring a more comprehensive trace element dataset for apatite (and other REE-bearing minerals) by sampling at frequent and regular intervals across the entirety of the orebody, particularly from the country rock to the barren zone. Precise geochronological data should also be acquired for apatite to allow accurate comparison between the same generations of apatite in other deposits on the Stuart Shelf. In addition, xenotime is recognised as being a valuable mineral target for geochronology and therefore may be useful in improving understanding of the age structure of the hydrothermal reactivation events throughout Carrapateena's history.

Another study could focus on the barren zone at Carrapateena to determine if it was in fact leached by examining the transition between the barren zone and surrounding mineralised volumes. If so, determining the likely temperatures of leaching and fluid compositions and quantifying the amount of copper involved allows for the development of a model for the transport and trapping of the mobilised copper. This may provide a new exploration opportunity, given that the geochronological data in this study provides evidence for the bornite zone being older than the barren zone.

8 ACKNOWLEDGMENTS

Thank you to my supervisors Dr. Richard Lilly, Prof. Martin Hand and Mitchell Neumann for all their invested time and invaluable advice throughout the year. To the Playford Trust and OZ Minerals for their generous financial support. Aoife McFadden and Sarah Gilbert at Adelaide Microscopy are thanked for their vital assistance and patience during data acquisition. Thanks to Brad Cave and Mitchell Bockmann for providing guidance with data processing, and to Carl Spandler for his technical insights during data interpretation. A special thank you to Becke Griggs for her help with learning Photoshop. Finally, a sincere thank you to the whole Honours cohort for making this a fantastic final year of university.

9 REFERENCES

Allen, S., McPhie, J., Ferris, G., Cadd, A. (2008). Evolution and architecture of a large felsic igneous province in western Laurentia: The 1.6 Ga Gawler Range Volcanics, South Australia. *Journal of Volcanology and Geothermal Research*, *172*, 132–147.

Apukhtina, O., Kamenetsky, V., Ehrig, K., Kamenetsky, M., Maas, R., Thompson, J., McPhie, J., Ciobanu, C., & Cook, N. (2017). Early, Deep Magnetite-Fluorapatite Mineralization at the Olympic Dam Cu-U-Au-Ag Deposit, South Australia. *Economic Geology and the Bulletin of the Society of Economic Geologists*, *112*(6), 1531–1542.

Barton, M. D. (2014). Iron Oxide(–Cu–Au–REE–P–Ag–U–Co) Systems. In K. K. T. Heinrich D. Holland (Ed.), *Treatise on Geochemistry Second ed*, *13*, 515-541.

Belperio, A., Flint, R., & Freeman, H. (2007). Prominent Hill: A Hematite-Dominated, Iron Oxide Copper-Gold System. *Economic Geology, 102*(8), 1499–1510.

Bett, P.G. and Giles, D. (2006). The 1800-1100 Ma tectonic evolution of Australia. *Precambrian Research, 144*, 92-125.

Bowden, B., Bowden, B., Fraser, G., Fraser, G., Davidson, G., Davidson, G., Meffre, S., Meffre, S., Skirrow, R., Skirrow, R., Bull, S., Bull, S., Thompson, J., & Thompson, J. (2017). Age constraints on the hydrothermal history of the Prominent Hill iron oxide copper-gold deposit, South Australia. *Mineralium Deposita*, *52*(6), 863–881.

Budd, A. (2006). *The Tarcoola Goldfield of the Central Gawler Gold province, and the Hiltaba Association Granites, Gawler Craton, South Australia* [Unpublished doctoral dissertation]. Australian National University.

Cherry, A., Kamenetsky, V., McPhie, J., Kamenetsky, M., Ehrig, K., & Keeling, J. (2017). Post 1590 Ma modification of the supergiant Olympic Dam deposit: links with regional tectonothermal events. In Proceedings, 14th SGA Biennial Meeting ‘Mineral Resources to Discover’, Québec City, QC, Canada, 20-23.

Cherry, A., Kamenetsky, V., McPhie, J., Thompson, J., Ehrig, K., Meffre, S., Kamenetsky, M & Krneta, S. (2018). Tectonothermal events in the Olympic IOCG Province constrained by apatite and REE-phosphate geochronology. *Australian Journal of Earth Science, 65*(5), 643-659.

Ciobanu, C., Wade, B., Cook, N., Schmidt Mumm, A., & Giles, D. (2013). Uranium-bearing hematite from the Olympic Dam Cu–U–Au deposit, South Australia: A geochemical tracer and reconnaissance Pb–Pb geochronometer. *Precambrian Research*, *238*, 129–147.

Corriveau, L & Potter, E. (2019). Alteration facies in ‘IOCG terranes’: a global view on mineral systems with IOCG and affiliated deposit types. *Geological Survey of South Australia*, 1-33.

Cowley, W., Conor, C & Zang, W. (2003). New and revised Proterozoic stratigraphic units on northern Yorke Peninsula. *MESA Journal*, *29*, 46–58.

CSIRO. 2019. Case Study: Maia x-ray imaging: finding hidden 'needles in a haystack'. Last updated 1 May 2019. https://www.csiro.au/en/Research/MRF/Areas/Orebody-knowledge/Resource characterisation-developments/Maia.

Cutts, K., Hand, M., & Kelsey, D. (2011). Evidence for early Mesoproterozoic (ca. 1590 Ma) ultrahigh temperature metamorphism in southern Australia. *Lithos*, *124*, 1–16.

Creaser, R & White, A. (1991). Yardea Dacite: Large-volume, high temperature felsic volcanism from the middle Proterozoic of South Australia. Geology, 19, 48-51.

Daly, S., Heithersay, P & McGeough, M. (2007). World-Class IOCG Deposits and Potential Deposits in South Australia. AusIMM. World Gold Conference, Cairns, QLD.

Davidson, G., Paterson, H., Meffre, S., & Berry, R. (2007). Characteristics and Origin of the Oak Dam East Breccia-Hosted, Iron Oxide Cu-U-(Au) Deposit: Olympic Dam Region, Gawler Craton, South Australia. *Economic Geology*, *102*(8), 1471–1498.

Dmitrijeva, M., Ciobanu, C. L., Ehrig, K, Cook, N, Metcalfe, A, Verdugo-Ihl, M, & McPhie, J. (2019). Mineralization-alteration footprints in the Olympic Dam IOCG district, South Australia: The Acropolis prospect. *Journal of Geochemical Exploration, 205*. doi:10.1016/j.gexplo.2019.106333.

Dodson, M. (1973). Closure temperature in cooling geochronological and petrological systems. *Contributions to Mineralogy and Petrology, 40*(3), 259–274.

Ehrig, K., McPhie, J & Kamenetsky, V. (2012). Geology and Mineralogical Zonation of the Olympic Dam Iron Oxide Cu U-Au-Ag Deposit, South Australia. *Society of Economic Geologists, 16,* 237-267.

Engi, M. (2017). Petrochronology Based on REE-Minerals: Monazite, Allanite, Xenotime, Apatite. *Reviews in Mineralogy and Geochemistry, 83*(1), 365–418.

Ferrero S, Grosch E. G, Lanari P, & Goncalves P. (2019). Garnet-Monazite Rare Earth Element Relationships in Sub-Solidus Metapelites: A Case Study from Bhutan. In *Metamorphic Geology - Microscale to Mountain Belts,* 1–2. Geological Society of London.

Ferris, G., Schwarz, M & Heithersay, P. (2002). The geological framework, distribution and controls of Fe-oxide Cu-Au mineralisation in the Gawler Craton, South Australia, Part I – Geological and tectonic framework. In TM Porter ed: *Hydrothermal Iron Oxide Copper-Gold and Related Deposits: A Global Perspective, 2,* 9–31.

Fletcher, I., McNaughton, N., Aleinikoff, J., Rasmussen, B., and Kamo, S. (2004). Improved calibration procedures and new standards for U-Pb and Th-Pb dating of Phanerozoic xenotime by ion microprobe. *Chemical Geology, 209*, 295–314.

Flint, R., Blissett, A., Conor, C., Cowley, W., Cross, K., Creaser, R., Daly, S., Krieg, G., Major, R., Teale, G., et al. (1993). Mesoproterozoic. In Drexel, J., Preiss, W., & Parker, A. (Eds), *The geology of South Australia; Volume 1, The Precambrian* (pp. 106–169). Geological Survey of South Australia.

Foden, J., Barovich, K., Jane, M., & O'Halloran, G. (2001). Sr-isotopic evidence for Late Neoproterozoic rifting in the Adelaide Geosyncline at 586 Ma: implications for a Cu ore forming fluid flux. *Precambrian Research, 106*(3), 291–308.

Forbes, C., Giles, D., Jourdan, F., Sato, K., Omori, S., & Bunch, M. (2012). Cooling and exhumation history of the northeastern Gawler Craton, South Australia. *Precambrian Research, 200,* 209-238.

Foden, J., Elburg, M., Dougherty-Page, J & Burtt A. (2006). The timing and duration of the delamerian orogeny: correlation with the ross orogen and implications for Gondwana assembly. *The Journal of Geology, 114,* 189-210.

Fraser, G., & Neumann, N. (2010). New SHRIMP U-Pb zircon ages from the Gawler Craton and Curnamona Province, South Australia, *Geoscience Australia*.

Gustafson, L. & Compston, W. (1979). Rb-Sr dating of Olympic Dam core samples, Report to Western Mining Corporation, Research School of Earth Sciences, *Australian National University, 18.*

Hand, M., Reid, A & Jagodzinski, L. (2007). Tectonic framework and evolution of the Gawler Craton, southern Australia. *Society of Economic Geologists Inc, 102,* 1377-1395.

Harlov, D., Förster, H., & Nijland, T. (2002). Fluid-induced nucleation of (Y+ REE)-phosphate minerals within apatite: Nature and experiment. Part I. Chlorapatite. *American Mineralogist, 87*(2-3), 245-261.

Hayward, N., & Skirrow, R. (2010). Geodynamic setting and controls on iron oxide Cu-Au (±U) ore in the Gawler Craton, South Australia. In: *Hydrothermal Iron Oxide Copper-Gold and Related Deposits: A global Perspective, 3*, 119-146.

Hazen, R., Ewing, R., & Sverjensky, D. (2009). Evolution of uranium and thorium minerals. *American Mineralogist, 94*(10), 1293–1311.

Henderson, P. (1984). General geochemical properties and abundances of the rare earth elements. In: Henderson, P. (Ed.), *Rare Earth Element Geochemistry, 2.* Elsevier, Amsterdam, pp. 1-32.

Hitzman, M, Oreskes, N & Einaudi, M. (1992). Geological characteristics and tectonic setting of Proterozoic iron oxide (Cu-U-Au-REE) deposits. *Precambrian Research, 58,* 241-287.

Holder, R., Yakymchuk, C., & Viete, D. (2020). Accessory Mineral Eu Anomalies in Suprasolidus Rocks: Beyond Feldspar. *Geochemistry, Geophysics, Geosystems : G3, 21*(8).

Howard, K., Hand, M., Barovich, K., Payne, J., Cutts, K & Belousova, E. (2011). U–Pb zircon, zircon Hf and whole-rock Sm–Nd isotopic constraints on the evolution of Paleoproterozoic rocks in the northern Gawler Craton. *Australian Journal of Earth Sciences*, *58*, 615–638.

Huang, Q., Kamenetsky, V., McPhie, J., Ehrig, K., Meffre, S., Maas, R., Thompson, J., Kamenetsky, M., Chambefort, I., Apukhtina, O., & Hu, Y. (2015). Neoproterozoic (ca. 820–830Ma) mafic dykes at Olympic Dam, South Australia: Links with the Gairdner Large Igneous Province. *Precambrian Research, 271*, 160–172.

Ismail, R., Ciobanu, C., Cook, N., Teale, G., Giles, D., Mumm, A., & Wade, B. (2014). Rare earths and other trace elements in minerals from skarn assemblages, Hillside iron oxide–copper–gold deposit, Yorke Peninsula, South Australia. *Lithos, 184-187*, 456–477.

Jagodzinski, E., Reid, A., Chalmers, N., Swain, G., Frew, R & Foudoulis, C. (2007). *Compilation of SHRIMP U-Pb geochronological data for the Gawler craton, South Australia.* Primary Industries and Resources South Australia, Division of Minerals and Energy Resources.

Johnson, J & Cross, K. (1995). U-Pb geochronological constraints on the genesis of the Olympic Dam Cu-U-Au-Ag deposit, South Australia. *Economic Geology, 90*(5), 1046–1063. doi:

Kendall, B., Creaser, R & Selby, D. (2006). Re-Os geochronology of postglacial black shales in Australia: Constraints on the timing of "Sturtian" glaciation. *Geology, 34*(9), 729–732. doi:

Kontonikas-Charos, A., Ciobanu, C., & Cook, N. (2014). Albitization and redistribution of REE and Y in IOCG systems: Insights from Moonta-Wallaroo, Yorke Peninsula, South Australia. *Lithos, 208-209*, 178–201.

Krneta, S., Ciobanu, C., Cook, N & Ehrig, K. (2018). Numerical Modeling of REE Fractionation Patterns in Fluorapatite from the Olympic Dam Deposit (South Australia). *Minerals, 8(8).*

Krneta, S., Ciobanu, C., Cook, N., Ehrig, K., & Kontonikas-Charos, A. (2017b). Rare Earth Element Behaviour in Apatite from the Olympic Dam Cu-U-Au-Ag Deposit, South Australia. *Minerals, 7*(8).

Krneta, S., Cook, N., Ciobanu, C., Ehrig, K., & Kontonikas-Charos, A. (2017a). The Wirrda Well and Acropolis prospects, Gawler Craton, South Australia: Insights into evolving fluid conditions through apatite chemistry. *Journal of Geochemical Exploration*, *181*, 276–291. https://doi.org/10.1016/j.gexplo.2017.08.004

Lane, K., Jagodzinski, E., Dutch R., Reid, A & Hand M. (2015). Age constraints on the timing of iron ore mineralisation in the southeastern Gawler Craton. *Australian Journal of Earth Sciences, 62*(1), 55–75.

Lloyd, J., Blades, M., Counts, J., Collins, A., Amos, K., Wade, B., Hall, J., Hore, S., Ball, A., Shahin, S., & Drabsch, M. (2020). Neoproterozoic geochronology and provenance of the Adelaide Superbasin. *Precambrian Research, 350*.

Maas, R., Kamenetsky, V., Ehrig, K., Meffre, S., McPhie, J., & Diemar, G. (2011). Olympic Dam U-Cu-Au deposit, Australia: New age constraints. *Mineralogical Magazine*, *75*, 1375.

McInnes, B., Keays, R., Lambert, D., Hellstrom, J., & Allwood, J. (2008). Re-Os geochronology and isotope systematics of the Tanami, Tennant Creek and Olympic Dam Cu-Au deposits. *Australian Journal of Earth Sciences, 55*(6-7), 967–981.

Mcphie, J., Ehrig, K., Kamenetsky, M., Crowley, J., & Kamenetsky, V. (2020). Geology of the Acropolis prospect, South Australia, constrained by high-precision CA-TIMS ages. *Australian Journal of Earth Sciences*, 1–18.

Mcphie, J., Kamenetsky, V., Allen, S., Ehrig, K., Agangi, A., & Bath, A. (2011). The fluorine link between a supergiant ore deposit and a silicic large igneous province. *Geology, 39*(1), 1003-1006.

Morrissey, L., Hand, M, Wade, B & Szpunar, M. (2013). Early Mesoproterozoic metamorphism in the Barossa Complex, South Australia: links with the eastern margin of Proterozoic Australia. *Australian Journal of Earth Sciences, 60,* 1–27.

Mortimer, G., Cooper, J., & Oliver, R. (1988). The geochemical evolution of proterozoic granitoids near Port Lincoln in the Gawler orogenic domain of South Australia. *Precambrian Research, 40*(C), 387-406.

Murphy, B., Betts, P & Funk, C. (2012). Interpretation of gravity and aeromagnetic data over the Carrapateena region, South Australia, and exploration targeting. *PGN Science.* 1-42.

Oreskes, N., & Einaudi, M. (1990). Origin of rare earth element-enriched hematite breccias at the Olympic Dam Cu-U-Au-Ag deposit, Roxby Downs, South Australia. *Society of Economic Geologists, 85*(1), 1-28.

Oreskes, N., & Einaudi, M. (1992). Origin of hydrothermal fluids at Olympic Dam; preliminary results from fluid inclusions and stable isotopes. *Economic Geology and the Bulletin of the Society of Economic Geologists, 87(*1), 64–90.

Otake, T., Wesolowski, D., Anovitz, L., Allard, L., & Ohmoto, H. (2007). Experimental evidence for non-redox transformations between magnetite and hematite under H 2-rich hydrothermal conditions. *Earth and Planetary Science Letters, 257*(1), 60–70. https://doi.org/10.1016/j.epsl.2007.02.022.

OZ Minerals. (2019). Carrapateena 2019 mineral resources and ore reserves statement and explanatory notes. Public report to the ASX, 30/06/2019, 1-56.

Payne, J., Hand, M., Barovich, K, & Wade, B. (2008). Temporal constraints on the timing of high-grade metamorphism in the northern Gawler Craton: implications for assembly of the Australian Proterozoic. *Australian Journal of Earth Sciences, 55*, 623–640.

Payne, J., Raimondo, T., Morrissey, L., Hand, M., Lilly, R., Tomkins, A., Reid, A., Dutch, R & Wade, C. (2017). Source to Spectrum: a new project investigating the range of mineral deposits in the Gawler Craton. *MESA Journal, 83,* 2, 8-10.

Porter, T. (2010). The Carrapateena iron oxide copper gold deposits, Gawler Craton, South Australia: A review. In: *Hydrothermal Iron Oxide Copper-Gold and Related Deposits: A global Perspective, 3*, 191-200.

Powell, C. (1998). Assembly and breakup of Rodinia leading to formation of Gondwanaland. In: Bird, R (Ed.), *The Assembly and Breakup of Rodinia,* (49-53). The Geological Society of Australia.

Preiss, W. (1987). The Adelaide Geosyncline : late Proterozoic stratigraphy, sedimentation, palaeontology and tectonics. *Geological Survey of South Australia.*

Preiss, W & Forbes, B. (1981). Stratigraphy, correlation and sedimentary history of Adelaidean (late Proterozoic) basins in Australia. *Precambrian Research, 15,* 255-304.

Reid, A. (2019). The Olympic Cu-Au Province, Gawler Craton: A Review of the Lithospheric Architecture, Geodynamic Setting, Alteration Systems, Cover Successions and Prospectivity. *Minerals, 9(* 6), 1-371.

Reid, A & Hand, M. (2008). Aspects of Palaeoproterozoic orogenesis in the Gawler Craton: the c. 1850 Ma Cornian Orogeny. *MESA Journal, 50,* 26-31.

Reid, A., Hand, M., Jagodzinski, E., Kelsey, D., & Pearson, N. (2008). Paleoproterozoic orogenesis in the southeastern Gawler Craton, South Australia. *Australian Journal of Earth Sciences, 55*(4), 449–471.

Reid, A & Hand, M. (2012). Mesoarchean to Mesoproterozoic evolution of the southern Gawler Craton, South Australia. *Episodes, 35,* 216–225.

Rubatto, D., Hermann, J & Buigk, I. (2006). Temperature and Bulk Composition Control on the Growth of Monazite and Zircon During Low-pressure Anatexis (Mount Stafford, Central Australia). *Journal of Petrology, 47*(10), 1973-1996.

Ryan, C., Kirkham, R., Parry, D., Moorhead, G., Jensen, M., Hogan, S., Faulks, A., Dunn, P., Dodanwela, R., Fisher, L., Pearce, M., Siddons, P., Kuczewski, A., Lundstrom, U., Trolliet, A., & Gao, N. (2018). Maia Mapper: High Definition XRF Imaging of Geological Samples at Intermediate Spatial Scales. *Microscopy and Microanalysis, 24*(s2), 108–109.

Ryan, C., Siddons, D., Kirkham, R., Kuczewski, A., Dunn, P., De Geronimo, G., Dragone, A., Li, Z., Moorhead, G., Jensen, M., Paterson, D., de Jonge, M., Howard, D., Dodanwela, R., Carini, G., Beuttenmuller, R., Pinelli, D., Fisher, L., Hough, R., … Davey, P. (2018). The Maia Detector Journey: Development, Capabilities and Applications. *Microscopy and Microanalysis*, *24(*S1), 720–721.

Sawyer et al. (2014). Geology of Carrapateena (internal report).

Sawyer, M., Whittaker, B & Delittle, J. (2017). Carrapateena Iron Oxide Copper-Gold-Silver-Uranium Deposit. *Australian Ore Deposits.* AusIMM.

Schmandt, D., Cook, N., Ciobanu, C., Ehrig, K., Wade, B., Gilbert, S., & Kamenetsky, V. (2017). Rare Earth Element Fluorocarbonate Minerals from the Olympic Dam Cu-U-Au-Ag Deposit, South Australia. *Minerals*, *7*(10).

Schmandt, D., Cook, N., Ciobanu, C., Ehrig, K., Wade, B., Gilbert, S., & Kamenetsky, V. (2019). Rare Earth Element Phosphate Minerals from the Olympic Dam Cu-U-Au-Ag Deposit, South Australia: Recognizing Temporal-Spatial Controls On Ree Mineralogy in an Evolved IOCG System. *The Canadian Mineralogist, 57*(1), 3–24.

Skirrow, R., Bastrakov, E., Barovich, K., Fraser, G., Creaser, R., Fanning, C., … Davidson, G. (2007). Timing of Iron Oxide Cu-Au-(U) Hydrothermal Activity and Nd Isotope Constraints on Metal Sources in the Gawler Craton, South Australia. *Economic Geology*, *102*(8), 1441–1470.

Smith, M., Moore, K., Kavecsanski, D., Finch, A., Kynicky, J & Wall, F. (2016). From mantle to critical zone: a review of large and giant sized deposits of the rare earth elements. *Geoscience Frontiers, 7*(3), 315-334.

Szpunar, M., Hand, M., Barovich, K., Belousova, E & Jagodzinski, E.A. (2011). Isotopic and geochemical constraints on the Paleoproterozoic Hutchison Group, southern Australia: Implications for Paleoproterozoic continental reconstructions. *Precambrian Res, 187,* 99–126.

Sun, S., & McDonough, W. (1989). Chemical and isotopic systematics of oceanic basalts: implications for mantle composition and processes. *Geological Society of London*, *42*(1), 313–345.

Swain G., Barovich K., Hand M., Ferris G. & Schwarz MP. (2008). Petrogenesis of the St Peter Suite, southern Australia: arc magmatism and Proterozoic crustal growth of the South Australian craton. *Precambrian Research, 166*(1–4):283–296.

Taylor, R. (2014). Comments and overview concerning recent observations on the textures and paragenetic data from the Carrapateena, Khamsin, and Freemantle Doctor mineralised zones. Retrieved from Tasmania (internal report).

Thomson, S., Gehrels, G., Ruiz, J & Buchwaldt, R. (2012). Routine low-damage apatite u-pb dating using laser ablation–multicollector–icpms. *Geochemistry, Geophysics, Geosystems*, *13*.

Thompson, J., Meffre, S., Maas, R., Kamenetsky, V., Kamenetsky, M., Goemann, K., Ehrig, K & Danyushevsky, L. (2016). Matrix effects in Pb/U measurements during LA-ICP-MS analysis of the mineral apatite. *Journal of Analytical Atomic Spectrometry*, *31*(6), 1206-1215.

Vella, L & Emerson, D. (2009). Carrapateena: Physical properties of a new iron-oxide copper-gold deposit. (internal report).

Verdugo, M., Ciobanu, C., Cook, N., Ehrig, K & Courtney-Davies, L. (2019). Defining early stages of IOCG systems: evidence from iron oxides in the outer shell of the Olympic Dam deposit, South Australia. *Mineralium Deposita, 55,* 429-452.

Vermeesch, P (2018). “IsoplotR: a free and open toolbox for geochronology.” *Geoscience Frontiers,* **9**, 1479-1493.

Weill, D & Drake, M. (1973). Europium Anomaly in Plagioclase Feldspar: Experimental Results and Semiquantitative Model. Science (American Association for the Advancement of Science), 180(4090), 1059–1060.

Williams P. (2012). Comments on Carrapateena Geology from Inspection of CAR075, CMG_27/1 (internal report).

Williams, P., Barton, M., Johnson, D., Fontbote, L., De Haller, A., Mark, G., Oliver, N & Marschik, R. (2005). Iron Oxide Copper-Gold Deposits: Geology, Space-Time Distribution, and Possible Modes of Origin. *Society of Economic Geologists, Inc, 100,* 371-405.

APPENDIX A: EXTENDED PETROLOGY

DD12CAR083
743.3m – 743.4m

Sample Lithology Description:
Polylithic ore breccia dominated by steely grey hematite and contains clasts of rock (Donnington Granite?) and colloform magnetite which has mostly been altered to hematite. Overprinted by red "earthy" hematite. Sulphides (chalcopyrite and pyrite) are abundant.

Main Fragments
Rock (donington granite?) (~1cm) - mostly composed of quartz.
Colloform hematite (2cm - 0.5cm)
Steely hematite (largest ~ 200 microns)
Chalcopyrite (largest ~150 microns)

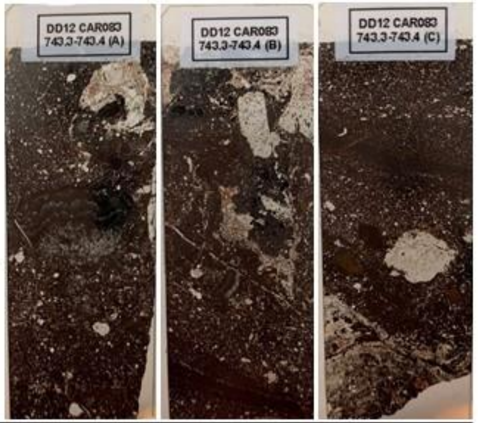

Veins/Infill
Sericite veins (~50 microns thick) being irregularly replaced by chalcopyrite and bornite.
Quartz veins (~75 microns thick) host subordinate amounts of chalcopyrite, pyrite and occasional bornite infill crystals.

Modal Proportions
Average: 70% Hematite, 20% quartz, 5% sericite, 5% limonite, 3% chalcopyrite, 1% pyrite, 1% bornite. Trace apatite (greater abundance in thin sections B and C).
Matrix: Dominantly hematite with lesser quartz.

REE Host Minerals
Apatite which is hosted in a range of minerals but dominantly hematite and quartz.

Summary
Polylithic breccia overprinted by earthy/red hematite. Matrix is dominated by fragments of steely grey hematite with quartz, sericite and minor limonite. The rock fragments are composed of variably sized, subangular quartz crystals and fine-grained hematite with occasional sericite infill. Chalcopyrite and bornite are disseminated throughout the matrix hematite as well as in veins.

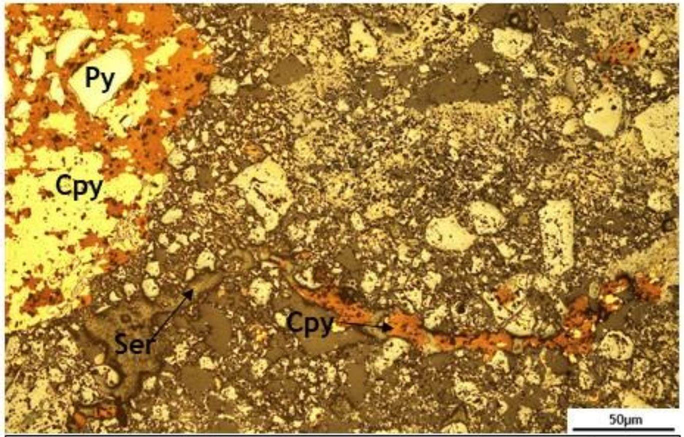

Above: Reflected light (RL) image of chalcopyrite (yellow and tarnished brown) partially replacing sericite veins (grey). Note chalcopyrite enveloping pyrite.
Below: RL image showing alteration of bornite to chalcocite (light blue) and covellite (darkest blue) at grain edges and along micro-fractures. Note bornite exsolving chalcopyrite.

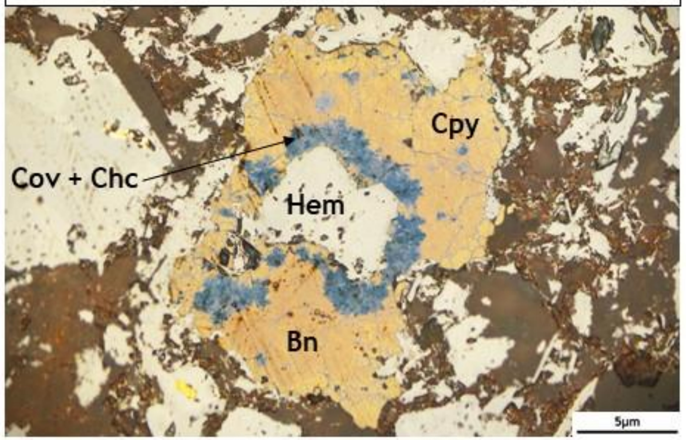

Abbreviations: Cpy: chalcopyrite, Hem: hematite, Mon: monazite, Dol: dolomite, Chl: chlorite, Carb: carbonate, Qtz: quartz, Ap: apatite, Anh: anhydrite, Bn: bornite, Cov: covellite.

DD12CAR085
978.5 m – 978.6 m

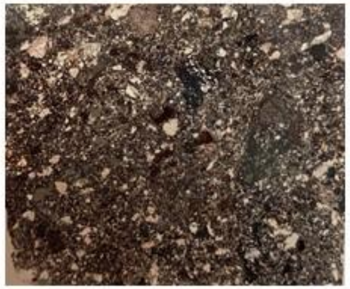

Sample Lithology Description:
Complex polymict ore breccia with multiple generations of matrix. Visible pyrite and chalcopyrite.

Main Fragments
Colloform hematite (2cm)
Carbonate (siderite?) (~200 microns)
Polymineralic aggregates of quartz (0.5-1cm)
Large grains of pyrite (~200 microns)

Veins/Infill
Veins are rare in these samples - only quartz veins: a large quartz vein (up to 0.8 cm wide) in thin section B containing infill crystals of chalcopyrite, and small quartz veins in carbonate clasts.
Pyrite and chalcopyrite are infilling grey hematite.

Modal Proportions
Average: 60% Hematite, 15% carbonate, 15% quartz, 5% pyrite, 5% limonite, trace chalcopyrite, bornite and chlorite.

REE Host Minerals
None observed.

Summary
Complex breccia dominated by grey hematite and contains rock fragments and colloform magnetite which has been completely altered to hematite (texturally retentive alteration). Sulphides (py and cpy) and hematite are intergrown in colloform textures. Carbonate overprints hematite. Quartz veins in carbonate suggest a paragentically later silica event in addition to early fragments of matrix quartz. Pyrite and Chalcopyrite are contained in grey hematite and lesser quartz fragments or veins.

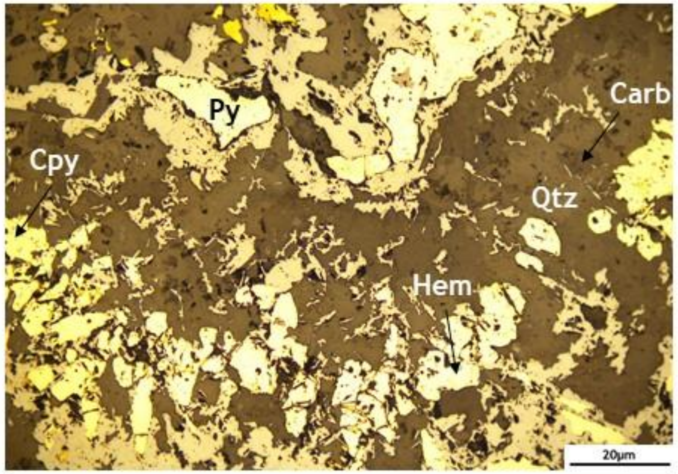

Above: RL image of colloform pyrite and hematite intergrowths with surrounding matrix of quartz and carbonate.
Below: RL image of bladed hematite intergrown with pyrite containing veins of chalcopyrite. Image by Martin Hand.

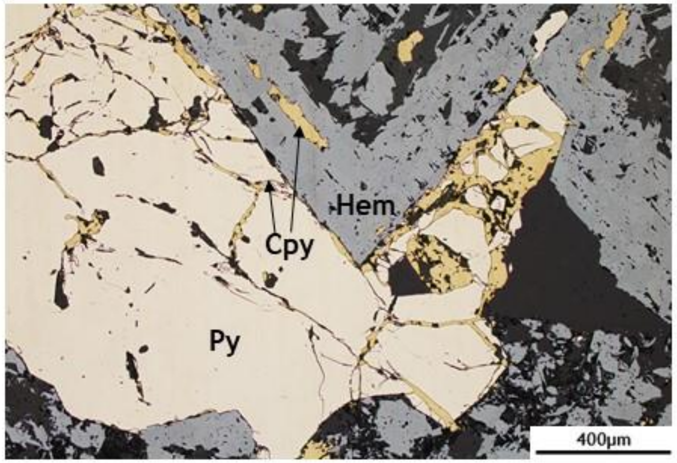

CAR031
874m

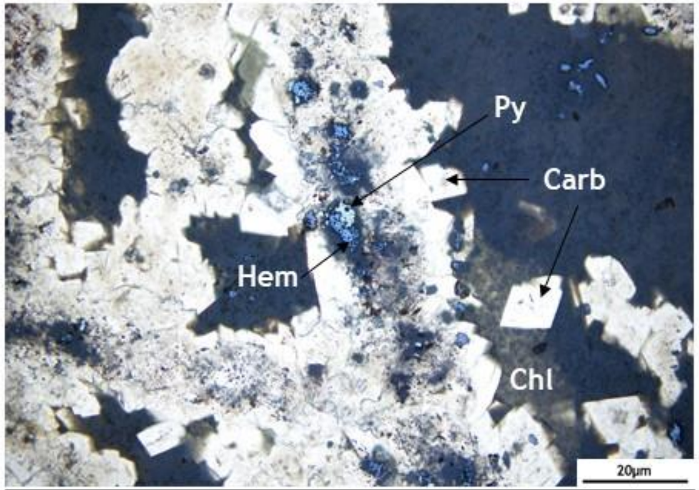

Above: Transmitted light (TL) image of rhombic carbonate crystals infilling veins which cut through chlorite altered clasts.
Below: Reflected light image of hematite (white) altering magnetite (light blue) and surrounded by chlorite and carbonate veins (grey).

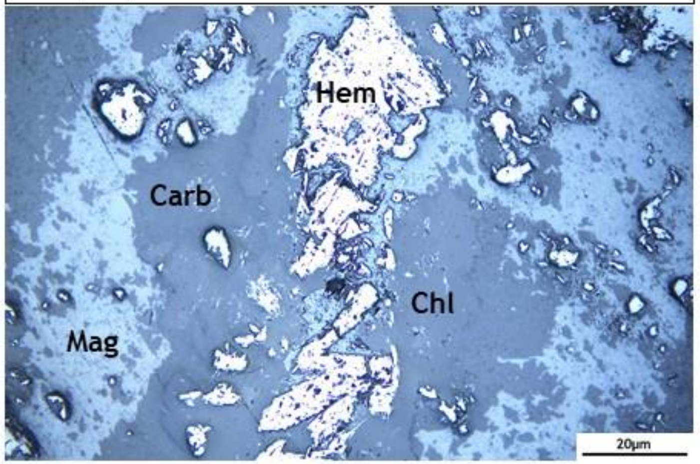

Sample Lithology Description:
Chlorite altered granite breccia

Main Fragments
Chlorite altered clasts (~10mm), most often encased in carbonate veins.
Steely/grey hematite fragments (blebs or blades).
Rhombic-euhedral carbonate crystals, some are reddened by earthy hematite.
Chalcopyrite fragments commonly intergrown with hematite in carbonate veins.

Veins/Infill
Rhombic-euhedral carbonate crystals (ankerite) present as infill.

Earthy hematite is altering/overprinting veins only.

Modal Proportions
50% Chlorite, 25% hematite, 20% carbonate, ~2% monazite, ~2% ilmenite, 1% rutile.

REE Hosts
Dominantly carbonate (rhombic crystals) and chlorite.

Summary
Complex granite breccia with abundant chloritised clasts. Carbonate appears to have replaced a pre-existing mineral (sulphate?) that had a cubic crystal habit up to 20x20 microns. Earthy hematite is exclusively present in veins. Steely/grey hematite is dispersed throughout the rock and present as either subrounded blebs (10-20 microns) or coarser blades (50 microns).

CAR032
1264.4m

Sample Lithology Description:
Dolomite with reddened vein networks

Veins/Infill
Fine bladed grey hematite diffuse veins intergrown with anhydrite and dolomite.

Chalcopyrite micro-veins in pyrite.

Modal Proportions
60% carbonate, 20% quartz, 15% anhydrite, 5% hematite, trace chalcopyrite and mica.

REE Hosts
Dolomite

Summary
Dominated by fine-grained patchy carbonate crystals with cross cutting bladed hematite veins intergrown with anhydrite. Anhydrite is the coarsest grained mineral in the sample which is poikiloblastic - contains inclusions of dolomite and rare chalcopyrite. Chalcopyrite and pyrite are present as disseminations throughout the sample with some localised within hematite veins. Chalcopyrite is present with two different textures: fine-grained and anhedral (intergrown with fine bladed hematite) and coarse-grained containing small pyrite crystals (bottom image). Pyrite is rimmed by blebby hematite.

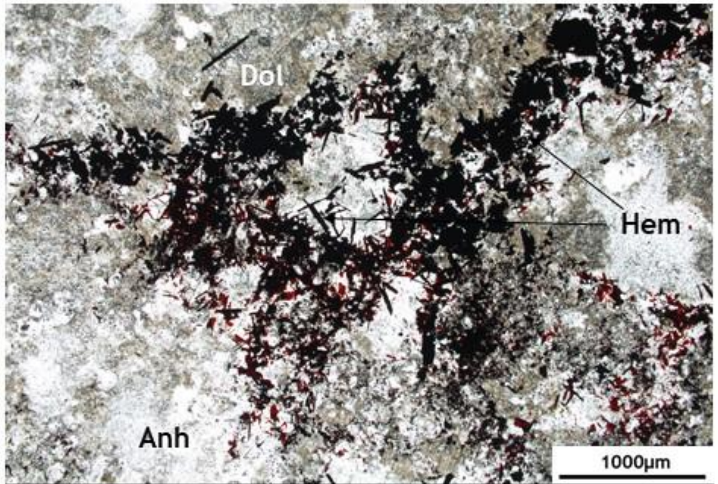

Above: TL image of a vein of fine-grained bladed hematite intergrown with dolomite and anhydrite.
Below: RL image of chalcopyrite present with two different textures.

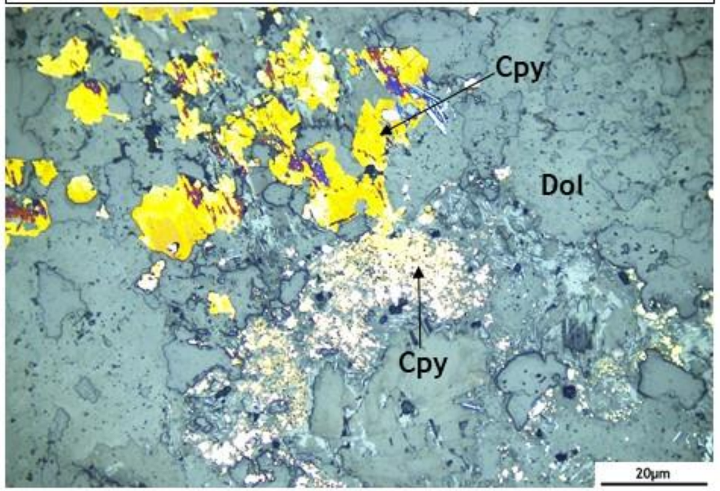

CAR032
623m

Sample Lithology Description:
Hematised siltstone interbedded with sandstone

Veins/Infill
Vein of blue mineral (chalcocite or covellite) running across the width of the thin section. Also cuts through a pale-yellow rounded mineral (pyrite?). Small vein in the middle of a light grey mineral vein - replacing pyrite and chalcopyrite.

Cross cutting hematite vein with pyrite. Small fragments (quartz?) overprinting the vein.

Modal Proportions
70% quartz, 20% hematite, >5% chlorite, trace chalcopyrite, pyrite, and covellite.

Summary
Forming the greater area of the thin section is a finer siltstone lithology composed of fine to medium grained quartz and hematite in a matrix of even finer grained hematite. A contact exists between the siltstone and a second domain of sandstone containing coarser fragments of hematite. Trace chalcopyrite and pyrite (pyrite>chalcopyrite). There are also larger composite clasts of quartz and chlorite within the second domain.

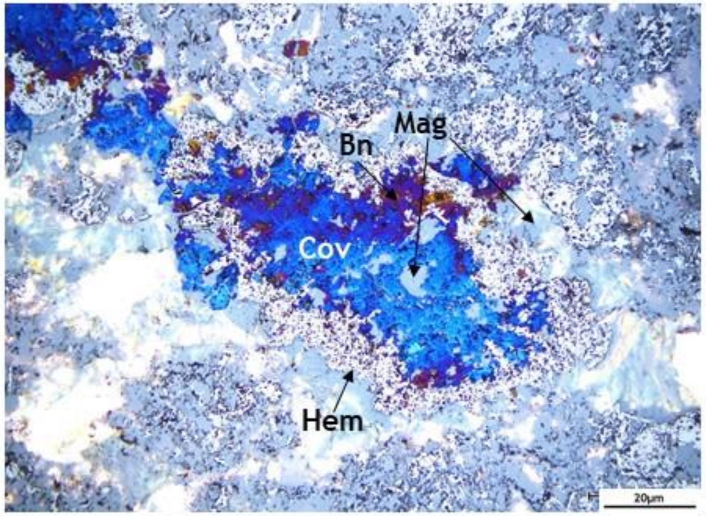

Above: RL image of covellite (deep blue) replacing bornite and rimmed by bladed hematite and magnetite successively.
Below: TL image (PPL) of chlorite within a polymineralic quartz aggregate encasing fragments of hematite.

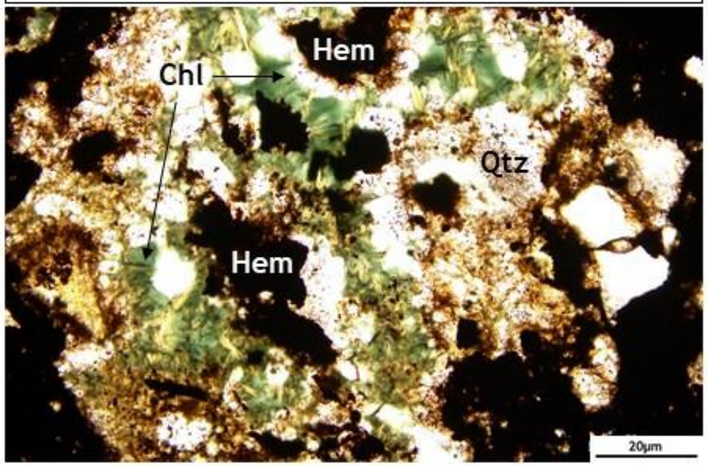

CAR031
966m

Sample Lithology Description:
Chlorite altered granite breccia

Main Fragments
Chlorite altered clasts (up to 2cm)
Quartz clasts (averaging 150 microns)
Steely hematite (averaging 20 microns)

Veins/Infill
One vein composed predominantly of sericite (70 microns thick) cross cuts altered clasts and contains a chalcopyrite crystal at its edge.
Micro quartz veins cross cut chlorite altered clasts.

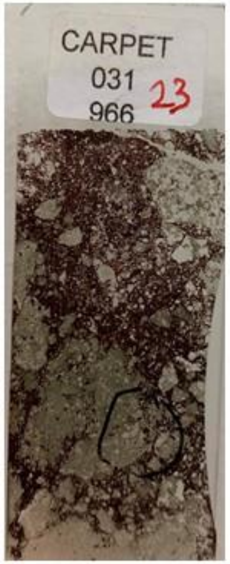

Modal Proportions
40% chlorite, 40% Quartz, 10% hematite, 10% sericite, trace chalcopyrite.

Summary
Macroscopic breccia with coarser clasts, which are variably altered to chlorite and sericite, in a matrix of quartz. The precursor mineral which has been dominantly altered to chlorite is unknown - possibly carbonate? Hematite is associated with chlorite and is less commonly intergrown with sericite. Trace chalcopyrite - inclusions are present in quartz.

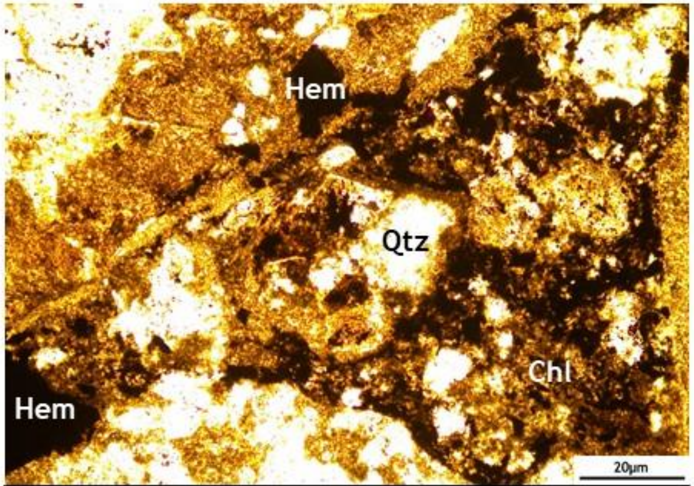

Above: TL image (PPL) of hematite (black) in a matrix of quartz, carbonate and chlorite (variably altering clasts).
Below: RL image of fine bladed hematite wrapping around a chlorite and sericite altered clast.

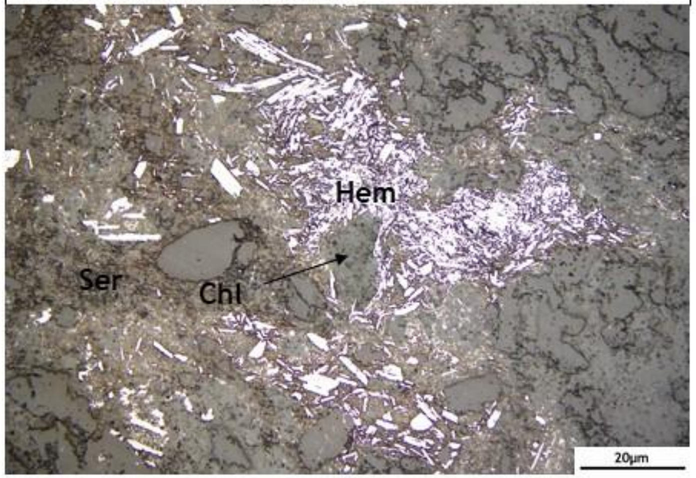

CAR056
719.6M

Sample Lithology Description:
Laminated sequence of colloform-banded, crystalline steely and earthy hematite. Cut by a smaller domain of a fine-grained, massive sericite matrix containing euhedral crystals of apatite.

Veins/Infill
Sericite vein (50 microns thick) follows microfault displacing the laminated sequence of colloform hematite.
Narrower sericite veins (~20 microns thick) cross cutting hematite throughout the sample.

Modal Proportions
95% hematite, 5% sericite, trace apatite and covellite.

REE Hosts
Apatite (hosted in sericite)

Summary
The colloform hematite is comprised of very fine feathery hematite branches linking the broad layers together (which are perpendicular to the branches) and interlaced with microcrystalline (earthy?) hematite. There is a second domain composed of a massive and very fine-grained matrix (possibly sericite) with euhedral crystals of apatite and trace amounts of copper sulphides (possibly covellite).

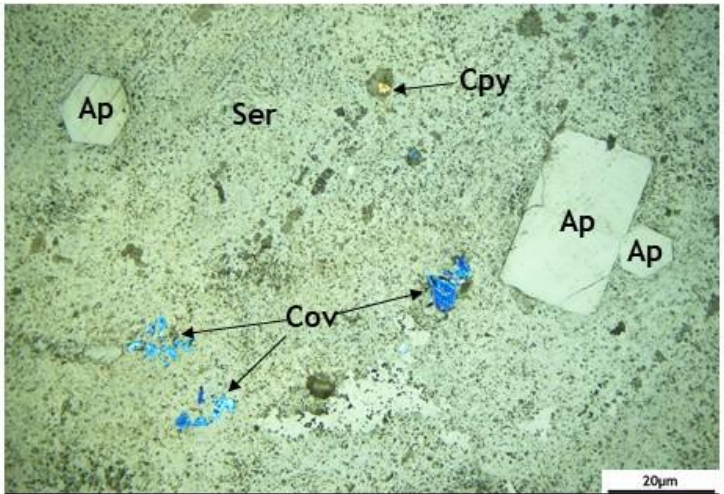

Above: RL image of massive sericite with scattered euhedral apatite crystals and covellite.
Below: RL image of very fine hematite branches linking a sequence of hematite bands (forming the colloform texture).

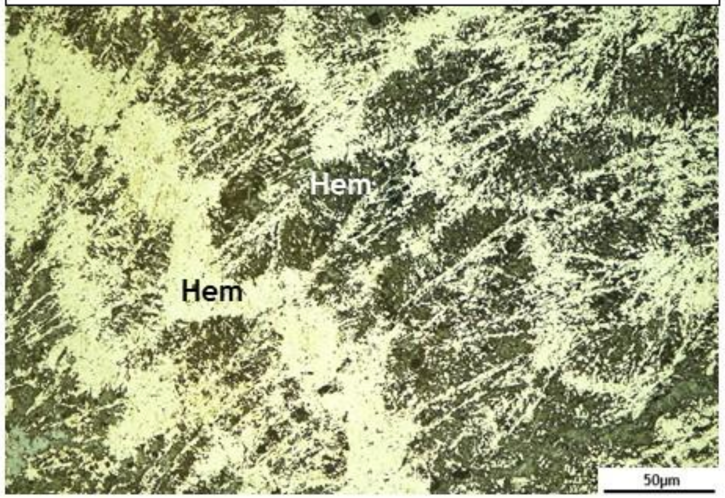

CAR034
508.02m

Sample Lithology Description:
Hematite breccia with quartz veins and quartz clasts. Hematite is present in various crystal habits. Barren of copper sulphides.

Main Fragments
Fan-like hematite averaging 75 microns wide and up to 200 microns long.
Individual blades of hematite averaging 100 microns long.
Granular hematite averaging 20 microns.

Veins/Infill
Quartz veins - variable width with abundant microcrystalline hematite blades.

Modal Proportions
80% hematite, 20% quartz.

Summary
The sample is dominantly composed of hematite with three different crystal habits - fan-like, individual blades (either ~100 microns long or microcrystalline) and granular masses. Quartz is present as both aggregates in veins and granular clusters which surround hematite. The microcrystalline hematite blades (earthy hematite) and granular quartz make up the interstitial material. It is common for the quartz veins to be overgrown by blades of hematite.

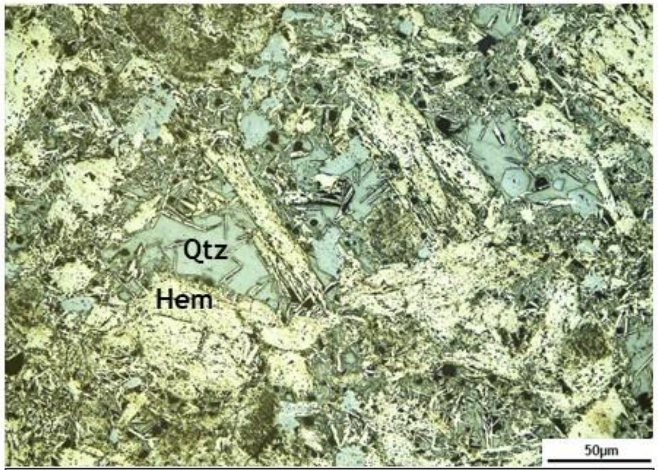

Above: RL image showing the various crystal habits of hematite (cream) - individual and microcrystalline blades.
Below: RL image of a fan-like clast of hematite surrounded by quartz and microcrystalline blades of hematite.

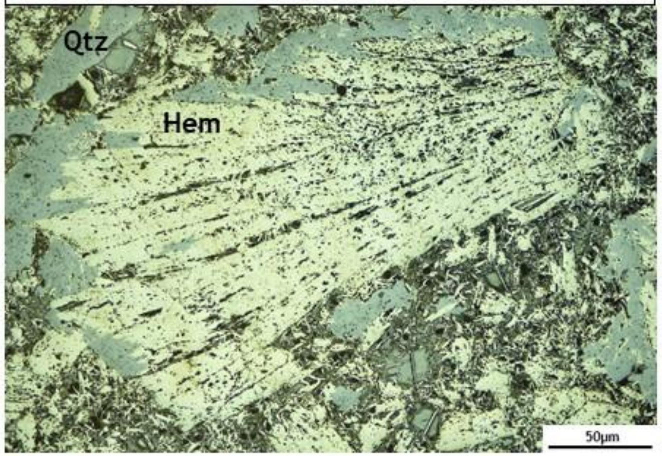

APPENDIX B: EXTENDED METHODS – LA-ICP-MS ANALYSIS OF STANDARDS

Throughout this study, two runs of monazite, xenotime and apatite data were collected. The MAdel monazite (Payne et al., 2008), MG-1 xenotime (Fletcher at al., 2004) and MAD apatite (Thomson et al., 2012) were used as primary standards for both runs which yielded 206Pb/238U ages of 518.82 ± 6.44 Ma (MSWD = 1.86) and 518.35 ± 0.37 Ma (MSWD = 0.87); 489.94 ± 0.96 Ma (MSWD = 1) and 491.30 ± 1.84 Ma (MSWD= 0.41); and 475.92 ± 19.18 Ma (MSWD = 0.0041) and 473.57 ± 0.70 Ma (MSWD= 0.76), respectively. These ages are all within error of their published values of 517.9 ± 2.6 Ma, 490 ± 0.3 Ma and 474.25 ± 0.41 Ma, respectively. Therefore, the U-Pb monazite, xenotime and apatite ages presented in this study are reliable. To perform accuracy checks, the secondary standards 222 (TIMS 206Pb/238U age = 445.55 ± 1.01 Ma; and 448.66 ± 1.33 Ma) and Ambat (TIMS 206Pb/238U age 515.7 ± 1.17 Ma; and 519.79 ± 1.74 Ma) were used for monazite (Adelaide Microscopy in-house), BS-1 (TIMS 206Pb/238U age = 514.44 ± 2.24 Ma; and 517.07 ± 3.99 Ma) (Fletcher et al., 2004) for xenotime and 401 (TIMS 206Pb/238U age = 530 ± 2.33 Ma; and 534.42 ± 2.63 Ma) and OD306 (TIMS 206Pb/238U age = 1595.1 ± 10.7 Ma) for apatite (Thomson et al., 2016). Another secondary standard, McClure (Schoene & Bowring, 2006), was used for the second apatite run. This yielded a 206Pb/238U age of 524.0 ± 16.7 Ma. For the secondary standards 222, Ambat, BS-1, 401 and OD306, the accepted published ages are 450.2 ± 3.4 Ma, 520-525 Ma, 508.9 ± 0.3 Ma, 530.3 ± 1.5 Ma and 1596.7 ± 7.1 Ma, respectively. The NIST610 reference material was used as the primary standard for all minerals to calibrate the 207Pb/206Pb isotopic abundances and correct instrument drift for trace element concentrations.

APPENDIX C: U-PB GEOCHRONOLOGY STANDARD ANALYSES

Samples	$^{207}Pb/^{235}U$	2σ	$^{206}Pb/^{238}U$	2σ	$^{207}Pb/^{235}U$ Age	2σ	$^{206}Pb/^{238}U$ Age	2σ	$^{207}Pb/^{206}Pb$ Age	2σ
Session 1 - Monazite Standards										
MAdel - 1	0.67636	0.02750	0.08368	0.00134	525	21	518	8	580	13
MAdel - 2	0.65978	0.02683	0.08378	0.00134	514	21	519	8	524	11
MAdel - 3	0.64406	0.02619	0.08378	0.00134	505	21	519	8	472	11
MAdel - 4	0.64450	0.02620	0.08291	0.00133	505	21	513	8	506	12
MAdel - 5	0.64713	0.02631	0.08311	0.00133	507	21	515	8	510	11
MAdel - 6	0.64424	0.02619	0.08271	0.00133	505	21	512	8	510	16
MAdel - 7	0.65150	0.02649	0.08316	0.00133	509	21	515	8	527	11
MAdel - 8	0.66557	0.02706	0.08372	0.00134	518	21	518	8	558	14
MAdel - 9	0.69306	0.02818	0.08434	0.00135	535	22	522	8	625	23
MAdel - 10	0.65864	0.02678	0.08510	0.00136	514	21	527	8	497	12
MAdel - 11	0.66361	0.02698	0.08519	0.00137	517	21	527	8	512	11
MAdel - 12	0.64362	0.02617	0.08432	0.00135	505	21	522	8	463	10
MAdel - 13	0.65751	0.02673	0.08394	0.00135	513	21	520	8	514	14
MAdel - 14	0.66771	0.02715	0.08348	0.00134	519	21	517	8	560	15
MAdel - 15	0.64439	0.02620	0.08435	0.00135	505	21	522	8	459	15
MAdel - 16	0.67915	0.02761	0.08386	0.00134	526	21	519	8	582	15
MAdel - 17	0.66425	0.02701	0.08391	0.00134	517	21	519	8	532	16
MAdel - 18	0.65072	0.02646	0.08318	0.00133	509	21	515	8	505	13
MAdel - 19	0.64817	0.02635	0.08284	0.00133	507	21	513	8	498	19
MAdel - 20	0.65503	0.02663	0.08329	0.00133	512	21	516	8	512	14
MAdel - 21	0.65019	0.02644	0.08369	0.00134	509	21	518	8	486	13
222 - 1	0.54195	0.02635	0.07145	0.00138	440	21	445	9	442	12

222 - 2	0.56099	0.02670	0.07167	0.00131	452	22	446	8	512	12
222 - 3	0.55133	0.02543	0.07105	0.00139	446	21	442	9	503	11
222 - 4	0.56171	0.02682	0.07153	0.00143	453	22	445	9	529	13
222 - 5	0.55182	0.02631	0.07150	0.00139	446	21	445	9	494	13
222 - 6	0.54447	0.02559	0.07123	0.00131	441	21	444	8	472	11
222 - 7	0.54000	0.02704	0.07134	0.00136	438	22	444	8	448	13
222 - 8	0.55196	0.02710	0.07199	0.00147	446	22	448	9	477	13
222 - 9	0.54242	0.02634	0.07201	0.00147	440	21	448	9	433	12
222 - 10	0.54633	0.02557	0.07227	0.00140	443	21	450	9	440	10
222 - 11	0.55256	0.02506	0.07163	0.00140	447	20	446	9	480	10
222 - 12	0.53739	0.02458	0.07131	0.00139	437	20	444	9	428	10
222 - 13	0.55054	0.02555	0.07174	0.00145	445	21	447	9	464	11
222 - 14	0.55976	0.02607	0.07155	0.00135	451	21	446	8	504	11
222 - 15	0.54681	0.02471	0.07141	0.00134	443	20	445	8	453	9
222 - 16	0.54176	0.02556	0.07169	0.00142	440	21	446	9	424	10
222 - 17	0.55383	0.02603	0.07159	0.00136	448	21	446	8	471	11
222 - 18	0.55667	0.02561	0.07127	0.00144	449	21	444	9	492	10
Ambat - 1	0.64145	0.02986	0.08203	0.00163	503	23	508	10	511	11
Ambat - 2	0.66990	0.03068	0.08449	0.00166	521	24	523	10	541	11
Ambat - 3	0.64678	0.03043	0.08264	0.00158	506	24	512	10	523	12
Ambat - 4	0.65045	0.03012	0.08426	0.00167	509	24	522	10	492	11
Ambat - 5	0.64642	0.02980	0.08206	0.00151	506	23	508	9	538	12
Ambat - 6	0.66589	0.03123	0.08296	0.00160	518	24	514	10	579	14
Ambat - 7	0.64441	0.03048	0.08347	0.00161	505	24	517	10	492	11
Ambat - 8	0.63853	0.03036	0.08229	0.00165	501	24	510	10	503	11
Ambat - 9	0.63973	0.02924	0.08246	0.00154	502	23	511	10	498	11
Ambat - 10	0.64802	0.02997	0.08312	0.00161	507	23	515	10	508	11

Ambat - 11	0.65644	0.03127	0.08442	0.00172	512	24	522	11	497	12
Ambat - 12	0.65613	0.03002	0.08408	0.00162	512	23	520	10	505	11
Ambat - 13	0.66342	0.03092	0.08397	0.00160	517	24	520	10	526	12
Ambat - 14	0.65874	0.03163	0.08373	0.00169	514	25	518	10	517	13
Ambat - 15	0.64202	0.02951	0.08292	0.00165	504	23	514	10	477	11
Ambat - 16	0.65730	0.03002	0.08387	0.00162	513	23	519	10	504	11
Ambat - 17	0.66344	0.03042	0.08340	0.00159	517	24	516	10	532	11
Ambat - 18	0.64764	0.02982	0.08348	0.00162	507	23	517	10	478	10
Session 2 - Monazite Standards										
MAdel - 1	0.65466	0.00616	0.08441	0.00117	511	5	522	7	491	14
MAdel - 2	0.66071	0.00621	0.08303	0.00115	515	5	514	7	548	16
MAdel - 3	0.65537	0.00481	0.08362	0.00079	512	4	518	5	538	14
MAdel - 4	0.65979	0.00484	0.08387	0.00080	514	4	519	5	546	16
MAdel - 5	0.65908	0.00640	0.08323	0.00085	514	5	515	5	541	14
MAdel - 6	0.65616	0.00637	0.08426	0.00086	512	5	521	5	504	14
MAdel - 7	0.65466	0.00813	0.08369	0.00012	511	6	518	1	473	15
MAdel - 8	0.66045	0.00821	0.08377	0.00012	515	6	519	1	492	13
MAdel - 9	0.66201	0.02526	0.08379	0.00131	516	20	519	8	520	15
MAdel - 10	0.65355	0.02494	0.08370	0.00131	511	19	518	8	496	14
MAdel - 11	0.64217	0.02597	0.08294	0.00145	504	20	514	9	555	15
MAdel - 12	0.67339	0.02723	0.08456	0.00148	523	21	523	9	614	16
MAdel - 13	0.66301	0.01117	0.08337	0.00072	516	9	516	4	548	15
MAdel - 14	0.65195	0.01098	0.08410	0.00073	510	9	521	5	495	14
MAdel - 15	0.65758	0.00030	0.08373	0.00000	513	0	518	0	594	15
222 - 1	0.54404	0.01863	0.07212	0.00143	441	15	449	9	432	13
222 - 2	0.55603	0.01647	0.07192	0.00112	449	13	448	7	506	12
222 - 3	0.54402	0.01745	0.07154	0.00122	441	14	445	8	450	12

222 - 4	0.56300	0.02039	0.07217	0.00096	453	16	449	6	470	14
222 - 5	0.53497	0.02506	0.07115	0.00147	435	20	443	9	415	10
222 - 6	0.53427	0.02991	0.07224	0.00164	435	24	450	10	450	16
222 - 7	0.55959	0.02022	0.07225	0.00119	451	16	450	7	495	14
222 - 8	0.54160	0.01881	0.07299	0.00122	439	15	454	8	469	12
Ambat - 1	0.65355	0.02337	0.08415	0.00249	511	18	521	15	496	15
Ambat - 2	0.64250	0.02106	0.08407	0.00167	504	17	520	10	479	14
Ambat - 3	0.63709	0.02165	0.08139	0.00140	501	17	504	9	519	16
Ambat - 4	0.66633	0.02171	0.08300	0.00139	518	17	514	9	537	16
Ambat - 5	0.66918	0.02062	0.08386	0.00109	520	16	519	7	539	14
Ambat - 6	0.63863	0.03097	0.08375	0.00188	501	24	518	12	508	15
Ambat - 7	0.66723	0.03284	0.08423	0.00193	519	26	521	12	551	14
Ambat - 8	0.64803	0.02361	0.08488	0.00132	507	18	525	8	521	14
Session 1 - Xenotime Standards										
MG-1 - 1	0.62356	0.01640	0.07887	0.00106	492	13	489	7	500	24
MG-1 - 2	0.61879	0.01627	0.07928	0.00107	489	13	492	7	471	21
MG-1 - 3	0.61675	0.01622	0.07872	0.00106	488	13	488	7	484	22
MG-1 - 4	0.61966	0.01629	0.07932	0.00107	490	13	492	7	472	19
MG-1 - 5	0.62198	0.01635	0.07865	0.00106	491	13	488	7	506	19
MG-1 - 6	0.59790	0.01572	0.07936	0.00107	476	13	492	7	397	16
MG-1 - 7	0.62306	0.01638	0.07883	0.00106	492	13	489	7	502	20
MG-1 - 8	0.62243	0.01637	0.07816	0.00105	491	13	485	7	522	21
MG-1 - 9	0.62036	0.01631	0.07958	0.00107	490	13	494	7	474	20
MG-1 - 10	0.62688	0.01648	0.07847	0.00106	494	13	487	7	524	21
MG-1 - 11	0.62920	0.01654	0.07996	0.00108	496	13	496	7	490	23
MG-1 - 12	0.62867	0.01653	0.07844	0.00106	495	13	487	7	532	21
BS-1 - 1	0.65651	0.05042	0.08293	0.00271	512	39	514	17	497	35

BS-1 - 2	0.69363	0.05901	0.08320	0.00267	535	46	515	17	611	52
BS-1 - 3	0.65506	0.04963	0.08385	0.00246	512	39	519	15	476	35
BS-1 - 4	0.59155	0.05430	0.08094	0.00246	472	43	502	15	328	29
BS-1 - 5	0.64720	0.05581	0.08258	0.00245	507	44	511	15	482	38
BS-1 - 6	0.66440	0.05917	0.08133	0.00271	517	46	504	17	572	50
BS-1 - 7	0.62838	0.05070	0.08219	0.00258	495	40	509	16	426	33
BS-1 - 8	0.62791	0.05208	0.08475	0.00248	495	41	524	15	360	28
BS-1 - 9	0.65482	0.05960	0.08334	0.00253	511	47	516	16	490	43
BS-1 - 10	0.66036	0.06216	0.08452	0.00280	515	48	523	17	477	42
BS-1 - 11	0.67403	0.04938	0.08402	0.00260	523	38	520	16	537	39
BS-1 - 12	0.66006	0.05223	0.08331	0.00262	515	41	516	16	508	36
Session 2 - Xenotime Standards										
MG-1 - 1	0.62356	0.01640	0.07887	0.00106	492	13	489	7	500	24
MG-1 - 2	0.61879	0.01627	0.07928	0.00107	489	13	492	7	471	21
MG-1 - 3	0.61675	0.01622	0.07872	0.00106	488	13	488	7	484	22
MG-1 - 4	0.61966	0.01629	0.07932	0.00107	490	13	492	7	472	19
MG-1 - 5	0.62198	0.01635	0.07865	0.00106	491	13	488	7	506	19
MG-1 - 6	0.59790	0.01572	0.07936	0.00107	476	13	492	7	397	16
MG-1 - 7	0.62306	0.01638	0.07883	0.00106	492	13	489	7	502	20
MG-1 - 8	0.62243	0.01637	0.07816	0.00105	491	13	485	7	522	21
MG-1 - 9	0.62036	0.01631	0.07958	0.00107	490	13	494	7	474	20
MG-1 - 10	0.62688	0.01648	0.07847	0.00106	494	13	487	7	524	21
MG-1 - 11	0.62920	0.01654	0.07996	0.00108	496	13	496	7	490	23
MG-1 - 12	0.62867	0.01653	0.07844	0.00106	495	13	487	7	532	21
BS-1 - 1	0.65651	0.05042	0.08293	0.00271	512	39	514	17	497	35
BS-1 - 2	0.69363	0.05901	0.08320	0.00267	535	46	515	17	611	52
BS-1 - 3	0.65506	0.04963	0.08385	0.00246	512	39	519	15	476	35

BS-1 - 4	0.59155	0.05430	0.08094	0.00246	472	43	502	15	328	29		
BS-1 - 5	0.64720	0.05581	0.08258	0.00245	507	44	511	15	482	38		
BS-1 - 6	0.66440	0.05917	0.08133	0.00271	517	46	504	17	572	50		
BS-1 - 7	0.62838	0.05070	0.08219	0.00258	495	40	509	16	426	33		
BS-1 - 8	0.62791	0.05208	0.08475	0.00248	495	41	524	15	360	28		
BS-1 - 9	0.65482	0.05960	0.08334	0.00253	511	47	516	16	490	43		
BS-1 - 10	0.66036	0.06216	0.08452	0.00280	515	48	523	17	477	42		
BS-1 - 11	0.67403	0.04938	0.08402	0.00260	523	38	520	16	537	39		
BS-1 - 12	0.66006	0.05223	0.08331	0.00262	515	41	516	16	508	36		
Session 1 - Apatite Standards												
MAD - 1	0.58339	0.02152	0.07392	0.00273	467	17	460	17	479	47		
MAD - 2	0.59921	0.02210	0.07576	0.00280	477	18	471	17	480	46		
MAD - 3	0.59452	0.02193	0.07497	0.00277	474	17	466	17	486	47		
MAD - 4	0.62708	0.02313	0.07927	0.00293	494	18	492	18	473	45		
MAD - 5	0.61856	0.02281	0.07837	0.00290	489	18	486	18	472	45		
MAD - 6	0.60936	0.02248	0.07708	0.00285	483	18	479	18	477	46		
MAD - 7	0.59575	0.02197	0.07576	0.00280	475	18	471	17	474	46		
MAD - 8	0.58943	0.02174	0.07530	0.00278	471	17	468	17	475	46		
MAD - 9	0.61330	0.02262	0.07786	0.00288	486	18	483	18	474	45		
MAD - 10	0.58775	0.02168	0.07433	0.00275	469	17	462	17	485	47		
MAD - 11	0.60185	0.02220	0.07671	0.00283	478	18	476	18	468	45		
MAD - 12	0.60523	0.02232	0.07719	0.00285	481	18	479	18	475	46		
MAD - 13	0.58906	0.02173	0.07474	0.00276	470	17	465	17	478	47		
MAD - 14	0.59965	0.02212	0.07605	0.00281	477	18	472	17	480	47		
MAD - 15	0.61524	0.02269	0.07791	0.00288	487	18	484	18	471	46		
MAD - 16	0.59781	0.02205	0.07580	0.00280	476	18	471	17	474	46		
MAD - 17	0.59755	0.02204	0.07577	0.00280	476	18	471	17	469	46		

MAD - 18	0.58664	0.02164	0.07464	0.00276	469	17	464	17	461	45
MAD - 19	0.60259	0.02223	0.07627	0.00282	479	18	474	18	473	46
MAD - 20	0.61221	0.02258	0.07790	0.00288	485	18	484	18	465	45
MAD - 21	0.59955	0.02211	0.07611	0.00281	477	18	473	17	467	46
MAD - 22	0.60738	0.02240	0.07685	0.00284	482	18	477	18	487	47
MAD - 23	0.59170	0.02182	0.07496	0.00277	472	17	466	17	471	47
MAD - 24	0.61391	0.02264	0.07742	0.00286	486	18	481	18	480	47
MAD - 25	0.58284	0.02150	0.07363	0.00272	466	17	458	17	490	49
MAD - 26	0.59452	0.02193	0.07561	0.00279	474	17	470	17	474	47
MAD - 27	0.59922	0.02210	0.07560	0.00279	477	18	470	17	487	48
MAD - 28	0.61835	0.02281	0.07865	0.00291	489	18	488	18	471	46
MAD - 29	0.59844	0.02207	0.07579	0.00280	476	18	471	17	486	48
MAD - 30	0.59719	0.02203	0.07564	0.00279	475	18	470	17	479	48
MAD - 31	0.61463	0.02267	0.07798	0.00288	486	18	484	18	477	47
MAD - 32	0.59771	0.02205	0.07590	0.00280	476	18	472	17	471	46
401 - 1	0.87968	0.10003	0.08621	0.00441	641	73	533	27	1016	111
401 - 2	0.74124	0.09081	0.08481	0.00488	563	69	525	30	695	82
401 - 3	0.87441	0.09976	0.08896	0.00463	638	73	549	29	932	102
401 - 4	0.91780	0.10267	0.08527	0.00428	661	74	527	26	1126	120
401 - 5	0.81704	0.09716	0.08692	0.00437	606	72	537	27	846	97
401 - 6	0.86160	0.09976	0.08567	0.00431	631	73	530	27	993	110
401 - 7	0.84450	0.09768	0.08773	0.00438	622	72	542	27	908	101
401 - 8	0.66043	0.08522	0.08637	0.00432	515	66	534	27	417	52
401 - 9	0.87778	0.10129	0.08608	0.00457	640	74	532	28	1024	113
401 - 10	0.86845	0.10031	0.08335	0.00439	635	73	516	27	1072	119
401 - 11	0.51085	0.07394	0.08462	0.00425	419	61	524	26	0	0
401 - 12	0.56049	0.07846	0.08372	0.00441	452	63	518	27	99	14

401 - 13	0.65328	0.08552	0.08617	0.00436	510	67	533	27	388	49
401 - 14	0.74236	0.09120	0.08216	0.00415	564	69	509	26	766	91
401 - 15	0.72346	0.11856	0.08482	0.00438	553	91	525	27	647	109
401 - 16	0.76857	0.09280	0.08384	0.00433	579	70	519	27	802	93
401 - 17	0.89420	0.10126	0.08480	0.00425	649	73	525	26	1083	117
401 - 18	0.78323	0.09379	0.08446	0.00424	587	70	523	26	823	95
401 - 19	0.88625	0.10103	0.08737	0.00437	644	73	540	27	999	109
401 - 20	0.96445	0.17596	0.08336	0.00458	686	125	516	28	1266	222
401 - 21	1.01405	0.10982	0.08532	0.00429	711	77	528	27	1312	135
401 - 22	0.88932	0.10150	0.08513	0.00428	646	74	527	26	1065	117
401 - 23	0.78203	0.09542	0.08690	0.00444	587	72	537	27	763	90
401 - 24	0.84080	0.09857	0.08697	0.00459	620	73	538	28	910	102
401 - 25	0.75556	0.09362	0.08531	0.00431	571	71	528	27	729	87
401 - 26	0.74479	0.09263	0.08553	0.00440	565	70	529	27	689	83
401 - 27	0.92123	0.10438	0.08623	0.00434	663	75	533	27	1109	120
401 - 28	0.65241	0.08560	0.08603	0.00464	510	67	532	29	382	49
401 - 29	0.93345	0.13767	0.08679	0.00437	669	99	537	27	1124	164
401 - 30	0.59009	0.08179	0.09111	0.00472	471	65	562	29	21	3
401 - 31	0.93737	0.10521	0.08651	0.00454	672	75	535	28	1135	122
401 - 32	0.86043	0.10033	0.08509	0.00435	630	74	526	27	1009	113
OD306 - 1	4.02532	0.27766	0.28660	0.01217	1639	113	1624	69	1635	90
OD306 - 2	4.01444	0.28680	0.27872	0.01182	1637	117	1585	67	1680	97
OD306 - 3	33.58517	2.15852	0.71925	0.03709	3598	231	3493	180	3642	76
OD306 - 4	3.91164	0.27115	0.28449	0.01193	1616	112	1614	68	1601	85
OD306 - 5	10.18044	0.95148	0.37952	0.01879	2451	229	2074	103	2767	161
OD306 - 6	3.99367	0.23558	0.28254	0.01185	1633	96	1604	67	1655	71
OD306 - 7	4.07476	0.27224	0.28934	0.01214	1649	110	1638	69	1647	87

OD306 - 8	5.56968	0.72350	0.29496	0.01349	1911	248	1666	76	2175	210
OD306 - 9	34.32117	1.66424	0.72349	0.03066	3619	176	3509	149	3664	63
OD306 - 10	4.27888	0.28727	0.28505	0.01211	1689	113	1617	69	1764	92
OD306 - 11	4.14118	0.29328	0.28874	0.01236	1662	118	1635	70	1677	99
OD306 - 12	4.05818	0.25919	0.28656	0.01230	1646	105	1624	70	1654	84
OD306 - 13	3.79424	0.27344	0.27900	0.01198	1592	115	1586	68	1578	90
OD306 - 14	4.13983	0.30251	0.28541	0.01242	1662	121	1619	70	1699	105
OD306 - 15	4.08643	0.26349	0.29225	0.01304	1652	106	1653	74	1627	88
OD306 - 16	3.82235	0.24828	0.28387	0.01229	1597	104	1611	70	1562	79
Session 2 - Apatite Standards										
MAD - 1	0.58424	0.02643	0.07624	0.00000	467	21	474	0	477	63
MAD - 2	0.62598	0.02832	0.07620	0.00229	494	22	473	14	478	62
MAD - 3	0.59733	0.02702	0.07747	0.00218	476	22	481	14	476	62
MAD - 4	0.57827	0.02616	0.07495	0.00211	463	21	466	13	478	64
MAD - 5	0.59637	0.02698	0.07661	0.00065	475	21	476	4	479	63
MAD - 6	0.59113	0.02674	0.07587	0.00064	472	21	471	4	476	63
MAD - 7	0.60316	0.02729	0.07602	0.00263	479	22	472	16	475	62
MAD - 8	0.60594	0.02741	0.07640	0.00264	481	22	475	16	476	63
MAD - 9	0.60728	0.02747	0.07782	0.00333	482	22	483	21	477	63
MAD - 10	0.58174	0.02632	0.07455	0.00319	466	21	464	20	479	64
MAD - 11	0.60586	0.02741	0.07735	0.00267	481	22	480	17	475	63
MAD - 12	0.58794	0.02660	0.07514	0.00259	470	21	467	16	476	63
MAD - 13	0.57367	0.02595	0.07517	0.00283	460	21	467	18	478	64
MAD - 14	0.59126	0.02675	0.07741	0.00291	472	21	481	18	475	63
MAD - 15	0.57605	0.02606	0.07493	0.00241	462	21	466	15	477	64
MAD - 16	0.59683	0.02700	0.07757	0.00250	475	22	482	16	479	63
MAD - 17	0.60955	0.02758	0.07690	0.00152	483	22	478	9	477	63

MAD - 18	0.59872	0.02709	0.07553	0.00149	476	22	469	9	479	63
MAD - 19	0.61431	0.02779	0.07678	0.00292	486	22	477	18	476	62
MAD - 20	0.60455	0.02735	0.07561	0.00288	480	22	470	18	477	62
MAD - 21	0.61727	0.02793	0.07790	0.00292	488	22	484	18	477	62
MAD - 22	0.59016	0.02670	0.07454	0.00279	471	21	463	17	477	64
MAD - 23	0.59542	0.02694	0.07579	0.00109	474	21	471	7	475	63
MAD - 24	0.60357	0.02731	0.07669	0.00110	479	22	476	7	478	63
MAD - 25	0.61030	0.02761	0.07674	0.00083	484	22	477	5	477	62
MAD - 26	0.60287	0.02728	0.07573	0.00082	479	22	471	5	479	63
MAD - 27	0.61578	0.02786	0.07617	0.00065	487	22	473	4	476	62
MAD - 28	0.61711	0.02792	0.07630	0.00065	488	22	474	4	476	62
MAD - 29	0.61851	0.02798	0.07664	0.00109	489	22	476	7	476	62
MAD - 30	0.61229	0.02770	0.07585	0.00107	485	22	471	7	476	62
MAD - 31	0.60979	0.02759	0.07571	0.00149	483	22	470	9	476	62
MAD - 32	0.61837	0.02798	0.07677	0.00151	489	22	477	9	476	62
401 - 1	0.73702	0.12005	0.07895	0.00456	561	91	490	28	754	119
401 - 2	0.76995	0.13153	0.08523	0.00487	580	99	527	30	694	116
401 - 3	0.87438	0.15257	0.08820	0.00493	638	111	545	30	1005	168
401 - 4	0.77104	0.13161	0.08910	0.00521	580	99	550	32	722	116
401 - 5	0.79454	0.12691	0.08727	0.00432	594	95	539	27	809	125
401 - 6	0.81983	0.14291	0.09147	0.00446	608	106	564	28	777	136
401 - 7	0.76456	0.12427	0.08841	0.00535	577	94	546	33	668	105
401 - 8	0.94564	0.15201	0.09054	0.00621	676	109	559	38	1058	155
401 - 9	0.76038	0.12441	0.08462	0.00555	574	94	524	34	778	124
401 - 10	0.86101	0.13399	0.08748	0.00571	631	98	541	35	970	146
401 - 11	0.74875	0.12408	0.08774	0.00525	567	94	542	32	666	107
401 - 12	0.73235	0.12248	0.08832	0.00533	558	93	546	33	604	102

401 - 13	0.80647	0.12868	0.09116	0.00560	600	96	562	35	793	122
401 - 14	0.73102	0.12251	0.09179	0.00566	557	93	566	35	571	93
401 - 15	0.75279	0.13031	0.08800	0.00515	570	99	544	32	705	131
401 - 16	0.68948	0.11852	0.08993	0.00566	532	92	555	35	462	77
401 - 17	0.70530	0.13065	0.08515	0.00473	542	100	527	29	568	98
401 - 18	0.77411	0.12580	0.08662	0.00457	582	95	536	28	738	116
401 - 19	0.78153	0.12761	0.08535	0.00544	586	96	528	34	770	122
401 - 20	0.77412	0.13399	0.08561	0.00542	582	101	530	34	741	131
401 - 21	0.97153	0.16319	0.08613	0.00534	689	116	533	33	1214	189
401 - 22	0.76709	0.12460	0.08479	0.00527	578	94	525	33	765	121
401 - 23	0.79017	0.13771	0.08762	0.00472	591	103	541	29	772	134
401 - 24	0.78367	0.12786	0.08141	0.00453	588	96	505	28	907	143
401 - 25	0.79520	0.12945	0.08468	0.00431	594	97	524	27	833	132
401 - 26	0.68284	0.11792	0.08497	0.00467	528	91	526	29	495	83
401 - 27	0.77981	0.12585	0.08614	0.00421	585	94	533	26	721	113
401 - 28	0.85367	0.13240	0.08534	0.00419	627	97	528	26	928	139
401 - 29	0.84818	0.13210	0.08382	0.00430	624	97	519	27	957	144
401 - 30	0.82830	0.12965	0.08296	0.00425	613	96	514	26	929	141
401 - 31	0.85334	0.13174	0.08603	0.00487	626	97	532	30	920	137
401 - 32	0.77202	0.12911	0.08176	0.00470	581	97	507	29	816	137
McClure - 1	2.00679	0.21734	0.09414	0.00480	1118	121	580	30	2320	231
McClure - 2	2.21406	0.20056	0.09815	0.00459	1185	107	604	28	2510	194
McClure - 3	2.70524	0.28343	0.10142	0.00491	1330	139	623	30	2770	277
McClure - 4	3.75376	0.35541	0.10946	0.00628	1583	150	670	38	3156	243
McClure - 5	3.42672	0.35418	0.10490	0.00719	1511	156	643	44	3095	308
McClure - 6	3.25534	0.32502	0.10793	0.00635	1470	147	661	39	2971	257
McClure - 7	2.82313	0.29189	0.10695	0.00695	1362	141	655	43	2790	264

McClure - 8	3.16311	0.26336	0.10836	0.00583	1448	121	663	36	2936	205
McClure - 9	3.81859	0.69320	0.11431	0.01112	1597	290	698	68	3107	220
McClure - 10	2.83190	0.28312	0.10052	0.00582	1364	136	617	36	2839	251
McClure - 11	3.77517	0.32024	0.11409	0.00516	1587	135	696	31	3105	219
McClure - 12	2.47584	0.27067	0.10054	0.00469	1265	138	618	29	2606	236
McClure - 13	3.90065	0.39003	0.10366	0.00561	1614	161	636	34	3268	300
McClure - 14	3.88374	0.56435	0.11440	0.01015	1610	234	698	62	3108	265
McClure - 15	2.29054	0.23286	0.09763	0.00491	1209	123	601	30	2505	223

APPENDIX D: U-PB GEOCHRONOLOGY MONAZITE ANALYSES

Samples	$^{207}Pb/^{235}U$	2σ	$^{206}Pb/^{238}U$	2σ	$^{207}Pb/^{235}U$ Age	2σ	$^{206}Pb/^{238}U$ Age	2σ	$^{207}Pb/^{206}Pb$ Age	2σ
Bn Zone - GranM 1	5.55126	0.41126	0.21653	0.01082	1909	141	1264	63	2721	79
Bn Zone - GranM 2	4.44488	0.32661	0.16844	0.00778	1721	126	1004	46	2764	110
Bn Zone - GranM 3	3.81156	0.26432	0.16093	0.00670	1595	111	962	40	2583	48
Bn Zone - GranM 4	4.23452	0.29491	0.18696	0.00773	1681	117	1105	46	2510	58
Bn Zone - GranM 5	3.98483	0.38366	0.15580	0.01161	1631	157	933	70	2715	51
Bn Zone - GranM 6	5.73695	0.41894	0.20241	0.00851	1937	141	1188	50	2879	86
Bn Zone - GranM 7	6.10509	0.63720	0.20953	0.01716	1991	208	1226	100	2917	161
Bn Zone - GranM 8	5.18341	0.53322	0.20845	0.01395	1850	190	1221	82	2656	129
Bn Zone - GranM 9	4.95997	0.49060	0.21519	0.01475	1813	179	1256	86	2576	141
Bn Zone - GranM 10	6.21092	0.47939	0.24344	0.01047	2006	155	1405	60	2696	122
Bn Zone - GranM 11	6.68483	0.76869	0.21554	0.01618	2071	238	1258	94	3013	151
Bn Zone - GranM 12	3.94408	0.32036	0.13711	0.00656	1623	132	828	40	2892	105
Bn Zone - GranM 13	4.72005	0.32503	0.18113	0.00704	1771	122	1073	42	2730	77
Bn Zone - GranM 14	4.06092	0.39207	0.15209	0.01321	1646	159	913	79	2772	104
Bn Zone - GranM 15	4.75510	0.46473	0.16464	0.01421	1777	174	982	85	2899	83
Bn Zone - GranM 16	2.80341	0.37007	0.11762	0.01270	1356	179	717	77	2582	83
Bn Zone - GranM 17	2.13897	0.19968	0.08249	0.00613	1161	108	511	38	2707	72
Bn Zone - GranM 18	5.44169	0.40567	0.22259	0.00945	1891	141	1296	55	2615	104
Bn Zone - GranM 19	5.65961	0.40408	0.21275	0.00912	1925	137	1243	53	2758	81
Bn Zone - GranM 20	4.91313	0.41296	0.19170	0.01050	1805	152	1131	62	2692	134
Bn Zone - GranM 21	3.35257	0.97057	0.13955	0.03550	1493	432	842	214	2637	249
Bn Zone - GranM 22	7.12038	2.35537	0.22450	0.04491	2127	703	1306	261	3123	423
Bn Zone - GranM 23	3.14227	0.42473	0.12897	0.01210	1443	195	782	73	2599	105

Bn Zone - GranM 24	5.12587	0.43624	0.20457	0.01187	1840	157	1200	70	2658	84
Bn Zone - GranM 25	7.24597	0.84437	0.24034	0.01627	2142	250	1388	94	2953	155
Bn Zone - GranM 26	4.15859	0.30678	0.16173	0.00873	1666	123	966	52	2690	88
Bn Zone - GranM 27	3.98754	0.42688	0.14308	0.01171	1632	175	862	71	2827	113
Bn Zone - GranM 28	1.68620	0.25982	0.06691	0.01062	1003	155	418	66	2658	94
Bn Zone - GranM 29	3.53339	0.29973	0.16293	0.00924	1535	130	973	55	2408	67
Bn Zone - GranM 30	2.01169	0.28673	0.07662	0.00942	1119	160	476	59	2717	100
Bn Zone - GranM 31	5.32340	0.43752	0.19695	0.00935	1873	154	1159	55	2772	86
Bn Zone - GranM 32	6.65320	1.24995	0.24030	0.03818	2066	388	1388	221	2804	234
Bn Zone - GranM 33	6.10548	0.91562	0.22976	0.02408	1991	299	1333	140	2741	152
Bn Zone - GranM 34	0.94012	0.14656	0.03597	0.00501	673	105	228	32	2811	91
Bn Zone - GranM 35	4.72867	0.33124	0.18219	0.00810	1772	124	1079	48	2704	86
Bn Zone - GranM 36	3.98438	0.47289	0.14263	0.01457	1631	194	860	88	2818	87
Bn Zone - GranM 37	5.39598	0.65560	0.19939	0.01957	1884	229	1172	115	2771	107
Bn Zone - GranM 38	5.47669	0.39999	0.21644	0.00965	1897	139	1263	56	2660	72
Cpy Zone - DolM 1	3.02249	0.20279	0.25005	0.00884	1413	95	1439	51	1391	31
Cpy Zone - DolM 2	2.78260	0.18470	0.23359	0.00836	1351	90	1353	48	1363	28
Cpy Zone - DolM 3	2.77379	0.20562	0.22769	0.00971	1349	100	1322	56	1408	33
Cpy Zone - DolM 4	2.84027	0.18903	0.22794	0.00824	1366	91	1324	48	1447	32
Cpy Zone - DolM 5	4.39777	0.31938	0.30718	0.01243	1712	124	1727	70	1709	63
Cpy Zone - DolM 6	3.32764	0.25298	0.25096	0.00978	1488	113	1443	56	1571	51
Cpy Zone - DolM 7	2.81409	0.21239	0.22797	0.00908	1359	103	1324	53	1430	62
Cpy Zone - DolM 8	3.20068	0.29143	0.25291	0.01188	1457	133	1453	68	1478	100
Cpy Zone - DolM 9	2.98534	0.22153	0.24429	0.00909	1404	104	1409	52	1420	53
Cpy Zone - DolM 10	2.84131	0.28616	0.23594	0.01638	1367	138	1366	95	1385	75
Cpy Zone - DolM 11	2.76573	0.18774	0.22823	0.00874	1346	91	1325	51	1409	39
Cpy Zone - DolM 12	2.90505	0.21497	0.24502	0.00927	1383	102	1413	53	1365	55

Barren Zone - M1	7.32815	0.76606	0.23227	0.01007	2152	225	1346	58	3071	321
Barren Zone - M2	3.38002	0.30115	0.16041	0.00948	1500	134	959	57	2387	174
Barren Zone - M3	2.58526	0.25964	0.15294	0.01709	1296	130	917	103	2031	184
Barren Zone - M4	3.57991	0.22105	0.19032	0.00602	1545	95	1123	36	2216	111
Barren Zone - M5	3.45164	0.41643	0.18848	0.02896	1516	183	1113	171	2185	255
Barren Zone - M6	3.25692	0.47930	0.17400	0.02549	1471	216	1034	152	2191	452
Barren Zone - M7	5.24346	0.41670	0.28834	0.01368	1860	148	1633	77	2179	154
Barren Zone - M8	5.65013	0.41205	0.24203	0.01721	1924	140	1397	99	2574	231
Barren Zone - M9	4.85755	0.58671	0.16229	0.01778	1795	217	970	106	2974	175
Barren Zone - M10	6.64829	0.29703	0.25394	0.01016	2066	92	1459	58	2739	105
Barren Zone - M11	4.08049	0.36155	0.21538	0.01102	1650	146	1257	64	2244	187
Barren Zone - M12	3.22826	0.19484	0.19247	0.00638	1464	88	1135	38	1986	106
Barren Zone - M13	5.40456	0.41144	0.23324	0.01187	1886	144	1351	69	2551	200
Barren Zone - M14	4.03077	0.25540	0.24459	0.01462	1640	104	1411	84	1965	93
Barren Zone - M15	2.89976	0.46138	0.17077	0.02697	1382	220	1016	160	2055	133
Barren Zone - M16	5.09899	0.33714	0.25326	0.01008	1836	121	1455	58	2311	107
Barren Zone - M17	4.12860	0.21672	0.23201	0.00794	1660	87	1345	46	2089	91
Barren Zone - M18	6.36603	0.40765	0.23181	0.01192	2028	130	1344	69	2825	92
Barren Zone - M19	3.34697	0.18067	0.18134	0.00658	1492	81	1074	39	2158	116
Barren Zone - M20	6.96000	1.99109	0.23224	0.01008	2106	603	1346	58	2973	824
Barren Zone - M21	3.24109	0.22481	0.18482	0.00666	1467	102	1093	39	2079	108
Barren Zone - M22	5.98474	0.37845	0.21529	0.00675	1974	125	1257	39	2897	137
Barren Zone - M23	4.78034	0.35759	0.20290	0.00838	1781	133	1191	49	2636	173
Barren Zone - M24	5.43652	0.33038	0.23979	0.00902	1891	115	1386	52	2522	141
Barren Zone - M25	6.03518	0.42069	0.24929	0.01367	1981	138	1435	79	2677	146
Barren Zone - M26	4.16107	0.27763	0.24015	0.00714	1666	111	1387	41	2114	93
Barren Zone - M27	3.78498	0.21050	0.21743	0.00751	1590	88	1268	44	2051	72

Barren Zone - M28	5.23955	0.30985	0.21841	0.00623	1859	110	1273	36	2605	129
Barren Zone - M29	5.66581	0.32941	0.22387	0.00670	1926	112	1302	39	2741	132
Barren Zone - M30	6.40898	0.33007	0.25843	0.01414	2033	105	1482	81	2657	121
Barren Zone - M31	4.94916	0.49621	0.26868	0.01144	1811	182	1534	65	2159	175
Barren Zone - M32	4.76270	0.35815	0.24924	0.07534	1778	134	1435	434	2263	280
Barren Zone - M33	4.97189	0.43899	0.26069	0.01096	1815	160	1493	63	2279	141

APPENDIX E: U-PB GEOCHRONOLOGY XENOTIME ANALYSES

Samples	$^{207}Pb/^{235}U$	2σ	$^{206}Pb/^{238}U$	2σ	$^{207}Pb/^{235}U$ Age	2σ	$^{206}Pb/^{238}U$ Age	2σ	$^{207}Pb/^{206}Pb$ Age	2σ
Bn Zone - BrecciaX 1	3.97591	0.13588	0.29519	0.00586	1629	56	1667	33	1578	26
Bn Zone - BrecciaX 2	2.72651	0.22595	0.21754	0.01360	1336	111	1269	79	1440	38
Bn Zone - BrecciaX 3	1.80074	0.38317	0.14131	0.02825	1046	223	852	170	1473	66
Cpy Zone - DolX 1	3.88850	0.12614	0.28581	0.00479	1611	52	1621	27	1598	23
Cpy Zone - DolX 2	1.84346	0.20472	0.17363	0.01136	1061	118	1032	68	1123	61
Cpy Zone - DolX 3	3.28846	0.19465	0.25122	0.01298	1478	88	1445	75	1524	39
Cpy Zone - DolX 4	2.52729	0.21810	0.20713	0.01473	1280	110	1213	86	1393	48
Cpy Zone - DolX 5	2.99358	0.14218	0.24683	0.00686	1406	67	1422	40	1377	42
Cpy Zone - DolX 6	2.84431	0.15788	0.24212	0.00959	1367	76	1398	55	1319	34
Cpy Zone - DolX 7	3.58460	0.46848	0.28167	0.02950	1546	202	1600	168	1473	40
Barren Zone - X1	0.46074	0.04081	0.03758	0.00323	385	34	238	20	1408	41
Barren Zone - X2	0.56925	0.07108	0.04188	0.00518	458	57	264	33	1615	57
Barren Zone - X3	0.63642	0.10467	0.04953	0.00790	500	82	312	50	1455	48
Barren Zone - X4	0.70811	0.09136	0.06141	0.00744	544	70	384	47	1285	36
Barren Zone - X5	1.17902	0.05674	0.09516	0.00498	791	38	586	31	1443	45
Barren Zone - X6	1.22331	0.35956	0.09088	0.01666	811	238	561	103	1564	488
Barren Zone - X7	1.27849	0.10008	0.09677	0.00739	836	65	595	45	1541	64
Barren Zone - X8	1.28132	0.07802	0.10095	0.00452	837	51	620	28	1450	47
Barren Zone - X9	1.29774	0.07663	0.11761	0.00466	845	50	717	28	1178	52
Barren Zone - X10	1.31068	0.05863	0.10373	0.00342	850	38	636	21	1461	38
Barren Zone - X11	1.32382	0.08123	0.10391	0.00497	856	53	637	30	1492	52
Barren Zone - X12	1.37238	0.08806	0.10701	0.00532	877	56	655	33	1466	42
Barren Zone - X13	1.37434	0.09819	0.12505	0.00658	878	63	760	40	1182	45

Barren Zone - X14	1.40667	0.09268	0.11053	0.00585	892	59	676	36	1476	45
Barren Zone - X15	1.42526	0.11209	0.10870	0.00754	900	71	665	46	1516	26
Barren Zone - X16	1.42977	0.10969	0.10921	0.00697	901	69	668	43	1509	66
Barren Zone - X17	1.45482	0.07767	0.12567	0.00392	912	49	763	24	1279	57
Barren Zone - X18	1.48393	0.10071	0.11490	0.00704	924	63	701	43	1483	30
Barren Zone - X19	1.57025	0.06167	0.12319	0.00555	959	38	749	34	1506	53
Barren Zone - X20	1.58845	0.12368	0.11787	0.00706	966	75	718	43	1594	49
Barren Zone - X21	1.67112	0.11596	0.13484	0.00729	998	69	815	44	1450	41
Barren Zone - X22	1.67183	0.12404	0.13452	0.00778	998	74	814	47	1437	36
Barren Zone - X23	1.69286	0.13478	0.13208	0.00847	1006	80	800	51	1475	38
Barren Zone - X24	1.75078	0.11676	0.13890	0.00915	1027	69	838	55	1477	40
Barren Zone - X25	1.79838	0.09521	0.13776	0.00546	1045	55	832	33	1514	34
Barren Zone - X26	1.84598	0.09474	0.13873	0.00505	1062	55	837	30	1549	45
Barren Zone - X27	1.89204	0.19483	0.15916	0.01450	1078	111	952	87	1344	33
Barren Zone - X28	1.96674	0.12090	0.14781	0.00598	1104	68	889	36	1537	39
Barren Zone - X29	2.02979	0.15205	0.16846	0.00898	1126	84	1004	53	1345	39
Barren Zone - X30	2.03524	0.08605	0.16461	0.00517	1127	48	982	31	1429	24
Barren Zone - X31	2.08189	0.12719	0.15649	0.00725	1143	70	937	43	1530	29
Barren Zone - X32	2.13987	0.14336	0.17248	0.00760	1162	78	1026	45	1476	59
Barren Zone - X33	2.20999	0.12825	0.17059	0.00822	1184	69	1015	49	1505	25
Barren Zone - X34	2.21325	0.18071	0.17084	0.01220	1185	97	1017	73	1504	40
Barren Zone - X35	2.23390	0.12238	0.17468	0.00747	1192	65	1038	44	1504	29
Barren Zone - X36	2.25836	0.11272	0.17695	0.00654	1199	60	1050	39	1450	34
Barren Zone - X37	2.29907	0.11718	0.17994	0.00861	1212	62	1067	51	1471	42
Barren Zone - X38	2.30378	0.13893	0.17814	0.00858	1213	73	1057	51	1472	24
Barren Zone - X39	2.39599	0.20265	0.18928	0.01287	1241	105	1117	76	1440	32
Barren Zone - X40	2.39800	0.11183	0.18603	0.00806	1242	58	1100	48	1525	46

Barren Zone - X41	2.45359	0.38158	0.17540	0.01355	1258	196	1042	80	1637	127
Barren Zone - X42	2.48976	0.13092	0.17799	0.00678	1269	67	1056	40	1651	50
Barren Zone - X43	2.67178	0.12582	0.20533	0.00598	1321	62	1204	35	1550	43
Barren Zone - X44	2.71588	0.27349	0.21638	0.01972	1333	134	1263	115	1470	51
Barren Zone - X45	2.74130	0.12703	0.21185	0.00665	1340	62	1239	39	1521	29

APPENDIX F: U-PB GEOCHRONOLOGY APATITE ANALYSES

Samples	$^{207}Pb/^{235}U$	2σ	$^{206}Pb/^{238}U$	2σ	$^{207}Pb/^{235}U$ Age	2σ	$^{206}Pb/^{238}U$ Age	2σ	$^{207}Pb/^{206}Pb$ Age	2σ
Bn Zone - 743BAp - 1	20.15829	2.50053	0.39084	0.03348	3099	384	2127	182	3787	216
Bn Zone - 743BAp - 2	15.66075	1.73913	0.30803	0.02809	2856	317	1731	158	3761	171
Bn Zone - 743BAp - 3	18.47693	0.87318	0.36821	0.01461	3015	142	2021	80	3749	70
Bn Zone - 743BAp - 4	16.17074	1.71985	0.32357	0.02252	2887	307	1807	126	3739	166
Bn Zone - 743BAp - 5	17.86172	1.48975	0.37678	0.01882	2982	249	2061	103	3669	205
Bn Zone - 743BAp - 6	18.43594	2.20751	0.39191	0.02700	3013	361	2132	147	3647	235
Bn Zone - 743BAp - 7	19.33814	2.07951	0.42168	0.03314	3059	329	2268	178	3626	207
Bn Zone - 743BAp - 8	18.73883	1.17151	0.40901	0.02032	3028	189	2210	110	3617	152
Bn Zone - 743BAp - 9	16.69560	3.28839	0.38291	0.05863	2918	575	2090	320	3537	180
Bn Zone - 743BAp - 10	15.28547	0.84034	0.36535	0.01684	2833	156	2007	93	3469	125
Bn Zone - 743BAp - 11	14.81424	1.33167	0.36172	0.02227	2803	252	1990	123	3438	154
Bn Zone - 743BAp - 12	12.69736	1.03847	0.31705	0.02353	2657	217	1775	132	3390	141
Bn Zone - 743BAp - 13	10.99471	1.96824	0.27689	0.03708	2523	452	1576	211	3378	222
Bn Zone - 743BAp - 14	12.78165	0.60611	0.32576	0.01368	2664	126	1818	76	3377	77
Bn Zone - 743BAp - 15	12.78848	0.66854	0.32820	0.01481	2664	139	1830	83	3361	103
Bn Zone - 743BAp - 16	9.09467	0.63027	0.23449	0.01303	2348	163	1358	75	3357	120
Bn Zone - 743BAp - 17	11.60879	0.75798	0.30716	0.01490	2573	168	1727	84	3317	109
Bn Zone - 743BAp - 18	11.07809	0.54940	0.29386	0.01313	2530	125	1661	74	3309	103
Bn Zone - 743BAp - 19	11.58523	0.72427	0.30891	0.01305	2571	161	1735	73	3306	139
Bn Zone - 743BAp - 20	10.79333	0.55838	0.28964	0.01250	2505	130	1640	71	3292	99
Bn Zone - 743BAp - 21	11.40769	0.63721	0.31440	0.01294	2557	143	1762	73	3249	78
Bn Zone - 743BAp - 22	8.85811	0.66606	0.24507	0.01414	2323	175	1413	82	3231	111
Bn Zone - 743BAp - 23	9.02332	1.11128	0.25639	0.02159	2340	288	1471	124	3214	164

Bn Zone - 743BAp - 24	10.89943	0.87956	0.30804	0.01339	2515	203	1731	75	3202	164
Bn Zone - 743BAp - 25	10.80751	0.87967	0.31316	0.01817	2507	204	1756	102	3166	120
Bn Zone - 743BAp - 26	16.39658	1.78996	0.48150	0.03216	2900	317	2534	169	3164	383
Bn Zone - 743BAp - 27	12.10895	0.88067	0.35491	0.01726	2613	190	1958	95	3159	159
Bn Zone - 743BAp - 28	9.37407	0.83682	0.27643	0.01719	2375	212	1573	98	3144	231
Bn Zone - 743BAp - 29	9.02837	0.98027	0.26775	0.01936	2341	254	1529	111	3115	163
Bn Zone - 743BAp - 30	10.51152	0.51774	0.32138	0.01290	2481	122	1796	72	3086	85
Bn Zone - 743BAp - 31	9.64604	0.89250	0.29632	0.01932	2402	222	1673	109	3074	142
Bn Zone - 743BAp - 32	10.28840	0.62684	0.31695	0.01243	2461	150	1775	70	3073	123
Bn Zone - 743BAp - 33	7.89833	0.43512	0.24932	0.01078	2219	122	1435	62	3035	98
Bn Zone - 743BAp - 34	7.67450	0.45221	0.24445	0.01187	2194	129	1410	68	3025	101
Bn Zone - 743BAp - 35	9.29623	0.42891	0.30312	0.01193	2368	109	1707	67	2986	60
Bn Zone - 743BAp - 36	8.11083	0.77631	0.27170	0.01848	2243	215	1549	105	2947	191
Bn Zone - 743BAp - 37	8.65039	0.69446	0.29097	0.01207	2302	185	1646	68	2936	156
Bn Zone - 743BAp - 38	7.96673	0.43657	0.27621	0.01135	2227	122	1572	65	2885	75
Bn Zone - 743BAp - 39	8.17000	0.45422	0.28418	0.01290	2250	125	1612	73	2875	51
Bn Zone - 743BAp - 40	6.73641	0.57480	0.25291	0.01540	2077	177	1453	89	2749	115
Bn Zone - 743BAp - 41	17.63780	1.24743	0.41779	0.02236	2970	210	2250	120	3486	95
Bn Zone - 743BAp - 42	13.49951	0.87479	0.38453	0.01823	2715	176	2097	99	3197	120
Bn Zone - 743BAp - 43	17.65090	1.10672	0.37682	0.01727	2971	186	2061	94	3638	132
Bn Zone - 743BAp - 44	14.51041	0.99911	0.37549	0.01784	2784	192	2055	98	3360	171
Bn Zone - 743BAp - 45	13.15187	0.99994	0.37473	0.02330	2691	205	2052	128	3210	219
Bn Zone - 743BAp - 46	13.23374	0.85773	0.36368	0.01908	2696	175	2000	105	3255	85
Bn Zone - 743BAp - 47	16.14184	0.86017	0.35956	0.01614	2885	154	1980	89	3581	92
Bn Zone - 743BAp - 48	12.75893	0.84740	0.35292	0.01722	2662	177	1949	95	3241	128
Bn Zone - 743BAp - 49	13.64943	0.78147	0.35057	0.01427	2726	156	1937	79	3364	123
Bn Zone - 743BAp - 50	15.27030	1.69581	0.34803	0.01587	2832	315	1925	88	3548	294

Bn Zone - 743BAp - 51	12.28127	1.41704	0.33900	0.02438	2626	303	1882	135	3237	153
Bn Zone - 743BAp - 52	11.80953	0.68563	0.34138	0.01576	2589	150	1893	87	3173	135
Bn Zone - 743BAp - 53	11.34865	0.66000	0.33633	0.01531	2552	148	1869	85	3136	111
Bn Zone - 743BAp - 54	10.43616	0.52367	0.32735	0.01367	2474	124	1826	76	3047	108
Bn Zone - 743BAp - 55	9.81451	0.57060	0.31718	0.01304	2418	141	1776	73	2992	101
Bn Zone - 743BAp - 56	10.06963	0.49618	0.31489	0.01212	2441	120	1765	68	3054	70
Bn Zone - 743BAp - 57	10.08990	0.54846	0.31438	0.01339	2443	133	1762	75	3055	65
Bn Zone - 743BAp - 58	11.59525	1.00107	0.31261	0.02137	2572	222	1754	120	3279	109
Bn Zone - 743BAp - 59	12.17456	0.52730	0.31343	0.01205	2618	113	1758	68	3359	41
Bn Zone - 743BAp - 60	10.30313	0.47668	0.30964	0.01191	2462	114	1739	67	3109	53
Bn Zone - 743BAp - 61	10.83082	0.48112	0.30780	0.01206	2509	111	1730	68	3204	48
Bn Zone - 743BAp - 62	8.57199	0.40104	0.30635	0.01192	2294	107	1723	67	2828	70
Bn Zone - 743BAp - 63	10.67434	0.52606	0.29976	0.01251	2495	123	1690	71	3223	92
Bn Zone - 743BAp - 64	8.46609	0.37396	0.29959	0.01151	2282	101	1689	65	2847	41
Bn Zone - 743BAp - 65	10.30494	0.70826	0.29784	0.01541	2463	169	1681	87	3181	89
Bn Zone - 743BAp - 66	8.45128	0.43627	0.29670	0.01153	2281	118	1675	65	2862	87
Bn Zone - 743BAp - 67	7.26205	0.33216	0.29513	0.01180	2144	98	1667	67	2624	45
Bn Zone - 743BAp - 68	9.70264	0.43784	0.29439	0.01122	2407	109	1663	63	3099	59
Bn Zone - 743BAp - 69	10.97731	1.06593	0.29463	0.01770	2521	245	1665	100	3293	204
Bn Zone - 743BAp - 70	8.48658	0.47218	0.29396	0.01164	2284	127	1661	66	2892	93
Bn Zone - 743BAp - 71	11.26933	0.72827	0.29067	0.01434	2546	165	1645	81	3343	120
Bn Zone - 743BAp - 72	8.08849	0.41681	0.29191	0.01151	2241	115	1651	65	2813	66
Bn Zone - 743BAp - 73	8.19935	0.50791	0.28945	0.01442	2253	140	1639	82	2848	63
Bn Zone - 743BAp - 74	9.04177	0.49591	0.29049	0.01281	2342	128	1644	72	3011	88
Bn Zone - 743BAp - 75	10.06324	0.52098	0.28446	0.01218	2441	126	1614	69	3220	105
Bn Zone - 743BAp - 76	8.74876	0.43134	0.28200	0.01126	2312	114	1601	64	3002	77
Bn Zone - 743BAp - 77	6.13292	0.26160	0.28075	0.01083	1995	85	1595	62	2425	37

Bn Zone - 743BAp - 78	7.02970	0.30881	0.27865	0.01085	2115	93	1585	62	2668	36
Bn Zone - 743BAp - 79	6.91144	0.31804	0.27653	0.01090	2100	97	1574	62	2649	40
Bn Zone - 743BAp - 80	7.23953	0.37683	0.27532	0.01224	2141	111	1568	70	2737	43
Bn Zone - 743BAp - 81	5.67120	0.24691	0.27259	0.01042	1927	84	1554	59	2343	27
Bn Zone - 743BAp - 82	7.09627	0.33063	0.26824	0.01074	2124	99	1532	61	2750	61
Bn Zone - 743BAp - 83	8.74461	1.06715	0.26562	0.02163	2312	282	1519	124	3100	171
Bn Zone - 743BAp - 84	8.82690	0.66409	0.26176	0.01297	2320	175	1499	74	3125	148
Bn Zone - 743BAp - 85	8.19812	0.52990	0.25806	0.01317	2253	146	1480	76	3038	115
Bn Zone - 743BAp - 86	8.27292	0.78459	0.25440	0.01668	2261	214	1461	96	3086	130
Bn Zone - 743BAp - 87	8.66108	0.91451	0.25009	0.01989	2303	243	1439	114	3181	108
Bn Zone - 743BAp - 88	6.84736	0.72353	0.24845	0.02212	2092	221	1430	127	2810	104
Bn Zone - 743BAp - 89	5.71867	0.54953	0.23183	0.01859	1934	186	1344	108	2635	59
Bn Zone - 743CAp - 1	17.39561	1.95165	0.33118	0.03261	2957	332	1844	182	3819	251
Bn Zone - 743CAp - 2	21.13008	1.36064	0.41077	0.01988	3145	202	2218	107	3788	90
Bn Zone - 743CAp - 3	18.12422	1.25801	0.36112	0.01711	2996	208	1987	94	3756	122
Bn Zone - 743CAp - 4	14.81439	1.45450	0.32059	0.01911	2803	275	1793	107	3622	177
Bn Zone - 743CAp - 5	14.64304	0.98126	0.33329	0.01736	2792	187	1854	97	3555	124
Bn Zone - 743CAp - 6	14.93418	0.76267	0.34325	0.01399	2811	144	1902	78	3531	94
Bn Zone - 743CAp - 7	8.08468	0.80222	0.19473	0.01917	2241	222	1147	113	3448	81
Bn Zone - 743CAp - 8	12.22051	0.61904	0.29858	0.01232	2621	133	1684	69	3433	95
Bn Zone - 743CAp - 9	12.74698	0.75386	0.32027	0.01494	2661	157	1791	84	3396	134
Bn Zone - 743CAp - 10	13.24052	0.84672	0.34559	0.01680	2697	172	1914	93	3334	83
Bn Zone - 743CAp - 11	12.58125	0.87375	0.33165	0.01579	2649	184	1846	88	3317	143
Bn Zone - 743CAp - 12	11.84611	0.59124	0.32778	0.01380	2592	129	1828	77	3244	104
Bn Zone - 743CAp - 13	10.99943	0.66415	0.30937	0.01890	2523	152	1738	106	3213	102
Bn Zone - 743CAp - 14	9.59043	0.65246	0.28086	0.01267	2396	163	1596	72	3142	155
Bn Zone - 743CAp - 15	9.74655	0.62991	0.29028	0.01502	2411	156	1643	85	3121	76

Bn Zone - 743CAp - 16	10.28840	0.48431	0.30761	0.01190	2461	116	1729	67	3118	68
Bn Zone - 743CAp - 17	9.37972	0.86648	0.28319	0.01613	2376	219	1607	92	3102	155
Bn Zone - 743CAp - 18	10.31751	0.47269	0.31562	0.01232	2464	113	1768	69	3081	70
Bn Zone - 743CAp - 19	9.89845	0.55614	0.30690	0.01370	2425	136	1725	77	3066	116
Bn Zone - 743CAp - 20	10.43104	0.52304	0.32560	0.01326	2474	124	1817	74	3058	96
Bn Zone - 743CAp - 21	8.53980	0.44708	0.27591	0.01095	2290	120	1571	62	2997	75
Bn Zone - 743CAp - 22	8.62795	0.71259	0.27983	0.01624	2300	190	1591	92	2991	105
Bn Zone - 743CAp - 23	8.19157	0.61678	0.27186	0.01382	2252	170	1550	79	2957	114
Bn Zone - 743CAp - 24	8.34100	1.04417	0.27810	0.01452	2269	284	1582	83	2956	240
Bn Zone - 743CAp - 25	7.76969	0.57863	0.26479	0.01422	2205	164	1514	81	2936	88
Bn Zone - 743CAp - 26	8.65561	0.90535	0.29067	0.01625	2302	241	1645	92	2928	192
Bn Zone - 743CAp - 27	8.24521	0.54732	0.27862	0.01176	2258	150	1584	67	2920	108
Bn Zone - 743CAp - 28	7.69171	0.38076	0.26335	0.01130	2196	109	1507	65	2900	79
Bn Zone - 743CAp - 29	7.76768	0.99071	0.27062	0.01888	2204	281	1544	108	2875	230
Bn Zone - 743CAp - 30	7.94821	0.38297	0.27815	0.01228	2225	107	1582	70	2857	72
Bn Zone - 743CAp - 31	8.43437	0.43164	0.29940	0.01232	2279	117	1688	69	2848	83
Bn Zone - 743CAp - 32	7.75382	0.61804	0.27589	0.01450	2203	176	1571	83	2839	149
Bn Zone - 743CAp - 33	8.38746	0.99057	0.30096	0.02588	2274	269	1696	146	2823	139
Bn Zone - 743CAp - 34	7.73862	0.58273	0.28370	0.01731	2201	166	1610	98	2798	84
Bn Zone - 743CAp - 35	7.32529	0.33293	0.28400	0.01180	2152	98	1611	67	2692	56
Bn Zone - 743CAp - 36	7.34706	0.37398	0.29002	0.01169	2155	110	1642	66	2671	63
Bn Zone - 743CAp - 37	5.76755	0.34958	0.22749	0.01076	1942	118	1321	63	2670	103
Bn Zone - 743CAp - 38	5.89738	0.38936	0.23563	0.01123	1961	129	1364	65	2654	133
Bn Zone - 743CAp - 39	5.15327	0.57047	0.20737	0.01158	1845	204	1215	68	2638	176
Bn Zone - 743CAp - 40	5.35219	0.51989	0.21559	0.01483	1877	182	1259	87	2632	116
Bn Zone - 743CAp - 41	5.17679	0.56055	0.21035	0.01211	1849	200	1231	71	2630	199
Bn Zone - 743CAp - 42	5.03875	0.43544	0.20413	0.01649	1826	158	1197	97	2617	132

Bn Zone - 743CAp - 43	6.12303	0.37848	0.25488	0.01198	1994	123	1464	69	2577	87
Bn Zone - 743CAp - 44	6.86545	0.73934	0.29280	0.01702	2094	226	1655	96	2537	154
Bn Zone - 743CAp - 45	5.57230	0.49956	0.23968	0.01569	1912	171	1385	91	2524	85
Bn Zone - 743CAp - 46	5.91426	0.33166	0.25857	0.01038	1963	110	1483	60	2498	91
Bn Zone - 743CAp - 47	5.79663	0.31920	0.25653	0.01031	1946	107	1472	59	2485	89
Bn Zone - 743CAp - 48	6.28253	0.34826	0.28055	0.01170	2016	112	1594	66	2467	80
Bn Zone - 743CAp - 49	5.97295	0.48381	0.27422	0.01338	1972	160	1562	76	2418	107
Bn Zone - 743CAp - 50	3.76475	0.47798	0.17275	0.01578	1585	201	1027	94	2407	143
Bn Zone - 743CAp - 51	5.19470	0.33885	0.24377	0.00983	1852	121	1406	57	2378	115
Bn Zone - 743CAp - 52	5.35914	0.39359	0.25275	0.01051	1878	138	1453	60	2368	114
Bn Zone - 743CAp - 53	5.59508	0.27173	0.26474	0.01055	1915	93	1514	60	2365	57
Bn Zone - 743CAp - 54	5.39176	0.24370	0.25781	0.01006	1884	85	1479	58	2353	58
Bn Zone - 743CAp - 55	5.17272	0.24427	0.25177	0.01004	1848	87	1448	58	2317	60
Bn Zone - 743CAp - 56	5.09315	0.28335	0.24896	0.01079	1835	102	1433	62	2314	77
Bn Zone - 743CAp - 57	5.53937	0.26359	0.26941	0.01034	1907	91	1538	59	2313	52
Bn Zone - 743CAp - 58	4.40088	0.27225	0.22009	0.01111	1713	106	1282	65	2263	124
Bn Zone - 743CAp - 59	4.40862	0.23493	0.22396	0.00937	1714	91	1303	55	2241	59
Bn Zone - 743CAp - 60	5.11489	0.22679	0.27111	0.01039	1839	82	1546	59	2170	36
Bn Zone - 743CAp - 61	4.85071	0.78706	0.26632	0.01941	1794	291	1522	111	2161	210
Bn Zone - 743CAp - 62	3.82160	0.21782	0.20535	0.00886	1597	91	1204	52	2138	90
Bn Zone - 743CAp - 63	3.31577	0.22414	0.18781	0.00810	1485	100	1109	48	2050	100
Bn Zone - 743CAp - 64	3.41773	0.22638	0.19482	0.00859	1508	100	1147	51	2037	86
Bn Zone - 743CAp - 65	11.39034	0.92532	0.36080	0.02331	2556	208	1986	128	3024	139
Bn Zone - 743CAp - 66	15.16540	0.84398	0.34980	0.01598	2826	157	1934	88	3531	119
Bn Zone - 743CAp - 67	13.44207	1.10088	0.34711	0.02126	2711	222	1921	118	3352	118
Bn Zone - 743CAp - 68	10.07643	1.17875	0.33974	0.01840	2442	286	1885	102	2925	243
Bn Zone - 743CAp - 69	11.89787	0.78175	0.33526	0.01593	2596	171	1864	89	3211	101

Bn Zone - 743CAp - 70	8.64445	0.39773	0.32796	0.01429	2301	106	1828	80	2741	58
Bn Zone - 743CAp - 71	12.43992	0.80825	0.32766	0.01638	2638	171	1827	91	3322	123
Bn Zone - 743CAp - 72	11.21994	0.66762	0.32069	0.01565	2542	151	1793	87	3191	64
Bn Zone - 743CAp - 73	8.95456	0.43636	0.32098	0.01422	2333	114	1794	79	2829	71
Bn Zone - 743CAp - 74	10.92037	0.53557	0.32112	0.01287	2516	123	1795	72	3145	71
Bn Zone - 743CAp - 75	9.70471	0.45903	0.31647	0.01298	2407	114	1772	73	2984	73
Bn Zone - 743CAp - 76	12.14214	0.81625	0.31386	0.01735	2615	176	1760	97	3353	86
Bn Zone - 743CAp - 77	9.31630	0.60793	0.30948	0.01263	2370	155	1738	71	2948	112
Bn Zone - 743CAp - 78	7.87553	0.37748	0.30346	0.01242	2217	106	1708	70	2714	44
Bn Zone - 743CAp - 79	8.91407	0.45872	0.30132	0.01201	2329	120	1698	68	2922	71
Bn Zone - 743CAp - 80	9.50138	0.58969	0.29786	0.01607	2388	148	1681	91	3053	106
Bn Zone - 743CAp - 81	8.75820	0.53544	0.29507	0.01319	2313	141	1667	74	2931	91
Bn Zone - 743CAp - 82	6.85772	0.29800	0.29423	0.01139	2093	91	1663	64	2530	31
Bn Zone - 743CAp - 83	9.30020	0.74841	0.29541	0.01442	2368	191	1669	81	3021	136
Bn Zone - 743CAp - 84	8.19042	0.35432	0.29237	0.01123	2252	97	1653	64	2836	53
Bn Zone - 743CAp - 85	7.07081	0.32559	0.28998	0.01130	2120	98	1641	64	2607	38
Bn Zone - 743CAp - 86	8.34532	0.38037	0.28660	0.01108	2269	103	1625	63	2895	49
Bn Zone - 743CAp - 87	9.14988	0.72132	0.28582	0.01903	2353	186	1621	108	3049	80
Bn Zone - 743CAp - 88	8.29736	0.43510	0.28545	0.01288	2264	119	1619	73	2889	57
Bn Zone - 743CAp - 89	7.91993	0.41609	0.28641	0.01196	2222	117	1624	68	2812	78
Bn Zone - 743CAp - 90	6.69118	0.29831	0.28341	0.01121	2071	92	1608	64	2551	32
Bn Zone - 743CAp - 91	6.47248	0.28308	0.28342	0.01078	2042	89	1609	61	2494	36
Bn Zone - 743CAp - 92	7.89029	0.37192	0.28349	0.01127	2219	105	1609	64	2824	47
Bn Zone - 743CAp - 93	6.35201	0.27887	0.28329	0.01111	2026	89	1608	63	2463	42
Bn Zone - 743CAp - 94	7.42525	0.36056	0.28309	0.01186	2164	105	1607	67	2726	40
Bn Zone - 743CAp - 95	7.26088	0.93612	0.27798	0.01883	2144	276	1581	107	2726	183
Bn Zone - 743CAp - 96	8.12034	0.42099	0.27658	0.01404	2245	116	1574	80	2909	71

Bn Zone - 743CAp - 97	4.59123	0.19602	0.27471	0.01058	1748	75	1565	60	1960	23
Bn Zone - 743CAp - 98	8.10519	0.38193	0.27005	0.01441	2243	106	1541	82	2936	79
Bn Zone - 743CAp - 99	4.58989	0.21531	0.27089	0.01065	1747	82	1545	61	1979	35
Bn Zone - 743CAp - 100	4.54758	0.21042	0.27061	0.01084	1740	80	1544	62	1967	35
Bn Zone - 743CAp - 101	5.78862	0.29155	0.26990	0.01098	1945	98	1540	63	2387	45
Bn Zone - 743CAp - 102	5.28478	0.30619	0.26813	0.01137	1866	108	1531	65	2246	51
Bn Zone - 743CAp - 103	6.45384	0.28779	0.26831	0.01049	2040	91	1532	60	2585	40
Bn Zone - 743CAp - 104	8.61728	0.47336	0.26603	0.01116	2298	126	1521	64	3074	102
Bn Zone - 743CAp - 105	4.90754	0.24440	0.26507	0.01087	1804	90	1516	62	2138	37
Bn Zone - 743CAp - 106	6.28544	0.33381	0.26254	0.01143	2016	107	1503	65	2575	56
Bn Zone - 743CAp - 107	6.14972	0.31752	0.25741	0.01039	1997	103	1477	60	2572	76
Bn Zone - 743CAp - 108	6.48887	0.36023	0.25551	0.01115	2044	113	1467	64	2670	112
Bn Zone - 743CAp - 109	7.03855	0.43364	0.25490	0.01082	2116	130	1464	62	2811	116
Bn Zone - 743CAp - 110	5.71537	0.35594	0.25446	0.01252	1934	120	1461	72	2464	65
Bn Zone - 743CAp - 111	6.39433	0.50040	0.25136	0.01315	2031	159	1445	76	2668	96
Bn Zone - 743CAp - 112	5.18856	0.39806	0.25009	0.01452	1851	142	1439	84	2331	87
Bn Zone - 743CAp - 113	5.24280	0.34901	0.24835	0.01119	1860	124	1430	64	2362	89
Bn Zone - 743CAp - 114	6.13227	0.34684	0.23432	0.00978	1995	113	1357	57	2719	94
Bn Zone - 743CAp - 115	4.30854	0.24754	0.22691	0.01008	1695	97	1318	59	2182	61
Bn Zone - 743CAp - 116	3.50975	0.27879	0.18839	0.01278	1529	121	1113	75	2130	56
Cpy Zone - DolAp - 1	12.91582	4.78865	0.43800	0.08793	2674	991	2342	470	2943	884
Cpy Zone - DolAp - 2	19.66537	5.54769	0.44508	0.12449	3075	867	2373	664	3559	908
Cpy Zone - DolAp - 3	14.00252	3.94160	0.42057	0.06569	2750	774	2263	353	3083	538
Cpy Zone - DolAp - 4	37.39488	8.24472	0.76859	0.15998	3704	817	3676	765	3703	647
Cpy Zone - DolAp - 5	5.31021	1.37286	0.28896	0.03631	1871	484	1636	206	2128	572
Cpy Zone - DolAp - 6	11.12457	2.34776	0.36776	0.05097	2534	535	2019	280	2968	486
Cpy Zone - DolAp - 7	4.01919	0.95547	0.31402	0.03217	1638	389	1760	180	1485	376

Cpy Zone - DolAp - 8	5.34922	1.23643	0.29957	0.02962	1877	434	1689	167	2102	495
Cpy Zone - DolAp - 9	4.28276	0.91743	0.28238	0.02229	1690	362	1603	127	1808	294
Cpy Zone - DolAp - 10	4.50228	0.74283	0.27347	0.02103	1731	286	1558	120	1927	305
Cpy Zone - DolAp - 11	4.17020	0.62753	0.28597	0.02139	1668	251	1621	121	1707	240
Cpy Zone - DolAp - 12	3.62929	0.49672	0.27579	0.01783	1556	213	1570	101	1509	191
Cpy Zone - DolAp - 13	4.04557	0.48327	0.29834	0.01663	1643	196	1683	94	1608	159
Cpy Zone - DolAp - 14	10.78070	1.03349	0.44504	0.02547	2504	240	2373	136	2623	190
Cpy Zone - SSAp - 1	32.02035	9.17195	0.59425	0.18878	3551	1,017.00	3007	955	3880	937
Cpy Zone - SSAp - 2	12.55337	4.47077	0.41116	0.10132	2647	943	2220	547	2973	996
Cpy Zone - SSAp - 3	21.34754	7.20397	0.48059	0.12457	3155	1,065.00	2530	656	3574	1,077.00
Cpy Zone - SSAp - 4	20.75159	6.97632	0.43359	0.11059	3127	1,051.00	2322	592	3694	1,129.00
Cpy Zone - SSAp - 5	17.72581	5.94735	0.45661	0.09943	2975	998	2425	528	3446	794
Cpy Zone - SSAp - 6	5.51055	2.00339	0.29804	0.05576	1902	692	1682	315	2154	767
Cpy Zone - SSAp - 7	8.16973	1.88026	0.38329	0.12056	2250	518	2092	658	2392	519
Cpy Zone - SSAp - 8	6.58214	2.33233	0.34818	0.06568	2057	729	1926	363	2211	758
Cpy Zone - SSAp - 9	49.62561	13.71116	0.83354	0.20185	3985	1,101.00	3908	946	4022	837
Cpy Zone - SSAp - 10	6.67624	3.06434	0.30986	0.01734	2069	950	1740	97	2432	1,041.00
Cpy Zone - SSAp - 11	6.53933	1.11748	0.38589	0.13245	2051	351	2104	722	2060	327
Cpy Zone - SSAp - 12	40.35496	11.24947	0.63238	0.14876	3779	1,054.00	3159	743	4106	863
Cpy Zone - SSAp - 13	96.43035	25.24180	1.49366	0.36062	4650	1,217.00	5890	1,422.00	4141	1,025.00
Cpy Zone - SSAp - 14	5.37564	1.32972	0.25106	0.05230	1881	465	1444	301	2402	581
Cpy Zone - SSAp - 15	5.14054	1.55141	0.28190	0.04313	1843	556	1601	245	2142	633
Cpy Zone - SSAp - 16	5.87835	1.77615	0.29813	0.02490	1958	592	1682	140	2264	456
Cpy Zone - SSAp - 17	9.38632	2.01027	0.26023	0.02907	2376	509	1491	167	3286	447
Cpy Zone - SSAp - 18	3.93524	0.83425	0.31250	0.03537	1621	344	1753	198	1483	302
Cpy Zone - SSAp - 19	5.78589	1.15704	0.33247	0.03361	1944	389	1850	187	2084	398
Cpy Zone - SSAp - 20	4.65268	0.91339	0.32198	0.03127	1759	345	1799	175	1748	327

Cpy Zone - SSAp - 21	6.73420	1.52212	0.30439	0.01820	2077	469	1713	102	2459	396
Cpy Zone - SSAp - 22	7.63477	1.56334	0.32683	0.02345	2189	448	1823	131	2547	439
Cpy Zone - SSAp - 23	3.96508	0.68815	0.31307	0.02605	1627	282	1756	146	1500	247
Cpy Zone - SSAp - 24	10.56218	1.67640	0.34552	0.03231	2485	394	1913	179	3007	358
Cpy Zone - SSAp - 25	15.33107	1.43524	0.42364	0.06714	2836	265	2277	361	3265	240
Cpy Zone - SSAp - 26	6.98327	1.13291	0.34609	0.02471	2109	342	1916	137	2316	323
Cpy Zone - SSAp - 27	5.31025	0.82579	0.32974	0.02481	1871	291	1837	138	1939	258
Cpy Zone - SSAp - 28	6.33490	0.92343	0.29804	0.02484	2023	295	1682	140	2405	333
Cpy Zone - SSAp - 29	4.28521	0.66435	0.28796	0.02118	1691	262	1631	120	1795	291
Cpy Zone - SSAp - 30	8.00198	1.25620	0.33407	0.02328	2231	350	1858	129	2625	350
Cpy Zone - SSAp - 31	3.85574	0.59046	0.29093	0.01947	1604	246	1646	110	1554	227
Cpy Zone - SSAp - 32	4.20643	0.56023	0.28729	0.02482	1675	223	1628	141	1769	185
Cpy Zone - SSAp - 33	4.50608	0.65145	0.33914	0.02528	1732	250	1883	140	1589	206
Cpy Zone - SSAp - 34	11.83545	1.66083	0.37577	0.02619	2591	364	2056	143	3055	359
Cpy Zone - SSAp - 35	9.62103	1.18839	0.30122	0.02521	2399	296	1697	142	3095	340
Cpy Zone - SSAp - 36	6.57774	1.00258	0.32221	0.01679	2056	313	1801	94	2321	290
Cpy Zone - SSAp - 37	4.38971	0.58519	0.28254	0.01999	1710	228	1604	113	1877	255
Cpy Zone - SSAp - 38	4.57753	0.64953	0.29678	0.01652	1745	248	1675	93	1857	185
Cpy Zone - SSAp - 39	4.22468	0.52741	0.31421	0.02107	1679	210	1761	118	1603	182
Cpy Zone - SSAp - 40	6.90017	0.91163	0.32375	0.01926	2099	277	1808	108	2394	219
Cpy Zone - SSAp - 41	5.06196	0.60007	0.32655	0.02159	1830	217	1822	120	1874	196
Cpy Zone - SSAp - 42	8.78200	1.01826	0.35281	0.02002	2316	268	1948	111	2649	229
Cpy Zone - SSAp - 43	4.46917	0.52258	0.30208	0.01451	1725	202	1702	82	1762	187
Cpy Zone - SSAp - 44	4.46980	0.45576	0.29825	0.01710	1725	176	1683	96	1813	162
Cpy Zone - SSAp - 45	4.52467	0.26103	0.29568	0.01315	1736	100	1670	74	1851	51
Barren Zone Ap - 1	82.18417	19.54373	1.00680	0.36849	4489	1,068.00	4490	1,643.00	4470	711
Barren Zone Ap - 2	8.60924	3.06641	0.18676	0.04474	2298	818	1104	264	3588	1,298.00

Barren Zone Ap - 3	56.73028	17.91533	0.73073	0.20437	4118	1,301.00	3536	989	4395	1,055.00
Barren Zone Ap - 4	6.94641	2.45294	0.13498	0.03239	2105	743	816	196	3761	1,398.00
Barren Zone Ap - 5	17.17464	5.21455	0.22448	0.06406	2945	894	1306	373	4329	1,162.00
Barren Zone Ap - 6	60.17919	18.10294	0.57412	0.16244	4177	1,257.00	2925	827	4814	1,137.00
Barren Zone Ap - 7	36.50252	12.76376	0.41200	0.09531	3680	1,287.00	2224	514	4583	986
Barren Zone Ap - 8	12.21161	4.01484	0.19067	0.04794	2621	862	1125	283	4092	1,379.00
Barren Zone Ap - 9	113.16160	32.63134	1.01592	0.28429	4810	1,387.00	4519	1,265.00	4902	899
Barren Zone Ap - 10	18.40053	4.08475	0.26736	0.08912	3011	668	1527	509	4187	892
Barren Zone Ap - 11	24.22715	7.03076	0.29560	0.07490	3278	951	1669	423	4497	1,244.00
Barren Zone Ap - 12	26.59600	7.65193	0.34921	0.08469	3369	969	1931	468	4346	1,158.00
Barren Zone Ap - 13	6.53273	2.04518	0.14390	0.03097	2050	642	867	187	3580	1,166.00
Barren Zone Ap - 14	22.34396	6.29788	0.26519	0.06490	3199	902	1516	371	4519	1,260.00
Barren Zone Ap - 15	36.47741	11.59375	0.41964	0.08735	3679	1,169.00	2259	470	4523	1,543.00
Barren Zone Ap - 16	31.57801	8.58547	0.40006	0.09755	3537	962	2169	529	4401	1,181.00
Barren Zone Ap - 17	30.24254	8.63685	0.45433	0.10409	3495	998	2414	553	4133	1,008.00
Barren Zone Ap - 18	13.38358	3.83185	0.18801	0.04265	2707	775	1111	252	4272	1,262.00
Barren Zone Ap - 19	53.77371	14.47083	0.69115	0.16687	4065	1,094.00	3387	818	4398	906
Barren Zone Ap - 20	7.18374	2.19091	0.14853	0.03038	2134	651	893	183	3681	1,167.00
Barren Zone Ap - 21	5.46596	1.72306	0.15078	0.02890	1895	597	905	174	3260	1,059.00
Barren Zone Ap - 22	54.93882	14.76029	0.85720	0.20255	4086	1,098.00	3991	943	4112	983
Barren Zone Ap - 23	12.53832	3.52927	0.19111	0.04184	2646	745	1127	247	4150	1,193.00
Barren Zone Ap - 24	103.43134	25.71159	0.91521	0.21865	4720	1,173.00	4189	1,001.00	4917	802
Barren Zone Ap - 25	6.47539	1.93213	0.16804	0.03168	2043	609	1001	189	3341	1,018.00
Barren Zone Ap - 26	43.90013	11.07161	0.44908	0.10357	3863	974	2391	551	4711	1,003.00
Barren Zone Ap - 27	29.18524	7.40666	0.36464	0.08345	3460	878	2004	459	4436	782
Barren Zone Ap - 28	58.91360	14.69488	0.63541	0.14753	4156	1,037.00	3171	736	4646	888
Barren Zone Ap - 29	274.98610	66.71181	2.51183	0.59101	5707	1,384.00	8098	1,905.00	4905	595

Barren Zone Ap - 30	9.41134	2.61321	0.20529	0.03995	2379	661	1204	234	3599	1,003.00
Barren Zone Ap - 31	156.06123	42.54028	1.36535	0.26356	5134	1,400.00	5550	1,071.00	4924	496
Barren Zone Ap - 32	26.52362	6.86886	0.31386	0.06409	3366	872	1760	359	4482	548
Barren Zone Ap - 33	27.02777	6.72379	0.33005	0.07017	3384	842	1839	391	4445	1,017.00
Barren Zone Ap - 34	59.54369	14.83087	0.60641	0.12870	4166	1,038.00	3056	649	4736	474
Barren Zone Ap - 35	6.23360	1.74910	0.13959	0.02506	2009	564	842	151	3542	1,031.00
Barren Zone Ap - 36	123.77749	28.33655	1.53761	0.34953	4901	1,122.00	6003	1,365.00	4419	409
Barren Zone Ap - 37	7.17522	1.90373	0.12677	0.02347	2133	566	769	142	3900	1,090.00
Barren Zone Ap - 38	78.38973	18.19004	0.75187	0.16390	4442	1,031.00	3614	788	4788	788
Barren Zone Ap - 39	44.49257	9.30674	0.46099	0.11094	3876	811	2444	588	4686	862
Barren Zone Ap - 40	4.63094	1.29506	0.13080	0.02171	1755	491	792	132	3208	927
Barren Zone Ap - 41	7.21911	1.91354	0.15180	0.02735	2139	567	911	164	3669	1,005.00
Barren Zone Ap - 42	12.17469	3.05470	0.21693	0.04183	2618	657	1266	244	3907	976
Barren Zone Ap - 43	27.54243	6.40364	0.32983	0.06566	3403	791	1838	366	4464	950
Barren Zone Ap - 44	11.24773	2.73137	0.16905	0.03132	2544	618	1007	187	4153	1,036.00
Barren Zone Ap - 45	206.33062	45.20311	1.85754	0.38470	5416	1,187.00	6768	1,402.00	4892	663
Barren Zone Ap - 46	14.17473	3.41720	0.24224	0.04481	2761	666	1398	259	3975	939
Barren Zone Ap - 47	5.59329	1.43766	0.14783	0.02355	1915	492	889	142	3302	869
Barren Zone Ap - 48	7.57534	1.78390	0.11210	0.02013	2182	514	685	123	4197	1,065.00
Barren Zone Ap - 49	7.75436	1.66175	0.14339	0.02802	2203	472	864	169	3852	853
Barren Zone Ap - 50	18.28785	3.89515	0.26178	0.05098	3005	640	1499	292	4194	854
Barren Zone Ap - 51	6.82648	1.69028	0.16765	0.02667	2089	517	999	159	3432	864
Barren Zone Ap - 52	130.44683	28.12236	1.25029	0.23688	4954	1,068.00	5228	991	4825	385
Barren Zone Ap - 53	9.07638	1.95685	0.16431	0.03076	2346	506	981	184	3878	853
Barren Zone Ap - 54	29.88538	5.58321	0.39415	0.07850	3483	651	2142	427	4332	705
Barren Zone Ap - 55	14.70971	3.12788	0.18213	0.03155	2797	595	1079	187	4429	959
Barren Zone Ap - 56	6.16986	1.43299	0.13050	0.01982	2000	465	791	120	3661	884

Barren Zone Ap - 57	74.89130	16.14950	0.73912	0.12000	4396	948	3567	579	4755	505
Barren Zone Ap - 58	36.50538	7.30754	0.48113	0.08245	3680	737	2532	434	4369	596
Barren Zone Ap - 59	15.65543	3.44127	0.21479	0.03145	2856	628	1254	184	4277	670
Barren Zone Ap - 60	46.12625	6.40065	0.48309	0.10891	3912	543	2541	573	4664	509
Barren Zone Ap - 61	216.68372	39.69739	2.14400	0.37274	5466	1,001.00	7384	1,284.00	4758	1,397.00
Barren Zone Ap - 62	6.69109	1.31432	0.15630	0.02445	2071	407	936	146	3514	698
Barren Zone Ap - 63	7.07035	1.47953	0.15574	0.02130	2120	444	933	128	3586	763
Barren Zone Ap - 64	54.37712	8.64354	0.59067	0.11003	4076	648	2992	557	4615	559
Barren Zone Ap - 65	10.25055	1.91692	0.17461	0.02542	2458	460	1037	151	3978	655
Barren Zone Ap - 66	19.81122	3.27129	0.32097	0.05329	3082	509	1794	298	4033	604
Barren Zone Ap - 67	8.03815	1.54414	0.16835	0.02334	2235	429	1003	139	3641	702
Barren Zone Ap - 68	7.09760	1.37386	0.15948	0.02091	2124	411	954	125	3558	695
Barren Zone Ap - 69	19.65554	3.35654	0.24535	0.03703	3075	525	1414	213	4451	727
Barren Zone Ap - 70	10.58533	1.85102	0.19260	0.02743	2487	435	1135	162	3886	672
Barren Zone Ap - 71	232.04296	24.33962	2.05077	0.43409	5535	581	7190	1,522.00	4914	218
Barren Zone Ap - 72	12.54275	2.17523	0.21372	0.02718	2646	459	1249	159	3958	668
Barren Zone Ap - 73	8.19256	1.35009	0.16664	0.01849	2253	371	994	110	3710	608
Barren Zone Ap - 74	66.73922	10.35368	0.64046	0.07391	4281	664	3191	368	4825	408
Barren Zone Ap - 75	46.12884	6.34921	0.44537	0.05858	3912	538	2375	312	4769	142
Barren Zone Ap - 76	17.20223	2.50841	0.24452	0.02872	2946	430	1410	166	4262	548
Barren Zone Ap - 77	333.28750	45.84336	3.01197	0.36119	5901	812	8956	1,074.00	4910	420
Barren Zone Ap - 78	415.96208	53.59073	3.71794	0.44219	6126	789	10001	1,189.00	4898	245
Barren Zone Ap - 79	304.01124	29.01578	2.71429	0.23667	5808	554	8459	738	4927	70
Barren Zone Ap - 80	350.35454	35.62532	3.20710	0.21727	5952	605	9262	627	4868	200
Barren Zone Ap - 81	321.53491	25.19651	2.75149	0.19091	5865	460	8523	591	4961	97
Barren Zone Ap - 82	394.69443	31.99734	3.57567	0.22132	6073	492	9803	607	4908	74

APPENDIX G: MONAZITE TRACE ELEMENT ANALYSES*

All values are in ppm and are not normalised.

Samples	Y	La	Ce	Pr	Nd	Sm	Eu	Gd	Tb	Dy	Ho	Er	Tm	Yb	Lu
Session 1 Standards															
NIST610 - 1	463	441	453	447	429	455	447	449	436	436	450	455	436	451	440
NIST610 - 2	462	439	452	446	428	453	446	448	435	435	449	454	433	449	438
NIST610 - 3	461	441	453	449	431	451	447	448	438	437	448	455	436	449	438
NIST610 - 4	462	441	454	450	432	453	448	450	439	439	449	456	437	451	440
NIST610 - 5	461	437	453	445	429	454	445	450	438	437	449	455	434	448	438
NIST610 - 6	462	438	454	447	429	454	447	452	438	437	450	455	435	449	439
NIST610 - 7	463	441	453	449	432	453	447	447	437	439	449	455	435	452	440
NIST610 - 8	462	442	452	449	432	452	447	448	436	437	449	455	435	451	439
NIST610 - 9	463	441	453	448	426	451	447	451	435	437	448	454	435	447	439
NIST610 - 10	462	440	452	447	427	450	445	446	434	436	447	453	433	446	438
NIST610 - 11	461	439	453	449	431	454	449	455	439	436	450	456	436	453	439
NIST610 - 12	462	440	454	449	434	456	449	452	440	438	451	457	437	454	440
NIST610 - 13	462	441	453	449	433	456	449	449	438	439	451	455	435	452	441
NIST610 - 14	462	442	453	448	432	456	449	450	438	439	451	455	437	451	440
NIST610 - 15	462	437	453	448	429	449	444	442	436	434	447	455	431	448	437
NIST610 - 16	462	438	453	448	428	450	445	443	436	435	447	455	433	448	437
NIST610 - 17	462	440	453	447	430	455	446	447	436	435	449	453	436	450	440
NIST610 - 18	462	440	453	446	430	454	447	447	437	435	449	454	436	450	440
NIST610 - 19	462	440	453	451	431	453	447	453	438	440	449	457	434	450	438
NIST610 - 20	462	440	453	450	430	452	447	452	437	439	449	456	434	450	438
NIST610 - 21	461	440	453	446	429	449	445	444	436	434	449	455	431	449	439

NIST610 - 22	462	440	454	449	431	451	447	450	437	437	450	456	434	450	441
NIST610 - 23	463	442	453	447	429	457	448	449	438	438	449	455	435	451	439
NIST610 - 24	462	440	452	447	429	455	447	452	437	437	448	454	436	450	437
NIST610 - 25	461	439	453	447	428	450	445	449	435	436	449	455	435	449	438
NIST610 - 26	462	441	455	449	430	453	446	452	437	437	450	457	436	451	439
NIST610 - 27	463	439	453	447	431	453	450	450	439	438	449	455	435	451	440
NIST610 - 28	462	439	451	447	430	453	448	449	437	437	448	453	434	449	439
NIST610 - 29	460	440	453	446	431	453	448	451	436	437	449	452	437	448	439
NIST610 - 30	462	440	455	447	431	453	449	449	438	438	451	454	436	450	441
NIST610 - 31	464	444	453	453	434	457	448	448	438	439	449	458	439	453	439
NIST610 - 32	462	440	451	449	429	453	445	442	436	436	446	456	434	450	437
NIST610 - 33	462	438	453	446	428	449	444	451	438	437	450	455	434	449	440
NIST610 - 34	462	439	453	448	430	451	446	451	438	438	450	455	434	449	440
NIST610 - 35	463	441	453	448	429	454	447	449	437	436	449	455	436	451	438
NIST610 - 36	462	440	452	448	429	455	448	448	436	436	448	454	436	450	438
NIST610 - 37	460	441	453	448	427	450	445	450	435	437	447	455	433	450	438
NIST610 - 38	462	442	455	449	430	452	447	452	437	439	449	457	435	452	440
NIST610 - 39	465	440	453	450	431	457	448	451	439	437	451	455	438	450	440
NIST610 - 40	462	438	451	447	430	454	447	449	437	435	449	453	435	448	438
NIST610 - 41	462	437	453	448	430	454	448	449	437	439	450	456	437	451	440
NIST610 - 42	462	439	453	448	430	455	448	449	437	440	450	457	436	451	440
NIST610 - 43	462	439	453	448	430	449	446	447	437	434	448	453	435	449	438
NIST610 - 44	462	441	453	448	430	450	446	447	437	434	448	453	434	449	438
NIST610 - 45	463	440	453	451	431	455	448	450	438	440	449	456	436	450	440
NIST610 - 46	462	439	452	449	429	452	446	450	436	439	448	455	435	449	439
NIST610 - 47	460	440	453	446	431	454	448	446	436	434	448	454	433	449	438
NIST610 - 48	462	441	455	448	431	454	448	449	438	436	450	455	435	451	439

NIST610 - 49	465	440	453	446	434	454	448	446	437	438	450	455	435	452	440
NIST610 - 50	462	437	450	445	430	450	446	444	434	434	448	452	434	449	438
NIST610 - 51	459	440	453	447	428	453	445	449	437	438	448	455	432	448	437
NIST610 - 52	462	443	456	452	430	456	449	453	440	440	451	458	436	451	440
NIST610 - 53	464	440	453	450	429	454	446	449	437	436	449	454	434	452	439
NIST610 - 54	462	438	450	447	428	452	444	448	435	435	446	451	432	450	437
NIST610 - 55	460	439	453	447	428	450	447	448	436	435	449	456	435	447	438
NIST610 - 56	462	442	456	449	432	454	450	451	439	439	452	459	438	450	441
NIST610 - 57	464	442	453	451	432	455	450	450	440	439	451	458	438	451	440
NIST610 - 58	462	440	451	450	430	454	448	447	438	437	450	456	436	449	439
NIST610 - 59	460	440	453	445	429	451	445	451	435	437	447	453	433	449	438
NIST610 - 60	462	440	454	447	430	452	446	450	436	437	448	454	434	451	439
Session 2 Standards															
NIST610 - 1	461	441	453	449	432	453	447	448	437	437	448	455	436	450	439
NIST610 - 2	462	441	454	449	433	453	446	448	437	438	448	454	435	450	439
NIST610 - 3	461	439	453	447	427	452	449	450	437	437	449	455	436	451	439
NIST610 - 4	462	439	454	447	427	452	448	450	437	437	449	455	435	451	439
NIST610 - 5	464	442	453	449	434	455	448	452	438	439	452	455	436	450	441
NIST610 - 6	462	441	451	447	432	454	446	450	436	437	450	453	434	448	439
NIST610 - 7	461	438	453	448	428	451	446	446	437	436	449	454	434	449	437
NIST610 - 8	462	439	454	449	428	452	447	448	437	437	450	455	434	450	438
NIST610 - 9	461	439	453	446	429	452	445	448	436	437	449	455	434	449	440
NIST610 - 10	462	440	454	447	429	453	447	449	437	437	450	457	435	450	441
NIST610 - 11	462	441	453	448	432	454	449	450	438	436	448	457	436	449	439
NIST610 - 12	462	440	453	448	432	453	450	449	438	436	448	457	436	450	440
NIST610 - 13	463	441	453	450	429	453	447	451	438	438	449	456	436	449	439
NIST610 - 14	462	441	452	449	429	453	448	450	438	438	449	457	436	449	438

NIST610 - 15	462	439	453	448	428	453	444	447	436	436	448	453	434	450	438
NIST610 - 16	462	439	453	448	428	453	445	448	437	435	448	453	434	451	438
NIST610 - 17	464	440	453	450	431	456	448	450	438	438	451	455	437	455	440
NIST610 - 18	462	440	452	449	430	455	448	449	437	437	450	454	437	454	439
NIST610 - 19	462	440	453	447	431	450	444	448	436	437	448	454	433	448	439
NIST610 - 20	462	440	453	447	431	451	445	449	436	436	448	454	434	448	439
NIST610 - 21	463	440	453	446	432	451	447	452	435	439	448	453	435	450	438
NIST610 - 22	462	440	452	446	432	451	446	451	435	438	447	452	435	449	438
NIST610 - 23	462	440	453	447	427	455	446	446	437	435	449	455	434	449	439
NIST610 - 24	462	440	453	448	427	456	446	447	438	435	449	456	435	450	440
NIST610 - 25	464	441	453	448	432	454	448	448	439	439	451	457	436	452	440
NIST610 - 26	462	439	451	446	430	452	446	446	437	437	449	455	435	450	439
NIST610 - 27	460	439	453	449	431	452	449	451	436	438	448	453	434	449	439
NIST610 - 28	462	441	455	452	433	454	450	452	438	440	450	455	436	451	441
NIST610 - 29	462	439	453	449	430	453	447	449	437	435	450	455	436	451	440
NIST610 - 30	462	439	453	449	430	453	446	449	437	435	449	454	435	451	439
NIST610 - 31	462	441	453	447	430	454	450	449	437	438	449	456	435	450	439
NIST610 - 32	462	441	453	446	430	453	449	449	436	437	448	455	435	449	438
NIST610 - 33	462	440	453	448	428	453	449	449	437	437	448	455	435	449	438
NIST610 - 34	462	439	453	448	428	452	448	448	437	437	448	455	435	449	437
NIST610 - 35	460	440	453	447	430	453	446	449	437	435	449	455	435	450	438
NIST610 - 36	462	441	455	449	431	454	446	450	437	437	450	456	435	451	439
NIST610 - 37	460	441	453	448	429	452	447	449	438	436	450	456	437	451	439
NIST610 - 38	462	442	455	449	430	453	448	451	438	438	451	457	437	452	440
NIST610 - 39	463	440	453	447	432	454	447	449	439	439	449	456	435	450	440
NIST610 - 40	462	438	452	446	430	453	445	448	437	438	447	454	433	448	439
NIST610 - 41	460	438	453	448	429	453	446	446	437	436	449	454	434	449	439

NIST610 - 42	462	439	455	449	430	454	448	447	437	438	450	456	435	450	441
NIST610 - 43	462	442	453	448	431	454	447	452	437	437	449	455	436	448	438
NIST610 - 44	462	441	453	447	430	452	446	451	436	437	448	454	435	448	438
NIST610 - 45	462	439	453	448	428	452	445	447	437	435	447	455	435	450	438
NIST610 - 46	462	439	453	448	428	451	445	447	437	435	447	455	435	451	438
NIST610 - 47	461	441	453	448	432	454	448	451	436	438	449	455	434	450	440
NIST610 - 48	462	441	454	449	433	455	449	451	437	439	449	456	435	451	440
NIST610 - 49	463	441	453	447	428	455	445	449	437	436	450	455	434	451	439
NIST610 - 50	462	441	452	447	428	455	446	449	437	435	450	455	435	451	439
NIST610 - 51	464	439	453	449	432	451	449	449	437	439	449	455	435	450	439
NIST610 - 52	462	439	451	449	432	451	449	449	437	437	449	454	435	449	439
Bn Zone - GranM 1	1683	170330	284915	23640	62030	7331	1510	4073	291	843	81	103	7	28	3
Bn Zone - GranM 2	2032	185462	290350	27262	68547	6837	1392	3729	279	870	87	128	10	54	7
Bn Zone - GranM 3	1907	180994	290789	26153	64068	6556	1328	3535	267	809	86	140	14	76	11
Bn Zone - GranM 4	1706	175869	285883	27118	64111	7771	1576	4363	295	830	77	119	10	49	7
Bn Zone - GranM 5	1759	177803	288778	25566	65435	7102	1447	3890	286	843	79	114	9	45	6
Bn Zone - GranM 6	1821	186969	290903	27199	67689	6756	1355	3728	274	842	80	110	7	29	3
Bn Zone - GranM 7	1710	176517	295209	26698	68422	8200	1638	4572	307	869	81	102	6	26	2
Bn Zone - GranM 8	1651	163201	292022	24535	71955	8897	1813	4957	321	847	72	94	7	28	3
Bn Zone - GranM 9	1375	158798	287356	24387	66051	7980	1629	4566	289	788	66	78	6	24	2
Bn Zone - GranM 10	1184	142552	251313	21655	57883	7244	1454	4036	267	687	59	71	4	15	1
Bn Zone - GranM 11	1445	171916	295760	26717	67216	8126	1603	4568	300	812	69	84	5	17	1
Bn Zone - GranM 12	2053	170546	292358	25813	64297	7451	1529	4121	304	916	90	144	14	74	10
Bn Zone - GranM 13	1663	177915	285334	26350	67264	6779	1369	3787	276	804	79	108	8	34	4
Bn Zone - GranM 14	1643	171425	273563	23984	61167	6684	1345	3749	268	788	72	94	8	33	5
Bn Zone - GranM 15	1819	173287	297012	26055	65235	7356	1518	4160	294	856	82	131	10	54	7
Bn Zone - GranM 16	1947	160551	281611	23991	61269	7113	1443	4023	286	840	90	138	15	83	10

Bn Zone - GranM 17	2363	169885	262896	23595	56292	6482	1266	3372	269	868	105	193	23	133	19
Bn Zone - GranM 18	1252	141434	244734	19406	56514	6801	1356	3801	260	721	62	72	4	13	1
Bn Zone - GranM 19	1385	166737	288354	24760	67868	8317	1702	4815	313	798	66	76	4	12	1
Bn Zone - GranM 20	1196	138053	235085	20805	53011	6091	1237	3557	240	655	58	68	4	15	2
Bn Zone - GranM 21	1293	132573	218060	20225	49488	6015	1185	3418	235	674	65	98	6	27	3
Bn Zone - GranM 22	1483	176534	292968	25115	68543	7919	1624	4520	304	801	70	90	7	30	4
Bn Zone - GranM 23	1611	180400	287764	27000	71289	7517	1522	4213	290	814	79	113	10	55	6
Bn Zone - GranM 24	1480	172449	279064	24466	61490	7163	1486	3971	276	753	68	93	7	33	4
Bn Zone - GranM 25	1384	165525	288009	22968	65792	7859	1578	4475	283	802	68	98	6	22	3
Bn Zone - GranM 26	1661	175746	292372	26828	64449	7385	1495	4186	286	816	78	115	9	47	6
Bn Zone - GranM 27	1815	185149	292516	22932	65324	7698	1501	4250	290	848	88	136	14	79	10
Bn Zone - GranM 28	1577	179780	293887	27083	64786	7646	1559	4380	299	830	76	106	8	38	4
Bn Zone - GranM 29	1401	181730	287472	26626	67514	7328	1464	4109	272	726	70	99	9	43	6
Bn Zone - GranM 30	1740	165917	275777	22967	58470	6562	1364	3743	271	798	82	126	12	74	10
Bn Zone - GranM 31	1653	176960	288108	26732	66629	7547	1528	4292	305	863	79	96	6	26	3
Bn Zone - GranM 32	1428	157720	284030	22568	64266	8278	1757	4806	295	774	70	82	5	16	1
Bn Zone - GranM 33	1649	166851	291126	25244	66263	8083	1620	4556	313	870	77	80	5	19	2
Bn Zone - GranM 34	1441	167810	280841	25934	65742	7808	1576	4423	294	787	70	91	6	21	2
Bn Zone - GranM 35	1785	174341	286035	26353	63880	7228	1463	3843	289	864	81	105	7	23	2
Bn Zone - GranM 36	1476	169894	286608	25869	64065	7758	1558	4181	286	791	70	90	5	19	2
Bn Zone - GranM 37	1501	167766	278094	24469	62782	7463	1544	4235	293	815	73	93	6	30	3
Bn Zone - GranM 38	1507	164421	287271	25789	68038	7603	1565	4295	299	827	71	83	5	15	1
Cpy Zone - DolM 1	954	135846	290481	32673	115562	13954	2049	6442	366	772	54	57	3	10	1
Cpy Zone - DolM 2	1473	128130	282857	33042	122848	15227	2291	7226	431	994	78	94	6	18	1
Cpy Zone - DolM 3	1588	128348	279908	32084	120223	14813	2192	6926	413	984	82	101	7	21	2
Cpy Zone - DolM 4	1038	132795	285065	32528	121958	14723	2185	6950	404	860	61	64	3	10	1
Cpy Zone - DolM 5	2341	135381	284443	32586	118208	13852	2098	7019	444	1191	110	146	9	27	2

Cpy Zone - DolM 6	3371	125429	278788	33069	120442	15060	2534	7859	564	1650	163	208	12	38	3
Cpy Zone - DolM 7	1916	147520	290511	30804	108582	11671	1548	5808	364	940	87	120	7	24	2
Cpy Zone - DolM 8	2204	142454	289971	31332	111478	11779	1593	5824	382	1043	100	132	8	22	1
Cpy Zone - DolM 9	3947	126344	282488	32691	120456	13770	1840	6977	515	1592	175	266	18	54	4
Cpy Zone - DolM 10	4543	132564	283964	32936	117865	12593	1649	6470	476	1594	191	301	21	66	5
Cpy Zone - DolM 11	1386	132414	283839	32628	120332	13748	2056	6878	404	939	73	86	5	18	1
Cpy Zone - DolM 12	1869	135655	285564	31650	115741	13099	1949	6620	407	999	86	116	7	24	2
Barren Zone - M1	1850	162437	282403	24922	73445	9361	2985	4348	309	904	97	142	14	102	7
Barren Zone - M2	5796	181926	277041	24712	73692	11547	5064	6571	413	1411	243	544	67	394	59
Barren Zone - M3	2581	190506	289280	22567	67716	5984	1338	3167	295	1137	143	198	18	41	4
Barren Zone - M4	3624	188111	280712	24056	76660	8104	2053	4393	371	1482	185	337	36	149	19
Barren Zone - M5	1948	192563	296713	26124	79140	8748	2230	4783	390	1276	112	150	9	24	1
Barren Zone - M6	4573	178252	300262	26130	83428	8130	1809	4767	439	1784	199	460	47	271	29
Barren Zone - M7	1811	161438	285963	25576	80225	10976	3126	5491	366	1140	105	147	9	29	2
Barren Zone - M8	2152	178322	289206	25859	77399	9555	2156	4836	405	1393	121	155	11	28	2
Barren Zone - M9	13634	159544	283633	25272	76808	9636	2313	6248	641	2988	574	1412	195	1159	154
Barren Zone - M10	4203	158295	282490	25511	77022	9304	1990	5388	466	1728	210	427	39	233	29
Barren Zone - M11	1984	181896	284472	25433	80593	8597	2000	4415	336	1169	111	116	8	40	2
Barren Zone - M12	1570	182434	284526	23920	73193	7730	1885	4135	321	1018	90	114	8	24	2
Barren Zone - M13	2704	165398	285512	26679	84580	15056	3285	7285	484	1541	159	196	12	37	2
Barren Zone - M14	1227	182693	283660	24776	74025	7830	2009	4116	313	926	77	89	5	18	2
Barren Zone - M15	27366	167315	257227	22554	68247	7346	2032	5751	832	5631	1110	2623	303	1490	188
Barren Zone - M16	2607	190909	290105	25246	75438	8444	2798	4974	358	1155	126	199	15	56	5
Barren Zone - M17	1529	180108	266802	23066	70931	7169	1840	3851	308	962	90	122	8	25	2
Barren Zone - M18	3319	160360	295634	26241	80851	9532	1951	5318	452	1667	175	272	24	121	14
Barren Zone - M19	1821	194789	297764	26045	77480	8406	2073	4468	350	1098	102	137	9	38	2
Barren Zone - M20	4352	172329	291881	26159	81747	9276	2003	5597	486	1847	229	417	46	237	29

Barren Zone - M21	3322	191451	290999	25235	79285	8343	2263	4498	406	1427	163	288	27	114	12
Barren Zone - M22	2101	160655	277286	25598	77258	9161	2258	5583	424	1425	123	157	10	32	3
Barren Zone - M23	2097	170617	290074	26837	79469	9701	2347	6461	455	1410	134	162	10	33	3
Barren Zone - M24	2966	167954	276180	26811	82770	13336	3062	7102	500	1657	177	230	16	52	4
Barren Zone - M25	1741	171651	284283	26803	82574	9208	2037	5257	406	1207	117	133	8	25	2
Barren Zone - M26	2358	181777	281264	26500	79166	9900	2253	5821	417	1299	131	186	12	46	4
Barren Zone - M27	2506	188088	282942	25131	77385	7900	1982	4440	384	1339	141	187	12	33	3
Barren Zone - M28	2359	163284	295177	26798	83904	10839	2362	6000	440	1390	141	184	11	38	3
Barren Zone - M29	2048	161161	281822	26024	78703	9415	2268	5556	430	1317	124	153	10	31	3
Barren Zone - M30	2354	169409	292846	25915	79628	9070	1875	6264	439	1438	141	180	11	40	4
Barren Zone - M31	3270	150012	314424	31244	102162	10045	1274	4705	339	1161	128	177	11	31	2
Barren Zone - M32	2050	157709	243329	22664	69859	9183	2031	5326	390	1146	113	143	10	34	3
Barren Zone - M33	2436	168186	279216	25504	77515	9751	2249	5765	415	1285	147	298	11	41	3

APPENDIX H: XENOTIME TRACE ELEMENT ANALYSES*

All values are in ppm and are not normalised.

Samples	Y	La	Ce	Pr	Nd	Sm	Eu	Gd	Tb	Dy	Ho	Er	Tm	Yb	Lu
Session 1 Standards															
NIST610_13 - 1	470	465	496	488	458	479	479	469	457	452	457	458	443	457	447
NIST610_13 - 2	486	477	498	492	461	489	480	465	458	458	471	472	453	466	450
NIST610_13 - 3	474	467	499	487	449	497	470	459	453	456	458	465	441	459	443
NIST610_13 - 4	478	474	511	487	466	474	476	487	459	458	464	472	454	465	453
NIST610_13 - 5	480	469	505	487	453	486	476	459	453	453	471	469	447	466	454
NIST610_13 - 6	487	476	500	493	465	503	476	472	461	456	473	470	453	452	455
NIST610_13 - 7	488	461	491	478	430	490	476	476	453	447	461	463	448	459	452
NIST610_13 - 8	473	468	501	479	461	477	470	470	449	446	457	462	442	452	447
NIST_13 - 1	477	469	488	477	456	470	462	476	448	449	459	465	442	460	448
NIST_13 - 2	474	472	493	494	474	496	474	470	456	452	465	471	452	466	455
NIST_13 - 3	481	475	509	486	474	480	471	480	458	466	465	480	452	466	455
NIST_13 - 4	482	469	493	492	455	469	469	470	452	442	469	467	446	464	453
NIST_13 - 5	479	472	490	481	456	464	469	468	454	450	467	464	446	459	448
NIST_13 - 6	474	464	497	481	450	473	468	475	453	449	462	468	448	457	449
Session 2 Standards															
NIST610 - 1	3768.2686	3814.0793	3982.9446	3805.6894	3767.9247	3753.6245	3785.7847	3832.1504	3586.9957	3712.9027	3670.9215	3741.1693	3510.1216	3610.4507	3570.2171
NIST610 - 2	3674.6441	3624.6984	3849.1005	3619.1949	3542.0736	3750.7779	3503.6907	3455.5993	3368.3992	3466.5123	3447.3543	3499.7965	3355.6304	3456.6745	3345.5549
NIST610 - 3	3463.793	3424.6132	3754.7654	3586.4149	3260.6603	3562.7539	3519.4858	3414.5173	3330.0553	3421.8737	3360.6291	3425.2252	3278.1707	3402.8343	3335.5617
NIST610 - 4	3694.9222	3668.7359	3967.8648	3796.2687	3693.4984	3851.7505	3664.9788	3597.9602	3550.47	3509.841	3589.4873	3630.5503	3474.5	3525.4689	3459.0617

NIST610 - 5	3782.3833	3741.312	3869.9902	3848.2914	3735.2649	4152.5499	3783.9419	3871.5506	3632.5429	3611.219	3677.0388	3675.0937	3562.4686	3712.2425	3584.7343
NIST610 - 6	3713.064	3678.0442	4057.6193	3894.8477	3667.1019	3779.154	3746.5234	3692.3576	3636.6141	3567.9723	3691.7919	3690.5378	3531.3664	3639.9423	3577.5273
NIST610 - 7	3590.3533	3393.3397	3659.808	3569.0249	3445.8802	3478.7981	3482.131	3494.5013	3373.9355	3312.631	3438.8574	3449.0985	3286.9558	3343.3081	3333.5509
NIST610 - 8	3470.605	3588.5471	3737.9143	3623.6246	3314.39	3675.3058	3379.5059	3610.1068	3305.7143	3316.6455	3410.6027	3448.0912	3255.3797	3400.3594	3301.8313
NIST610 - 9	3631.28	3661.6849	3884.59	3760.0404	3581.954	3603.8362	3616.8141	3556.2019	3470.7809	3519.1458	3560.5157	3670.8327	3462.708	3524.852	3480.2517
NIST610 - 10	3662.9792	3745.1239	3947.1426	3840.2197	3620.0632	3879.2108	3697.0636	3666.5388	3586.7766	3657.7525	3664.6565	3682.7071	3479.3075	3552.692	3580.1054
NIST610 - 11	3630.697	3554.5576	3783.7846	3690.4688	3452.0644	3504.7786	3574.7781	3492.6083	3446.6573	3457.4262	3505.9333	3561.4864	3322.5237	3548.6046	3397.749
NIST610 - 12	3834.8539	3859.9095	4109.6206	4033.9074	3795.7257	3885.834	3927.4867	3704.2985	3716.9086	3767.4117	3708.3987	3865.3157	3631.6226	3703.3713	3707.7583
NIST610 - 13	3622.8204	3558.7746	3854.5497	3656.051	3680.8922	3486.0583	3581.029	3583.027	3426.9097	3406.0158	3512.0195	3583.1992	3347.7501	3621.2763	3396.7545
Barren Zone - X3	358264	68	467	109	1097	3628	2597	21654	5055	46284	12364	40119	5726	36895	4965
Barren Zone - X4	373663	60	369	118	1447	3717	2548	20795	5455	49330	12805	40060	5689	35280	4597
Barren Zone - X5	328665	3370	4912	533	2412	5371	3443	25028	5431	45179	11037	35958	5146	33358	4635
Barren Zone - X6	245626	884	1634	189	1195	4739	4278	19487	4395	38064	8425	25080	3915	25174	3080
Barren Zone - X7	327048	13555	15358	1249	4005	6715	4846	34061	6254	48122	11657	35824	4987	31650	4194
Barren Zone - X8	360364	768	1747	218	1642	3660	2613	21209	5127	47655	11945	39081	5602	34431	4705
Barren Zone - X9	353585	39	417	156	2036	5081	3505	26438	5691	46133	11470	37923	5439	35181	4803
Barren Zone - X10	358811	62	401	99	1268	3982	2902	23000	5439	49773	12465	39196	5665	36073	4646
Barren Zone - X11	338577	645	1156	142	1289	3825	2760	21544	5170	46417	12061	37422	5278	33787	4405
Barren Zone - X12	344965	45	367	98	1037	3538	2735	21086	4890	45427	12043	39066	5468	34726	4630
Barren Zone - X13	354944	67	559	103	1368	4002	2851	26350	6299	54978	13395	41923	5942	38823	5036
Barren Zone - X14	330355	85	340	70	794	2910	2066	16675	4322	42418	11300	36530	5210	33694	4388
Barren Zone - X15	357709	45	311	81	876	2570	1862	15484	4075	41864	11249	38586	5536	35129	4762
Barren Zone - X16	367857	38	335	85	920	4182	3063	22423	5240	49053	12532	41914	5892	38442	4880

Barren Zone - X17	360444	104	1097	345	3500	5276	2986	22855	5792	53117	13014	42586	5857	36893	4772
Barren Zone - X18	352999	52	302	82	896	2799	2064	16396	4314	42737	11427	38599	5535	33878	4632
Barren Zone - X19	348085	454	919	159	1578	4321	3114	23225	5306	45898	11701	37293	5157	32638	4360
Barren Zone - X20	364171	3176	4652	424	1690	2975	2181	17687	4698	44664	11835	39749	5406	34496	4690
Barren Zone - X21	370119	29	241	62	817	3339	2494	20671	5070	48502	12502	41856	5961	37361	4728
Barren Zone - X22	336956	43	361	74	896	2895	2104	17761	4419	44522	11550	38379	5565	34672	4637
Barren Zone - X23	361628	51	452	79	863	2920	2189	18327	4660	46081	12120	40884	5854	37457	4898
Barren Zone - X24	373726	26	237	64	826	2567	1887	16393	4370	46130	12382	41364	5860	38062	4892
Barren Zone - X25	378670	26	212	65	800	2638	1956	16091	4023	39954	11366	37241	5101	31904	4527
Barren Zone - X26	375374	32	330	81	991	3048	2183	17455	4577	45801	12091	40159	5571	35780	4727
Barren Zone - X27	367323	1176	1699	238	1450	2903	2009	15965	4932	49428	12912	43097	6487	42447	5197
Barren Zone - X28	360900	2044	3450	308	1652	3568	2433	18925	4695	47880	12083	41651	6106	38115	4918
Barren Zone - X29	323308	1181	2240	224	1537	3179	2338	17299	4783	44965	11097	37428	5314	34954	4260
Barren Zone - X30	349872	20	248	55	757	3155	2378	19630	4810	46713	12166	41435	6006	37379	4681
Barren Zone - X31	365519	33	321	85	956	2760	1936	16599	4199	42089	11418	37664	5105	31964	4465
Barren Zone - X32	364883	26	254	76	898	3351	2346	19234	4763	46681	12337	41685	5934	38439	4783
Barren Zone - X33	354655	26	255	68	811	3208	2243	19071	4569	44761	11967	39847	5713	36682	4889
Barren Zone - X34	365968	65	462	170	2020	4253	2928	22556	5276	48637	12702	41960	5950	37206	4662
Barren Zone - X35	355295	35	244	62	787	3807	2879	21737	4814	44586	11833	40794	5827	37622	4814
Barren Zone - X36	351854	130	1131	354	3211	4138	2261	18285	4503	44382	12614	45563	6642	40689	5149
Barren Zone - X37	364586	161	1862	629	5820	6197	2980	23080	5783	52927	13268	42251	5570	31257	3595
Barren Zone - X38	357152	48	506	74	809	3360	2324	18933	4453	43152	11601	40261	6147	39714	5203

Barren Zone - X39	358164	124	538	87	887	1961	1396	11827	3905	44334	12202	42609	6336	41416	5076
Barren Zone - X40	360834	557	3766	787	6823	6861	2432	20659	4752	41805	10894	37558	5618	39315	6054
Barren Zone - X41	370758	257	664	104	832	2626	1845	16216	4367	45298	12157	42960	6265	39773	4839
Barren Zone - X42	351646	1699	2871	331	2193	3513	2172	15929	4218	42588	11657	40029	6001	39801	5252
Barren Zone - X43	369828	17	159	51	657	2547	1816	16219	4270	44877	12383	42414	6415	40796	5136
Barren Zone - X44	339353	801	2354	324	2075	4951	3436	25807	5466	47802	12625	42829	6625	44191	5780
Barren Zone - X45	356867	18	158	37	545	3095	2214	18250	4204	42061	11574	40040	5902	38559	4934

APPENDIX I: APATITE TRACE ELEMENT ANALYSES

Samples	Y	La	Ce	Pr	Nd	Sm	Eu	Gd	Tb	Dy	Ho	Er	Tm	Yb	Lu
Session 1 Standards															
NIST610 - 1	458	438	450	446	426	451	445	447	435	435	447	455	432	446	436
NIST610 - 2	467	442	455	450	434	456	449	451	439	439	451	456	438	454	442
NIST610 - 3	460	441	454	449	431	451	448	451	438	437	449	455	435	450	440
NIST610 - 4	460	439	453	447	429	452	446	447	437	437	449	455	435	450	440
NIST610 - 5	456	436	445	442	425	450	441	446	430	431	446	450	430	443	433
NIST610 - 6	470	445	460	455	435	457	454	453	444	444	453	462	440	456	445
NIST610 - 7	457	434	447	444	425	451	443	447	434	432	445	449	433	447	432
NIST610 - 8	465	442	456	453	435	454	452	451	441	442	454	457	437	451	440
NIST610 - 9	457	436	450	440	425	449	439	443	432	431	441	452	428	445	436
NIST610 - 10	473	450	461	456	436	465	455	455	443	443	457	466	442	460	449
NIST610 - 11	459	434	450	446	428	445	446	448	435	436	446	448	435	448	437
NIST610 - 12	462	442	453	450	432	454	448	450	439	438	452	456	435	448	440
NIST610 - 13	463	442	455	451	431	456	447	451	439	440	451	460	437	455	441
NIST610 - 14	461	441	453	445	429	451	447	447	435	435	447	453	433	448	439
NIST610 - 15	454	429	444	445	428	443	442	444	434	434	445	448	431	443	430
NIST610 - 16	462	442	455	451	432	456	453	454	441	441	453	456	439	452	440
NIST610 - 17	460	441	452	445	426	453	443	446	433	433	445	453	432	451	438
NIST610 - 18	470	447	461	451	434	461	452	452	441	441	453	463	438	454	444
NIST610 - 19	459	435	449	444	425	451	442	445	434	433	444	452	431	445	439
NIST610 - 20	470	446	458	452	436	460	452	453	441	441	454	458	439	456	444
NIST610 - 21	458	435	449	444	426	450	443	447	434	435	446	453	433	448	434
NIST610 - 22	464	442	455	452	434	453	451	451	440	439	452	455	437	451	440

NIST610 - 23	458	437	448	448	426	448	446	448	436	437	447	452	434	444	437
NIST610 - 24	462	440	451	448	434	450	448	450	439	437	451	454	436	452	439
NIST610 - 25	459	439	452	445	429	451	444	446	434	432	446	455	431	450	438
NIST610 - 26	467	446	462	451	431	461	450	452	440	442	452	460	439	455	442
NIST610 - 27	458	437	449	446	428	451	445	446	435	435	446	454	434	446	436
NIST610 - 28	462	441	453	450	432	455	449	452	439	439	452	455	437	451	440
NIST610 - 29	461	434	447	444	424	445	442	444	433	432	444	450	430	446	434
NIST610 - 30	468	447	460	453	436	462	453	454	442	443	455	461	441	456	446
NIST610 - 31	452	429	443	439	422	443	437	439	428	427	440	447	425	439	430
NIST610 - 32	470	450	462	456	437	462	456	458	445	447	457	463	444	459	447
Session 2 Standards															
NIST610 - 1	464	441	455	450	433	454	449	453	439	439	450	456	436	451	440
NIST610 - 2	460	439	451	447	427	452	445	448	435	434	448	454	434	449	438
NIST610 - 3	465	443	457	448	432	455	450	452	441	441	452	459	438	454	443
NIST610 - 4	457	437	449	443	428	451	441	442	433	433	446	451	432	446	435
NIST610 - 5	464	439	452	449	428	452	449	448	437	437	450	455	435	451	440
NIST610 - 6	464	441	454	452	432	454	450	452	437	437	448	456	435	449	438
NIST610 - 7	461	440	453	448	428	452	444	447	436	436	450	455	434	450	438
NIST610 - 8	462	440	453	448	432	454	448	448	438	438	448	455	436	450	440
NIST610 - 9	463	443	456	449	434	454	447	452	440	440	452	457	437	455	443
NIST610 - 10	455	437	449	442	426	452	441	448	434	433	446	453	433	445	435
NIST610 - 11	465	439	454	449	432	454	449	451	436	437	448	456	436	451	441
NIST610 - 12	463	441	452	449	429	453	449	451	438	437	450	454	434	449	437
NIST610 - 13	460	436	449	446	425	449	446	446	433	435	445	450	431	445	436
NIST610 - 14	468	444	457	453	435	457	452	456	441	439	453	460	439	456	442
NIST610 - 15	461	440	453	446	429	455	445	447	438	438	449	456	436	452	440
NIST610 - 16	459	440	453	447	431	451	446	445	436	436	449	454	434	448	438

NIST610 - 17	460	437	451	447	429	451	444	445	434	435	446	454	433	449	438
NIST610 - 18	464	443	455	449	431	455	450	450	440	439	452	456	437	451	441
NIST610 - 19	463	440	454	449	428	455	446	450	437	437	450	455	435	450	439
NIST610 - 20	463	440	452	449	432	451	449	450	437	437	448	455	435	450	439
NIST610 - 21	461	439	452	446	431	453	445	450	437	436	449	454	434	448	438
NIST610 - 22	459	441	454	447	429	453	446	447	437	437	449	456	436	452	440
NIST610 - 23	464	443	456	452	434	454	450	452	438	440	451	457	437	451	440
NIST610 - 24	462	437	450	447	426	452	446	449	436	434	447	453	433	449	438
NIST610 - 25	459	438	452	444	427	453	445	448	436	435	447	452	434	449	440
NIST610 - 26	464	442	454	449	433	453	447	449	438	439	451	458	436	451	438
NIST610 - 27	463	438	451	448	429	452	445	450	436	435	447	454	434	448	437
NIST610 - 28	465	442	455	451	431	454	452	452	438	439	451	456	436	452	441
NIST610 - 29	459	438	451	445	428	453	443	446	436	435	447	454	433	447	437
NIST610 - 30	462	442	455	450	432	453	449	448	438	439	451	456	437	453	441
NIST610 - 31	461	439	453	447	428	451	446	448	436	437	448	453	433	449	438
NIST610 - 32	464	441	453	449	432	455	448	451	438	437	450	457	437	451	440
NIST610_20 - 1	476	451	472	462	439	463	457	456	443	447	456	464	441	456	444
NIST610_20 - 2	2188	2111	2164	2139	2045	2110	2099	2116	2049	2047	2110	2134	2025	2132	2061
NIST610_20 - 3	452	435	451	446	430	450	441	445	427	427	434	444	424	440	424
NIST610_20 - 4	441	424	436	431	420	430	426	433	415	415	427	434	413	429	413
NIST610_20 - 5	460	442	462	448	429	453	446	446	436	439	445	457	433	451	438
NIST610_20 - 6	458	435	453	449	431	450	442	440	428	419	439	446	427	434	429
NIST610_20 - 7	457	436	455	451	433	450	449	449	429	428	442	452	426	438	429
NIST610_20 - 8	456	442	460	452	438	457	444	440	431	439	444	456	433	448	434
NIST610_20 - 9	456	440	454	447	427	448	448	443	430	432	443	450	428	444	431
NIST610_20 - 10	472	451	466	464	436	465	458	455	442	445	453	454	439	458	442
NIST610_20 - 11	450	436	451	443	431	443	438	440	427	431	439	443	420	440	429

NIST610_20 - 12	454	429	448	438	414	442	439	441	420	420	435	440	417	428	420
NIST610_20 - 13	456	437	455	444	429	448	444	451	429	428	440	448	427	440	430
NIST610_20 - 14	437	419	433	428	412	425	424	421	410	409	421	430	409	425	414
NIST610_20 - 15	482	462	483	469	451	477	469	450	454	451	463	472	448	464	452
NIST610_20 - 16	455	441	460	451	428	460	444	447	432	435	441	449	429	448	428
Bn Zone - 743BAp - 1	1430	51	273	62	468	264	96	698	105	505	69	129	12	57	6
Bn Zone - 743BAp - 2	912	25	134	29	223	150	62	526	78	345	45	80	7	34	4
Bn Zone - 743BAp - 3	2011	22	89	17	114	76	38	347	62	379	66	154	17	94	12
Bn Zone - 743BAp - 4	2084	79	428	99	756	379	133	872	134	665	95	186	18	86	10
Bn Zone - 743BAp - 5	2208	60	353	86	664	354	130	866	135	684	101	198	19	91	10
Bn Zone - 743BAp - 6	884	28	153	35	259	149	59	510	76	324	43	75	7	32	4
Bn Zone - 743BAp - 7	1442	34	197	49	398	257	99	787	116	517	68	124	11	53	6
Bn Zone - 743BAp - 8	831	13	77	20	181	302	133	1045	98	329	39	71	6	27	3
Bn Zone - 743BAp - 9	707	53	177	32	216	138	58	496	73	298	37	62	5	22	2
Bn Zone - 743BAp - 10	922	13	78	19	164	227	112	884	91	333	44	84	7	33	4
Bn Zone - 743BAp - 11	1240	24	135	31	242	158	63	556	88	414	58	107	10	49	5
Bn Zone - 743BAp - 12	1071	32	171	38	283	177	69	541	81	374	51	92	8	40	5
Bn Zone - 743BAp - 13	1601	50	295	75	602	330	117	780	112	532	73	141	14	70	8
Bn Zone - 743BAp - 14	1430	28	161	37	293	190	77	610	95	459	66	126	12	53	7
Bn Zone - 743BAp - 15	1293	30	170	39	298	194	75	602	94	434	60	116	10	48	6
Bn Zone - 743BAp - 16	1070	26	158	38	297	197	81	687	104	454	55	90	8	34	4
Bn Zone - 743BAp - 17	837	23	124	27	204	146	62	512	75	327	42	71	6	27	3
Bn Zone - 743BAp - 18	884	18	108	27	229	155	66	577	97	417	48	73	6	24	2
Bn Zone - 743BAp - 19	1239	48	320	77	584	289	107	770	115	506	63	107	9	42	5
Bn Zone - 743BAp - 20	738	13	77	19	163	280	135	1063	99	306	36	63	5	25	3
Bn Zone - 743BAp - 21	1997	63	344	74	513	248	90	647	104	547	84	177	17	85	10
Bn Zone - 743BAp - 22	1418	52	299	71	536	302	117	760	109	502	67	129	12	59	7

Bn Zone - 743BAp - 23	1405	31	169	37	273	174	71	618	97	463	64	122	11	50	6
Bn Zone - 743BAp - 24	1880	56	295	63	422	211	83	620	100	531	81	163	16	77	9
Bn Zone - 743BAp - 25	1206	63	212	41	285	178	71	596	90	410	56	104	10	47	6
Bn Zone - 743BAp - 26	1189	30	166	37	280	185	73	626	91	396	54	101	9	43	5
Bn Zone - 743BAp - 27	1572	40	227	53	399	230	83	638	101	499	73	141	13	62	7
Bn Zone - 743BAp - 28	836	20	102	22	160	114	52	500	77	319	40	72	6	31	4
Bn Zone - 743BAp - 29	1802	49	261	59	434	248	89	688	109	551	80	164	16	77	10
Bn Zone - 743BAp - 30	2498	63	359	85	672	372	143	987	161	820	117	231	21	97	10
Bn Zone - 743BAp - 31	805	27	181	46	329	244	122	835	87	318	38	69	6	28	3
Bn Zone - 743BAp - 32	1596	64	287	61	411	213	76	567	92	466	68	136	14	67	8
Bn Zone - 743BAp - 33	1135	23	139	35	299	203	87	699	110	479	57	96	8	34	4
Bn Zone - 743BAp - 34	989	21	126	32	272	188	81	637	100	436	53	85	7	30	3
Bn Zone - 743BAp - 35	1540	48	247	53	351	192	76	564	91	460	68	134	12	60	7
Bn Zone - 743BAp - 36	815	30	153	32	240	145	58	520	76	321	40	68	6	27	3
Bn Zone - 743BAp - 37	1946	25	108	21	140	102	47	493	93	496	77	155	15	75	9
Bn Zone - 743BAp - 38	1622	30	178	44	350	227	97	738	119	562	77	144	13	60	7
Bn Zone - 743BAp - 39	2146	49	209	39	236	120	48	410	69	413	73	175	19	103	13
Bn Zone - 743BAp - 40	1925	41	243	57	418	251	100	782	128	627	90	171	16	71	8
Bn Zone - 743BAp - 41	1424	374	846	107	547	242	91	676	100	471	66	124	11	51	6
Bn Zone - 743BAp - 42	1084	25	148	36	284	196	83	589	79	362	50	96	9	43	5
Bn Zone - 743BAp - 43	773	18	94	22	179	251	116	911	90	299	37	67	6	29	3
Bn Zone - 743BAp - 44	968	31	179	43	332	238	95	604	74	327	45	86	8	39	4
Bn Zone - 743BAp - 45	755	23	123	29	229	154	64	477	66	292	37	67	6	28	3
Bn Zone - 743BAp - 46	1377	36	200	44	339	210	84	648	99	463	64	120	11	50	6
Bn Zone - 743BAp - 47	1343	30	178	44	370	233	90	639	94	446	63	119	11	54	6
Bn Zone - 743BAp - 48	963	24	139	31	241	172	69	589	84	355	46	80	7	32	4
Bn Zone - 743BAp - 49	1922	57	315	69	497	260	98	725	117	587	86	170	16	79	9

Bn Zone - 743BAp - 50	1785	69	376	81	565	269	95	628	101	524	80	160	15	72	8
Bn Zone - 743BAp - 51	1126	292	589	72	361	183	77	678	103	443	54	91	8	32	4
Bn Zone - 743BAp - 52	1014	46	264	59	416	210	77	546	80	363	49	87	8	36	4
Bn Zone - 743BAp - 53	1169	34	175	40	302	199	75	592	89	400	55	102	9	45	5
Bn Zone - 743BAp - 54	1419	28	166	40	316	217	93	733	117	535	70	123	11	47	5
Bn Zone - 743BAp - 55	1992	161	373	54	305	168	67	590	98	529	84	180	19	96	12
Bn Zone - 743BAp - 56	925	18	80	17	113	65	25	212	35	193	32	76	9	50	7
Bn Zone - 743BAp - 57	1037	14	68	14	98	79	33	324	54	265	41	85	9	51	6
Bn Zone - 743BAp - 58	1447	30	177	42	328	232	104	820	121	536	69	123	11	50	6
Bn Zone - 743BAp - 59	795	18	95	21	144	97	44	384	61	281	37	67	6	30	4
Bn Zone - 743BAp - 60	1557	41	246	55	381	181	64	435	69	369	59	130	14	74	10
Bn Zone - 743BAp - 61	2058	55	299	66	467	254	108	803	132	650	93	180	18	88	10
Bn Zone - 743BAp - 62	1766	166	501	84	556	273	103	701	108	544	79	156	15	70	8
Bn Zone - 743BAp - 63	940	20	112	25	195	233	108	846	91	342	45	84	7	33	4
Bn Zone - 743BAp - 64	1497	37	156	28	166	90	38	327	56	310	52	118	12	65	8
Bn Zone - 743BAp - 65	1775	66	368	81	540	242	88	592	96	505	76	158	17	86	11
Bn Zone - 743BAp - 66	1495	21	91	18	119	78	33	314	56	312	53	120	13	70	9
Bn Zone - 743BAp - 67	1640	70	319	66	423	190	66	461	76	415	66	134	13	63	8
Bn Zone - 743BAp - 68	1777	22	107	22	158	109	47	437	76	423	68	145	15	77	10
Bn Zone - 743BAp - 69	1013	44	286	69	489	296	121	791	98	392	51	87	8	34	4
Bn Zone - 743BAp - 70	2225	36	196	45	352	255	120	939	145	711	100	195	19	87	10
Bn Zone - 743BAp - 71	1697	59	336	69	452	237	103	845	135	622	82	146	13	58	6
Bn Zone - 743BAp - 72	1685	51	271	58	394	189	70	526	90	480	72	144	13	66	7
Bn Zone - 743BAp - 73	1653	35	195	46	348	208	84	582	92	477	70	146	15	74	9
Bn Zone - 743BAp - 74	1428	35	223	53	381	227	98	775	125	554	71	117	10	42	5
Bn Zone - 743BAp - 75	1368	46	220	51	399	265	112	854	129	561	70	118	10	42	5
Bn Zone - 743BAp - 76	1566	35	210	48	342	202	85	615	95	458	65	136	14	71	9

Bn Zone - 743BAp - 77	1472	9	51	14	126	152	80	653	90	409	59	124	12	63	8
Bn Zone - 743BAp - 78	1023	24	120	27	210	133	57	419	64	320	43	86	8	39	5
Bn Zone - 743BAp - 79	1879	51	238	42	245	122	49	432	73	416	70	154	16	80	10
Bn Zone - 743BAp - 80	1359	27	146	34	269	174	81	639	99	465	63	117	11	50	6
Bn Zone - 743BAp - 81	261	25	82	12	60	35	14	96	12	63	9	21	2	14	2
Bn Zone - 743BAp - 82	1487	34	218	52	376	239	107	852	127	552	72	126	11	47	5
Bn Zone - 743BAp - 83	1224	41	205	45	328	231	105	866	123	515	62	101	8	34	4
Bn Zone - 743BAp - 84	1420	130	484	91	566	250	87	597	92	456	65	126	12	58	7
Bn Zone - 743BAp - 85	2202	38	211	47	358	234	98	736	121	649	98	197	19	91	11
Bn Zone - 743BAp - 86	1023	39	254	62	447	270	117	838	106	416	52	89	7	33	4
Bn Zone - 743BAp - 87	2065	32	149	33	241	168	86	731	127	651	93	180	17	85	11
Bn Zone - 743BAp - 88	1139	27	160	39	318	191	75	522	75	363	52	102	11	52	6
Bn Zone - 743BAp - 89	1969	31	179	40	298	193	83	627	103	537	83	174	18	101	14
Bn Zone - 743CAp - 1	746	8	49	13	119	110	52	497	73	295	37	58	5	22	3
Bn Zone - 743CAp - 2	1833	38	180	40	297	178	65	530	82	426	64	132	13	70	8
Bn Zone - 743CAp - 3	2194	31	162	37	273	149	53	464	80	437	71	155	16	86	11
Bn Zone - 743CAp - 4	2183	43	224	51	382	227	83	691	107	543	82	167	17	83	10
Bn Zone - 743CAp - 5	1244	56	288	60	405	197	74	594	96	449	59	103	9	43	5
Bn Zone - 743CAp - 6	1481	52	282	59	399	181	57	454	72	366	58	127	13	68	9
Bn Zone - 743CAp - 7	2181	19	95	23	186	151	68	585	93	495	81	175	20	102	14
Bn Zone - 743CAp - 8	1820	27	147	35	283	221	89	749	111	514	72	134	12	59	7
Bn Zone - 743CAp - 9	1437	63	320	66	433	209	79	630	100	467	63	116	11	47	5
Bn Zone - 743CAp - 10	2240	103	592	124	768	330	121	898	147	718	101	194	17	78	9
Bn Zone - 743CAp - 11	1643	44	234	52	367	197	71	579	88	430	64	126	13	64	8
Bn Zone - 743CAp - 12	1444	35	227	52	372	204	86	737	117	512	67	117	11	45	5
Bn Zone - 743CAp - 13	2217	87	434	86	534	215	72	553	89	490	79	177	19	106	14
Bn Zone - 743CAp - 14	1306	34	203	45	314	167	62	560	91	422	58	108	10	44	5

Bn Zone - 743CAp - 15	2391	65	312	65	453	283	106	841	130	641	95	188	18	90	11
Bn Zone - 743CAp - 16	2039	49	314	69	425	211	87	707	122	599	87	171	16	78	10
Bn Zone - 743CAp - 17	1685	64	364	85	616	295	108	790	121	570	76	138	13	58	6
Bn Zone - 743CAp - 18	1664	62	308	61	390	183	61	478	72	372	61	144	16	87	12
Bn Zone - 743CAp - 19	1709	91	456	93	615	260	95	683	109	547	77	148	14	64	7
Bn Zone - 743CAp - 20	1292	41	253	58	416	238	98	707	105	467	60	106	9	41	5
Bn Zone - 743CAp - 21	1659	35	176	39	287	155	56	448	70	374	62	141	15	87	11
Bn Zone - 743CAp - 22	2260	59	267	56	409	271	102	840	126	609	88	168	17	80	9
Bn Zone - 743CAp - 23	1093	20	110	26	198	132	49	454	67	299	44	87	9	49	6
Bn Zone - 743CAp - 24	1840	32	171	39	304	206	81	695	108	512	75	141	14	71	9
Bn Zone - 743CAp - 25	1990	37	191	42	289	177	65	587	96	506	81	178	20	109	14
Bn Zone - 743CAp - 26	1755	33	160	35	268	183	69	616	96	479	74	162	17	91	11
Bn Zone - 743CAp - 27	1858	49	214	43	277	132	46	389	63	356	62	155	18	108	15
Bn Zone - 743CAp - 28	1053	22	107	23	179	122	47	437	67	302	45	95	10	56	7
Bn Zone - 743CAp - 29	1149	23	117	26	191	125	45	443	71	329	47	99	11	55	7
Bn Zone - 743CAp - 30	1699	29	152	36	280	179	67	586	91	441	65	129	13	65	8
Bn Zone - 743CAp - 31	1933	72	319	62	385	169	53	406	62	361	64	163	19	110	15
Bn Zone - 743CAp - 32	1479	55	331	71	464	212	75	680	114	525	70	123	10	45	5
Bn Zone - 743CAp - 33	854	28	163	35	237	130	53	524	80	333	41	70	6	25	3
Bn Zone - 743CAp - 34	1875	94	429	81	523	230	95	700	112	559	86	173	18	95	11
Bn Zone - 743CAp - 35	2166	26	139	29	198	140	60	574	107	568	88	184	18	98	12
Bn Zone - 743CAp - 36	2223	105	441	82	491	191	58	447	73	421	74	179	21	118	16
Bn Zone - 743CAp - 37	1037	27	172	39	261	132	53	511	85	385	49	84	8	35	4
Bn Zone - 743CAp - 38	1060	23	118	26	179	122	48	483	75	342	47	89	9	42	6
Bn Zone - 743CAp - 39	1028	12	70	17	134	118	52	461	70	321	44	84	8	39	5
Bn Zone - 743CAp - 40	1324	50	282	58	376	162	58	524	90	447	61	115	11	52	6
Bn Zone - 743CAp - 41	856	20	95	21	155	109	46	405	59	264	37	71	7	37	5

Bn Zone - 743CAp - 42	2474	108	332	57	354	183	68	578	93	520	87	210	24	133	19
Bn Zone - 743CAp - 43	1092	26	153	33	229	130	52	494	80	361	48	91	8	37	4
Bn Zone - 743CAp - 44	935	22	115	25	175	124	47	470	73	321	41	77	7	37	4
Bn Zone - 743CAp - 45	1463	30	146	31	219	141	56	493	77	382	59	127	14	74	10
Bn Zone - 743CAp - 46	1427	84	396	75	444	171	52	393	62	322	54	129	16	89	12
Bn Zone - 743CAp - 47	628	15	85	18	121	96	47	427	61	252	32	54	5	21	2
Bn Zone - 743CAp - 48	1808	48	198	38	263	142	48	431	71	388	66	155	18	98	13
Bn Zone - 743CAp - 49	1397	59	283	54	327	151	50	399	61	313	53	124	14	82	11
Bn Zone - 743CAp - 50	2267	22	113	25	188	154	67	591	97	511	84	197	23	131	18
Bn Zone - 743CAp - 51	1615	41	189	38	246	137	51	462	77	402	66	148	17	93	12
Bn Zone - 743CAp - 52	873	26	145	30	187	88	36	350	63	306	40	74	7	32	4
Bn Zone - 743CAp - 53	1445	44	202	40	261	128	45	382	61	313	49	112	13	79	11
Bn Zone - 743CAp - 54	1970	31	146	28	189	121	49	459	85	480	77	170	19	98	13
Bn Zone - 743CAp - 55	1404	30	122	24	170	107	41	373	61	315	51	121	14	83	12
Bn Zone - 743CAp - 56	991	30	169	34	217	96	38	383	73	348	47	86	8	34	4
Bn Zone - 743CAp - 57	1416	44	193	37	246	119	42	342	54	297	51	124	15	91	12
Bn Zone - 743CAp - 58	1288	32	160	33	227	135	52	469	73	377	56	118	12	60	8
Bn Zone - 743CAp - 59	1889	33	160	34	241	154	57	500	81	447	74	171	20	108	15
Bn Zone - 743CAp - 60	1364	22	83	16	111	61	20	202	37	231	43	111	14	86	12
Bn Zone - 743CAp - 61	1800	63	270	52	333	163	53	452	75	426	72	171	19	110	14
Bn Zone - 743CAp - 62	1147	21	103	22	161	119	51	460	71	342	51	104	11	56	7
Bn Zone - 743CAp - 63	792	19	94	20	146	103	45	389	57	263	35	71	7	35	5
Bn Zone - 743CAp - 64	844	24	132	27	177	103	46	415	70	327	42	74	6	28	3
Bn Zone - 743CAp - 65	1032	47	231	46	295	145	50	417	61	288	42	88	9	51	7
Bn Zone - 743CAp - 66	1240	50	306	72	510	252	90	660	103	461	60	105	9	41	5
Bn Zone - 743CAp - 67	1164	33	209	49	350	267	122	842	100	405	53	99	9	43	5
Bn Zone - 743CAp - 68	1443	44	253	54	353	192	73	623	95	447	62	117	11	48	6

Bn Zone - 743CAp - 69	1464	46	232	48	328	163	55	471	72	357	54	115	12	63	8
Bn Zone - 743CAp - 70	1280	38	222	51	372	202	76	575	89	416	56	104	9	43	5
Bn Zone - 743CAp - 71	1250	44	267	62	451	240	94	656	95	430	57	105	9	46	5
Bn Zone - 743CAp - 72	1579	569	1005	121	523	176	57	431	64	333	57	142	17	102	14
Bn Zone - 743CAp - 73	1406	29	141	31	231	162	61	513	74	369	57	127	14	74	9
Bn Zone - 743CAp - 74	1485	907	1797	214	873	233	71	473	66	332	55	131	15	82	11
Bn Zone - 743CAp - 75	1110	47	226	46	312	168	66	568	93	410	53	88	7	32	3
Bn Zone - 743CAp - 76	1528	63	396	93	688	325	119	824	122	550	73	130	11	49	6
Bn Zone - 743CAp - 77	2125	71	450	105	736	354	130	866	139	681	95	186	17	79	9
Bn Zone - 743CAp - 78	1215	83	215	33	189	98	30	245	38	216	39	102	13	75	10
Bn Zone - 743CAp - 79	1369	50	254	54	362	177	68	484	79	390	58	115	11	54	6
Bn Zone - 743CAp - 80	2685	114	508	98	581	253	80	623	100	557	92	213	23	124	15
Bn Zone - 743CAp - 81	1679	49	303	69	465	243	94	739	113	535	74	139	13	57	7
Bn Zone - 743CAp - 82	1365	98	373	67	408	166	59	425	70	363	55	113	11	59	7
Bn Zone - 743CAp - 83	2229	153	617	107	616	236	76	587	90	492	79	178	19	99	13
Bn Zone - 743CAp - 84	1570	93	375	71	456	212	77	592	96	469	66	127	12	61	7
Bn Zone - 743CAp - 85	1015	29	102	18	102	66	25	216	33	182	32	79	10	62	9
Bn Zone - 743CAp - 86	976	23	86	17	121	72	26	228	36	191	32	75	8	50	7
Bn Zone - 743CAp - 87	2635	89	567	132	928	426	151	1055	171	827	116	215	21	95	11
Bn Zone - 743CAp - 88	1371	31	125	26	196	131	55	469	70	340	51	111	12	69	9
Bn Zone - 743CAp - 89	1831	36	172	36	260	155	55	486	82	440	72	170	20	113	15
Bn Zone - 743CAp - 90	960	31	174	40	292	154	57	431	66	304	41	77	7	33	4
Bn Zone - 743CAp - 91	1148	53	193	31	164	69	24	194	32	179	33	87	11	71	10
Bn Zone - 743CAp - 92	1961	37	232	50	317	174	81	698	126	613	85	160	15	71	8
Bn Zone - 743CAp - 93	1121	33	128	23	146	94	36	290	43	219	37	88	11	64	9
Bn Zone - 743CAp - 94	829	19	67	12	74	48	19	160	25	133	23	58	7	45	7
Bn Zone - 743CAp - 95	1234	30	134	27	183	117	48	415	64	314	49	106	11	61	8

Bn Zone - 743CAp - 96	1356	30	142	30	224	140	53	444	68	347	55	124	14	76	10
Bn Zone - 743CAp - 97	302	209	514	61	262	56	10	71	11	59	9	21	2	13	2
Bn Zone - 743CAp - 98	2084	91	407	81	527	244	99	713	118	608	90	184	18	96	12
Bn Zone - 743CAp - 99	235	12	51	10	64	37	9	70	9	46	7	15	2	9	1
Bn Zone - 743CAp - 100	769	40	178	32	188	70	16	136	20	114	19	45	5	30	4
Bn Zone - 743CAp - 101	1889	146	508	83	460	164	51	368	59	344	62	154	19	110	15
Bn Zone - 743CAp - 102	1336	38	207	46	326	179	68	520	82	397	56	110	11	56	7
Bn Zone - 743CAp - 103	999	31	141	26	150	72	30	252	43	236	36	76	8	45	6
Bn Zone - 743CAp - 104	1988	47	287	64	437	250	91	746	119	584	86	162	14	65	8
Bn Zone - 743CAp - 105	967	119	663	121	644	180	30	219	34	194	35	89	10	63	8
Bn Zone - 743CAp - 106	1304	43	180	33	190	103	36	295	44	229	40	99	12	71	10
Bn Zone - 743CAp - 107	1206	33	205	45	300	152	60	556	94	428	56	96	8	34	4
Bn Zone - 743CAp - 108	1268	15	77	18	140	139	68	576	87	400	56	107	11	54	7
Bn Zone - 743CAp - 109	1195	37	230	51	334	169	65	597	98	443	57	96	8	34	4
Bn Zone - 743CAp - 110	1731	34	187	39	258	190	81	650	101	490	72	145	15	74	9
Bn Zone - 743CAp - 111	1614	31	135	28	219	160	66	542	82	419	66	147	16	89	12
Bn Zone - 743CAp - 112	2680	61	284	58	374	209	93	755	135	706	106	224	23	123	16
Bn Zone - 743CAp - 113	1584	32	140	28	203	128	49	422	69	371	62	146	16	87	12
Bn Zone - 743CAp - 114	1185	24	139	30	216	136	56	481	77	359	51	99	10	46	6
Bn Zone - 743CAp - 115	977	23	103	21	147	104	45	405	61	292	41	85	8	47	6
Bn Zone - 743CAp - 116	3349	25	98	19	142	109	51	503	95	574	105	272	32	203	28
Cpy Zone - DolAp - 1	1236	129	540	99	556	200	44	268	42	260	47	112	12	63	7
Cpy Zone - DolAp - 2	396	142	447	67	326	89	19	110	14	75	13	33	4	19	2
Cpy Zone - DolAp - 3	1605	369	1623	289	1495	349	64	352	48	288	56	149	17	90	10
Cpy Zone - DolAp - 4	473	184	573	84	413	107	19	127	17	90	15	40	4	25	3
Cpy Zone - DolAp - 5	1902	455	1526	236	1109	299	31	331	49	291	59	164	22	131	20
Cpy Zone - DolAp - 6	2842	321	1245	220	1215	402	61	525	80	502	101	274	32	172	21

Cpy Zone - DolAp - 7	951	2470	6925	887	3415	512	89	360	41	207	35	84	10	53	7
Cpy Zone - DolAp - 8	1949	814	2543	369	1673	373	46	389	52	321	64	178	21	122	16
Cpy Zone - DolAp - 9	1712	693	2054	294	1324	315	42	338	48	295	58	153	19	106	14
Cpy Zone - DolAp - 10	1865	834	2557	361	1600	335	36	354	48	289	60	163	21	121	17
Cpy Zone - DolAp - 11	1860	485	1590	239	1156	304	51	368	55	333	64	165	19	100	12
Cpy Zone - DolAp - 12	1647	881	2627	359	1545	320	36	311	43	261	53	150	19	111	16
Cpy Zone - DolAp - 13	2229	919	2709	385	1748	402	50	430	61	373	74	200	25	142	19
Cpy Zone - DolAp - 14	2009	1178	3311	448	1890	392	42	392	53	327	65	182	23	135	19
Cpy Zone - SSAp - 1	446	78	347	61	310	79	16	82	11	71	14	43	6	34	5
Cpy Zone - SSAp - 2	632	174	725	121	607	135	16	130	17	108	22	63	8	47	6
Cpy Zone - SSAp - 3	449	76	320	55	289	76	15	82	12	69	15	41	5	31	4
Cpy Zone - SSAp - 4	358	66	285	48	244	67	14	75	10	61	12	32	4	25	3
Cpy Zone - SSAp - 5	1662	1130	3692	520	2351	454	49	375	50	284	55	150	18	111	15
Cpy Zone - SSAp - 6	507	148	539	85	398	95	20	101	14	88	18	52	7	39	5
Cpy Zone - SSAp - 7	1012	316	1027	154	723	172	27	191	27	159	31	80	9	51	6
Cpy Zone - SSAp - 8	1155	182	623	97	488	136	26	189	29	191	38	97	11	53	5
Cpy Zone - SSAp - 9	503	112	440	72	355	94	21	99	14	89	18	51	7	39	5
Cpy Zone - SSAp - 10	821	1425	3942	495	1920	294	36	218	27	151	28	75	9	52	7
Cpy Zone - SSAp - 11	879	258	880	137	673	165	18	177	25	143	28	75	9	50	7
Cpy Zone - SSAp - 12	458	103	412	68	343	84	18	86	12	75	15	44	6	38	5
Cpy Zone - SSAp - 13	451	82	354	60	311	82	18	89	12	71	15	41	5	36	5
Cpy Zone - SSAp - 14	407	74	247	40	210	69	14	93	13	73	14	35	4	25	3
Cpy Zone - SSAp - 15	2448	238	927	164	896	303	40	415	69	454	92	245	28	145	14
Cpy Zone - SSAp - 16	1290	893	2938	418	1873	390	45	342	45	245	45	114	13	65	7
Cpy Zone - SSAp - 17	1895	1111	3376	483	2139	480	66	491	60	329	60	148	16	83	11
Cpy Zone - SSAp - 18	976	981	2827	381	1596	320	51	278	37	202	37	90	11	53	6
Cpy Zone - SSAp - 19	666	371	1295	188	862	174	24	163	21	113	23	60	8	45	6

Cpy Zone - SSAp - 20	4530	433	1614	275	1443	492	58	698	114	742	157	445	56	316	39
Cpy Zone - SSAp - 21	932	532	1583	222	1025	206	25	196	26	151	30	83	11	66	10
Cpy Zone - SSAp - 22	2260	960	2994	424	1890	491	67	516	75	447	83	221	27	144	16
Cpy Zone - SSAp - 23	1411	500	1927	315	1511	340	39	320	41	234	44	114	13	71	9
Cpy Zone - SSAp - 24	805	185	569	87	432	109	18	138	19	118	25	72	10	60	9
Cpy Zone - SSAp - 25	581	389	1413	210	920	166	22	140	18	102	20	54	7	41	6
Cpy Zone - SSAp - 26	705	265	767	107	489	110	18	124	16	105	22	65	9	60	10
Cpy Zone - SSAp - 27	1065	1861	5361	707	2849	506	70	379	46	244	41	99	11	53	5
Cpy Zone - SSAp - 28	626	308	1039	152	667	140	21	134	18	109	21	59	7	42	6
Cpy Zone - SSAp - 29	647	1569	4596	595	2339	328	41	209	24	130	24	65	7	45	6
Cpy Zone - SSAp - 30	718	623	1741	229	955	186	27	164	22	123	24	67	8	50	7
Cpy Zone - SSAp - 31	1525	1000	3164	458	2025	425	51	385	52	297	54	137	16	86	9
Cpy Zone - SSAp - 32	1189	442	1422	205	918	203	24	212	29	174	37	114	15	90	14
Cpy Zone - SSAp - 33	3214	657	2245	358	1863	591	92	723	104	625	117	311	38	217	26
Cpy Zone - SSAp - 34	644	862	2729	361	1485	237	23	188	21	114	22	60	7	43	6
Cpy Zone - SSAp - 35	997	1113	3333	471	2116	511	104	489	51	245	39	94	10	60	8
Cpy Zone - SSAp - 36	2161	2187	6055	776	3159	549	64	477	60	358	70	190	24	140	18
Cpy Zone - SSAp - 37	2141	1131	3751	553	2423	490	51	462	59	341	67	185	23	136	19
Cpy Zone - SSAp - 38	1960	1289	3887	541	2305	440	52	412	54	322	63	172	21	128	18
Cpy Zone - SSAp - 39	796	536	1482	193	822	170	22	172	22	137	27	74	10	54	8
Cpy Zone - SSAp - 40	2080	2291	6293	805	3259	549	63	476	59	345	67	185	22	131	18
Cpy Zone - SSAp - 41	691	678	2095	280	1162	202	26	175	21	120	23	63	8	46	6
Cpy Zone - SSAp - 42	1984	1378	3772	494	2063	443	62	422	61	370	72	194	25	139	18
Cpy Zone - SSAp - 43	1173	1939	5650	718	2857	443	50	320	39	213	40	111	13	78	11
Cpy Zone - SSAp - 44	807	1677	4546	545	2024	288	39	224	25	141	26	69	8	44	6
Cpy Zone - SSAp - 45	2724	549	1761	277	1324	438	28	488	88	560	97	217	21	91	10
Barren Zone Ap - 1	154	0	5	3	45	147	91	562	35	83	7	10	1	4	0

Barren Zone Ap - 2	305	1	8	4	67	244	165	1219	100	219	16	21	2	7	1
Barren Zone Ap - 3	182	2	12	6	86	282	165	1152	86	171	11	12	1	3	0
Barren Zone Ap - 4	470	1	11	6	103	420	268	2069	172	380	27	31	2	8	1
Barren Zone Ap - 5	426	2	11	5	76	292	202	1568	134	303	22	29	2	11	1
Barren Zone Ap - 6	155	6	14	5	70	229	140	1009	74	144	9	9	1	2	0
Barren Zone Ap - 7	309	3	13	5	71	252	168	1244	100	219	16	21	2	8	1
Barren Zone Ap - 8	338	1	10	6	89	324	208	1559	129	278	20	22	2	7	1
Barren Zone Ap - 9	156	3	15	6	87	270	159	1096	80	153	10	10	1	2	0
Barren Zone Ap - 10	407	1	11	5	81	292	195	1518	134	300	22	28	2	10	1
Barren Zone Ap - 11	200	1	8	5	72	233	145	1058	83	169	11	13	1	4	0
Barren Zone Ap - 12	412	3	15	6	95	363	235	1789	152	338	24	27	2	7	1
Barren Zone Ap - 13	370	1	10	5	81	300	198	1564	132	290	21	25	2	8	1
Barren Zone Ap - 14	350	2	8	3	50	177	123	796	55	153	15	25	2	11	1
Barren Zone Ap - 15	399	4	16	6	84	308	206	1601	137	306	22	27	2	8	1
Barren Zone Ap - 16	466	8	21	7	93	360	240	1869	163	365	26	31	2	10	1
Barren Zone Ap - 17	538	2	16	7	118	457	301	2296	197	439	31	36	3	9	1
Barren Zone Ap - 18	470	6	16	7	99	388	255	1995	170	374	27	32	2	9	1
Barren Zone Ap - 19	160	1	7	4	58	181	115	775	53	112	8	11	1	4	0
Barren Zone Ap - 20	397	1	12	6	89	327	211	1627	144	313	23	27	2	9	1
Barren Zone Ap - 21	515	1	12	6	94	376	254	2011	173	392	28	35	3	11	1
Barren Zone Ap - 22	368	4	20	7	110	389	238	1675	133	288	21	26	2	7	1
Barren Zone Ap - 23	437	1	11	6	100	388	246	1861	157	344	25	30	2	9	1
Barren Zone Ap - 24	156	7	22	6	75	235	141	991	75	145	9	10	1	3	0
Barren Zone Ap - 25	432	1	11	6	91	334	222	1728	150	335	24	29	2	9	1
Barren Zone Ap - 26	181	1	8	4	59	205	129	921	68	139	10	12	1	4	0
Barren Zone Ap - 27	485	4	16	5	76	271	185	1369	111	270	23	34	3	14	1
Barren Zone Ap - 28	162	1	7	4	57	181	116	787	54	111	8	10	1	3	0

Barren Zone Ap - 29	389	28	70	14	164	513	283	1880	134	295	22	26	2	7	1
Barren Zone Ap - 30	314	1	9	5	75	264	174	1319	106	231	17	20	2	6	1
Barren Zone Ap - 31	163	26	51	8	79	223	134	964	72	144	10	11	1	3	0
Barren Zone Ap - 32	447	4	13	4	58	201	142	940	68	190	18	33	3	14	2
Barren Zone Ap - 33	361	8	24	7	102	367	223	1688	137	303	21	23	2	7	1
Barren Zone Ap - 34	548	8	23	6	71	256	180	1231	92	247	24	40	4	16	2
Barren Zone Ap - 35	436	1	10	5	77	303	205	1626	140	315	24	30	2	11	1
Barren Zone Ap - 36	385	8	28	8	99	352	224	1702	144	319	22	25	2	7	1
Barren Zone Ap - 37	483	1	10	5	77	308	207	1579	133	310	24	32	3	13	1
Barren Zone Ap - 38	202	4	17	6	92	308	179	1225	90	178	12	14	1	3	0
Barren Zone Ap - 39	368	58	151	19	105	178	114	661	48	141	15	26	2	12	1
Barren Zone Ap - 40	524	1	11	6	91	346	239	1866	164	374	28	35	3	13	1
Barren Zone Ap - 41	461	1	10	5	86	330	222	1781	156	353	25	31	2	10	1
Barren Zone Ap - 42	302	1	8	4	67	237	160	1170	91	201	15	21	2	8	1
Barren Zone Ap - 43	277	2	11	5	77	276	176	1338	110	230	16	18	1	5	0
Barren Zone Ap - 44	454	1	10	5	75	286	198	1534	128	295	23	31	2	11	1
Barren Zone Ap - 45	179	35	73	9	79	200	132	930	70	143	10	12	1	4	0
Barren Zone Ap - 46	288	1	9	4	66	231	152	1098	83	187	14	19	2	8	1
Barren Zone Ap - 47	467	1	10	5	78	308	210	1596	132	302	24	31	3	12	1
Barren Zone Ap - 48	495	1	11	5	86	319	219	1724	148	348	27	34	3	13	1
Barren Zone Ap - 49	488	1	10	5	76	286	193	1429	112	274	24	33	3	13	2
Barren Zone Ap - 50	435	2	12	5	80	315	212	1673	147	329	24	30	2	9	1
Barren Zone Ap - 51	425	1	9	4	71	255	176	1308	105	247	20	29	3	13	1
Barren Zone Ap - 52	458	94	163	21	129	303	207	1571	134	308	23	32	3	12	1
Barren Zone Ap - 53	485	1	12	5	84	323	219	1722	148	337	26	33	3	12	1
Barren Zone Ap - 54	394	1	10	5	82	303	198	1566	135	305	22	27	2	9	1
Barren Zone Ap - 55	456	2	12	5	82	318	218	1721	151	340	25	30	2	11	1

Barren Zone Ap - 56	478	1	10	5	74	276	192	1442	116	278	23	34	3	13	1
Barren Zone Ap - 57	443	9	28	6	79	264	179	1324	104	254	21	32	3	13	1
Barren Zone Ap - 58	481	9	25	7	90	339	229	1777	151	343	26	33	2	10	1
Barren Zone Ap - 59	605	4	10	3	39	193	135	840	66	216	24	46	4	20	2
Barren Zone Ap - 60	432	12	33	8	87	298	203	1586	136	307	23	30	2	10	1
Barren Zone Ap - 61	157	32	69	11	92	243	148	1051	79	150	10	10	1	2	0
Barren Zone Ap - 62	587	1	9	5	72	284	196	1382	105	271	26	43	4	19	2
Barren Zone Ap - 63	519	1	10	5	77	292	197	1496	119	287	25	38	3	15	1
Barren Zone Ap - 64	453	11	36	9	105	374	242	1880	165	364	26	30	2	8	1
Barren Zone Ap - 65	623	1	11	5	74	276	193	1364	104	280	27	45	4	19	2
Barren Zone Ap - 66	459	4	16	5	80	295	203	1543	126	294	23	31	3	12	1
Barren Zone Ap - 67	522	1	9	5	69	260	180	1279	98	253	23	37	3	16	2
Barren Zone Ap - 68	558	1	9	4	70	271	188	1333	102	264	25	40	4	17	2
Barren Zone Ap - 69	507	1	11	6	88	340	227	1813	159	358	27	34	3	13	1
Barren Zone Ap - 70	550	1	11	5	75	286	202	1475	115	286	25	39	3	16	2
Barren Zone Ap - 71	301	188	338	29	154	317	197	1456	120	258	17	20	1	6	1
Barren Zone Ap - 72	485	1	8	4	53	210	144	960	70	196	21	36	3	16	2
Barren Zone Ap - 73	569	0	5	2	42	195	137	862	66	202	23	43	4	18	2
Barren Zone Ap - 74	536	3	41	15	133	267	177	1207	90	240	24	37	3	17	2
Barren Zone Ap - 75	593	1992	4659	548	2117	735	351	2467	211	472	33	40	3	12	1
Barren Zone Ap - 76	577	1	7	4	50	219	152	1002	74	221	23	42	4	20	2
Barren Zone Ap - 77	166	133	244	26	133	202	123	862	59	123	9	11	1	4	0
Barren Zone Ap - 78	169	55	148	19	106	183	114	778	51	119	9	11	1	3	0
Barren Zone Ap - 79	518	448	973	105	429	267	157	997	72	206	21	38	3	16	2
Barren Zone Ap - 80	535	96	205	24	126	229	156	1013	73	213	23	40	4	17	2
Barren Zone Ap - 81	488	707	1681	185	708	400	226	1708	142	322	25	34	2	12	1
Barren Zone Ap - 82	179	1671	2868	282	923	316	157	1069	79	156	11	12	1	4	0